AN IMPROVED SIZE, MATCHING, AND SCALING SYNTHESIS METHOD FOR THE DESIGN OF MESO-SCALE TRUSS STRUCTURES

A Thesis
Presented to
The Academic Faculty

by

Patrick Chang

In Partial Fulfillment
of the Requirements for the Degree
Master of Mechanical Engineering in the
The George W. Woodruff School of Mechanical Engineering

Georgia Institute of Technology
August 2011

Copyright © 2011 by Patrick Chang

AN IMPROVED SIZE, MATCHING, AND SCALING SYNTHESIS METHOD FOR THE DESIGN OF MESO-SCALE TRUSS STRUCTURES

Approved by:

Professor David Rosen, Advisor,
Committee Chair
The George W. Woodruff School of
Mechanical Engineering
Georgia Institute of Technology

Professor Christiaan Paredis
The George W. Woodruff School of
Mechanical Engineering
Georgia Institute of Technology

Professor Seung-Kyum Choi
The George W. Woodruff School of
Mechanical Engineering
Georgia Institute of Technology

Date Approved: June 15, 2011

ACKNOWLEDGEMENTS

I would like to thank my advisor, Dr. David W. Rosen and my committee members, Dr. Christiaan Paredis and Dr. Seung-Kyum Choi for providing their expertise and knowledge in the completion of my Master's thesis. I would also like to acknowledge Dr. Janet K. Allen and Dr. Farrokh Mistree for providing me with academic and professional mentorship throughout my tenure at the Georgia Institute of Technology

In addition, I would like to thank my labmates, Amit Jariwala, Jane Kang, Namin Jeong, Wenchao Zhou, Jason Nguyen, and Chad Hume, as well as the former members of the now defunct Systems Realization Laboratory, Benjamin Lee, Alek Kerzhner, Roxanne Moore, Jiten Patel, Aditya Shah, Abhishek Kumar, Mukul Singhee, Gregory Graf, Jane Chu, and Sarah Engelbrecht, for their support and friendship.

Finally, I would like to thank my friends and family for their unending and oftentimes unrequited love and support.

Thank you all!

TABLE OF CONTENTS

LIST OF TABLES

LIST OF FIGURES

SUMMARY

The recent improvement of additive manufacturing has allowed designers to achieve a level of complexity and customizability that is difficult or impossible to accomplish using traditional manufacturing processes. As a result, much research has been conducted on developing new methods to utilize the larger design space brought by additive manufacturing. One such research area is in the design of mesoscale lattice structures. Mesoscale lattice structures are a type of cellular structure with support element sizes on the order of magnitude of centimeters. These types of structures are engineered for high performance and have applications in industries where both low weight and high strength are desired. However, due to the small size of their struts, these structures can easily have hundreds to thousands of individual struts. As a result, design poses a unique challenge. Current methods approach design of mesoscale lattice structures as a topological optimization problem, treating each strut diameter in the structure as a design variable. For structures with a fewer number struts, these optimization methods can converge, but will generally be very time-consuming. For structures with a large number of struts, the optimization problem becomes too large for current algorithms to solve.

In previous research, a new, highly efficient design method for mesoscale lattice structures was presented that eliminates the need for global size or topological optimization. This method, termed the Size, Matching and Scaling method, used a unique combination of a solid-body finite element analysis and a library of pre-defined lattice configurations, termed the unit-cell library, to generate lattice topologies. The results from this method were highly promising: design time was significantly reduced when compared to optimization methods. Furthermore, lattices designed using the SMS

method had performance results that were either comparable or better than their optimized counterparts. However, the method developed was highly conceptual, lacking a true systematic methodology for generating topologies and suffering from some gaps in implementation.

In this research, we present a modified Size Matching and Scaling (SMS) design method. Firstly, we introduce and outline the modified methodology. This methodology particularly includes an optimization step for determining strut diameters that replaces the manual search used in the original method. Secondly, we expand and explore the unit-cell library in an attempt to improve the performance of lattices generated using the SMS method. In particular, we optimize several unit-cell configurations and compare their performance in the context of the SMS method. Finally, we test the updated SMS methodology and unit-cell library using various design examples.

Results from the various example problems indicate that optimization is not only a viable systematic method for determining diameter values, but is actually preferred to the manual, iterative process used in the original method. Furthermore, various optimization algorithms and approaches yield different results. Between the two optimization algorithms utilized in this method: constrained optimization and least-squares minimization, constrained minimization converges faster, but least-squares minimization yields slightly improved performance results. In addition to these algorithms, a one-variable approach using an untested, simplifying assumption, dubbed the "28% approach," was tested. Results indicate that this assumption was incorrect and cannot be utilized. Finally, results from the expanded unit-cell library indicate that the best unit-cell configuration is still the same original unit-cell configuration utilized in the first SMS method. The addition of more unit-cell does not improve the performance of structures generated using the SMS method. In fact, both performance and design time worsen when additional configurations are utilized.

CHAPTER I

INTRODUCTION, BACKGROUND AND MOTIVATION

1.1 Introduction

The challenges facing designers today have reached an unprecedented level. The demands for lighter, stronger, and more customizable parts have necessitated the research and development of new technologies, tools, and methodologies that can satisfy the new demands of the modern world. In particular, the introduction and continual improvement of one technology, additive manufacturing, has dramatically changed the way engineers pursue design and manufacturing. This new and promising technology has eliminated many barriers to manufacturing and has allowed designers to achieve a level of complexity and customizability difficult or impossible to achieve using traditional, "removal manufacturing" processes. As a result, much research has been conducted on developing new methods to utilize the larger design space brought by additive manufacturing. One such research area is in the design of mesoscale lattice structures. Mesoscale lattice structures are a type of cellular structure with support element sizes on the order of magnitude of centimeters. These types of structures are engineered for high performance and have applications in industries where both low weight and high strength are desired. Such structures will be the focus of this work. In particular, this research will present a design method for the design of mesoscale truss structures.

1.2 Background

1.2.1 Additive Manufacturing

Additive manufacturing (AM), once referred to as Rapid Prototyping (RP), can be defined as a collection of automated processes that fabricate 3-D objects from a series

of nominally 2-D cross-sectional layers of specialized materials [33]. Typically, all parts designed with AM technologies begin with a 3-D CAD model representation of the component. This model is then typically converted into an STL file and sent to the AM machine, which builds the part layer-by-layer.

Currently, many technologies exist that fit into the broad definition of AM. These technologies are supported by several, distinct process categories. These categories include: photopolymerization processes, powder bed fusion processes, extrusion-based systems, printing processes, sheet lamination processes, beam deposition processes, and direct write technologies [42]. Each of these processes has its own distinct set of advantages and disadvantages regarding characteristics such as manufacturing speed and layer resolution. Of these different processes, two particular manufacturing technologies are most commonly used: stereolithography (SLA) and selective laser sintering (SLS). These two processes will be briefly outlined in the following sections.

1.2.1.1 Stereolithography

Stereolithography (SLA) is a type of photopolymerization processes that makes use of a liquid vat filled with resins filled with curable photopolymers. These photopolymers react to certain wavelengths of light, with the most common photopolymers reacting within the ultraviolet wavelengths. Once irradiated, the resin undergoes a chemical reaction to become solid called photopolymerization [42]. In SLA, a platform is suspended in the resin vat. During the manufacture of a component, the platform begins at the top of the vat. A scanning laser then traces the 2-D cross-section of the part, curing the exposed resin. After the cross-section is traced, the platform moves down an incremental amount and the laser cures the next cross-section. This process continues until the part is complete. Because SLA uses photopolymers as the main material for manufacture, components built using SLA must be some sort of plastic material.

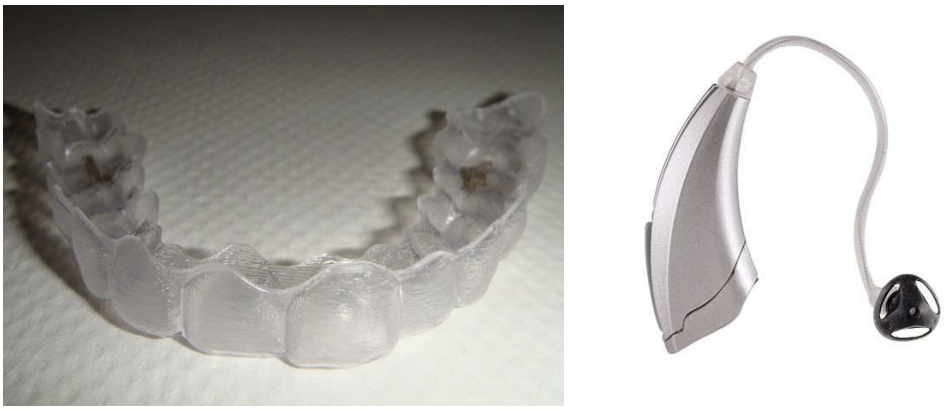

Figure 1: A specialized Invisalign® brace (left), that is constructed using a mold generated by SLA, and Phonax hearing aid (right) built using SLA processes [2, 4].

Although initially used primarily as a prototyping technology, SLA has begun to be more frequently used in manufacturing applications, particularly where mass-customization is required. For instance, Align Technologies, developers of the Invisalign® braces technology, uses stereolithography to develop molds for their customized braces [57]. Also, hearing-aid manufacturing companies such as Siemens, Phonak, and Widex use stereolithography machines to mass-produce customized hearing-aid shells [30]. Figure 1 shows examples of these products manufactured in SLA machines.

1.2.1.2 Selective Laser Sintering

Selective laser sintering (SLS) or melting (SLM) technologies were the first AM technologies to use the powder bed fusion (PBF) process [42]. The principal driving feature of these methods is the melting and fusion of powder to form part cross-sections. In the SLS process, a build platform exists containing a thin layer of powder. An infrared heater heats the powder bed to just below the melting point of the powder. Then, a laser beam traces the cross-section of the part, heating the powder to its melting point and fusing the powder. The platform bed then lowers an incremental amount. Rollers spread a uniform layer of powder along the platform bed, and the melting process is repeated. This step continues until the part is complete.

Figure 2: An exhaust manifold manufactured using SLS [5].

Because SLS uses a powder bed instead of a photopolymer vat, it can build both plastic and metal components. As a result, SLS can be used in industries where metal parts are required. For instance, the Boeing Company uses laser sintering to build over 80 separate components for their F-18 military jet [58]. The motorsports industry uses additive manufacturing SLS techongy to manufacture items as diverse as electrical housings and aerodynamic elements [57]. An example of an SLS-manufactured exhaust manifold is shown in Figure 2.

1.2.1.3 The Advantages of Additive Manufacturing

AM has several key advantages that can make it more desirable than removal, or subtractive manufacturing technologies, such as computer numerical controlled (CNC) machining. These advantages are listed below [42]:

- **Design Intuition**: AM processes follow the concept of What You See Is What You Get (WYSIWYG); since AM generally begin with a 3-D CAD model, the design intent of the desired component is apparent. Furthermore, transition between the CAD model and the AM processes is automated and generally seamless. This eliminates confusion that may occur between the design and the manufacture of a component.

- **Process Planning**: Because AM processes are robust in nature, any part can generally be made in one step, regardless of size or complexity. On the other hand, removal manufacturing such as CNC machining requires lengthy planning and multiple machining steps. These steps also generally increase in number as part complexity increases. Also, a small change in the part design may change the entire process planning of the part. All these issues do not exist for AM processes.

- **Build Time**: Because part complexity and process planning are reduced in AM, many components can be built in a much smaller time frame than if they were machined using traditional processes.

- **Customizability**: AM processes allow for the quick manufacture of specific components without the need for a change of the manufacture process. Variations and customization of components that can significantly change the manufacturing process and process planning of traditional subtractive technologies do not affect the AM process at all; only the CAD model needs to be changed for the customization to be reflected in the final component. As a result of this property, AM processes have begun to be exclusively used in industries where high customization is a necessity.

- **Complexity**: One of the key disadvantages that traditional machining processes have is the inability to manufacture components of very high complexity. This drawback occurs because these machining processes generally have accessibility constraints that can prevent the access of certain regions in a part geometry. Because AM processes build layer-by-layer, these accessibility constraints do not exist. As a result, subtractive machining processes may need to manufacture multiple pieces and assemble a component that could otherwise be built as one part in additive manufacturing.

1.2.2 Design for Additive Manufacturing

The great potential of additive manufacturing removes nearly all limits in the manufacturing of parts. However, because of the enormous freedom conferred by AM, the challenge of AM is not the manufacturing of the part itself, but the design of component [56]. The principal challenge in the design for additive manufacturing (DFAM) is to develop new methods for exploring large, complex, design spaces [19]. These larger design spaces are brought on by an increased complexity in three areas: shape, material, and hierarchy [18]. Shape complexity encompasses the ability of AM to produce virtually any shape and geometry. Material complexity encompasses the ability of AM to process different materials on different layers of a structure, allowing complex material composition. Hierarchical complexity deals with the ability of AM to fabricate on multiple structural scales, from the microstructure to the part-scale macrostructure. This thesis focuses primarily on developing methods that enable designers to utilize the design space conferred by shape complexity. In particular, we focus on the design of cellular structures.

1.2.3 Cellular Structures

Cellular structures in the context of manufacturing are structures, such as foams, honeycombs, and lattices, that contain material only where it is needed for specific application. Advantages of these structures over their solid-body counterparts include good energy absorption characteristics, strong thermal and acoustic insulation properties, and, most importantly, a high strength to low mass correlation [25]. As a result, cellular structures have increasing application and use in industries where weight minimization is critical, such as the aerospace and racing industries [31]. Some examples of human-made cellular structures are shown in Figure 3.

Classification of cellular structures can be divided into two categories: those produced using stochastic processes and those designed using deterministic processes.

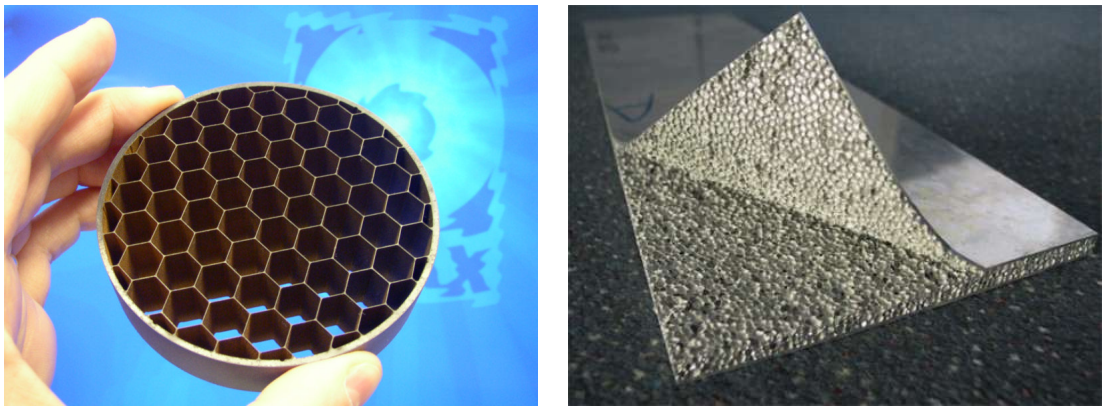

Figure 3: Examples of human-made cellular structures: a honeycomb lattice (left) and metallic foam (right) [1, 3].

Stochastic cellular structures are cellular structures generated with processes that cannot be entirely controlled, such as foaming. As a result, the topology of these structures cannot be explicitly defined. The principal advantage of these structures is that their design and manufacture is relatively autonomous, simple, and fast [25]. Stochastic cellular structures have strength that scales roughly to $\rho^{1.5}$, where ρ is the volumetric density of the structure's material [21].

Deterministic cellular structures, on the other hand, are structures that are designed with lattices specifically meant to support specific loading and boundary conditions. In their research, Wallach and Gibson propose that, because their lattices are highly specialized, deterministic cellular structures will have higher strength than stochastic cellular structures [50]. In their work, Deshpande et al. found confirm this statement, determining that the strength of deterministic cellular structures scale to their volumetric density, ρ [21]. Therefore, a designed lattice structure with a volumetric density of $\rho = 0.1$ will be roughly three times stronger than its stochastic counterpart. It is theorized that this difference in strength occurs because stochastic cellular structures are dominated primarily by bending whereas deterministic structures are dominated by compression and tension, thus resulting in higher failure stresses [20]. Because designed cellular structure have such a significant strength advantage, much

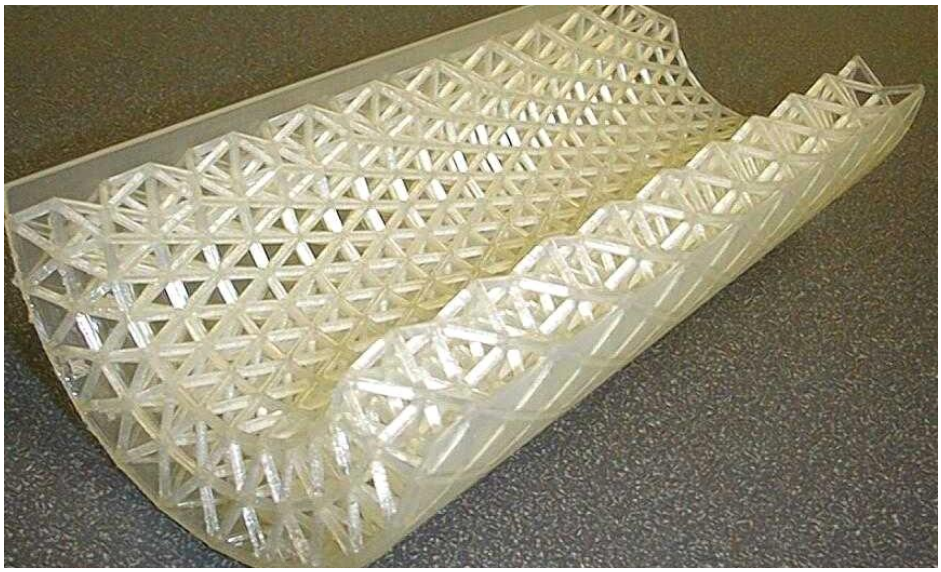

Figure 4: Example of a meso-scale truss structure. The structure pictured is roughly 10 in long.

research has gone into developing synthesis methods for these structures.

1.2.4 Meso-Scale Truss Structures

In this work, the particular focus will be on a specific subset of cellular structures: mesoscale truss structures (MSTS)–structures with strut diameters in the range of 0.1 to 10 mm and strut lengths on the order of centimeters. An example of a meso-scale truss structure is shown in Figure 4. It is important to note that Figure 4 contains a uniformly-generated, or stochastically generated, lattice. The focus of this work, on the other hand, will be deterministic MSTS.

1.3 Motivation

1.3.1 Design of Meso-Scale Truss Structures

The advantages conferred by deterministic cellular structures, and in particular meso-scale truss structures, make them highly desirable as a design option for components that require high strength and low weight. However, although the introduction of AM has allowed these structures to be manufactured with relative ease, their inherent

design complexity limits their use in industry. Depending on their size and scale, components designed with MSTS can contain upwards of hundreds of thousands of individual struts. If just the diameter of each strut is considered a design variable, then the design of MSTS will have as many design variables as struts. If the problem is expanded to consider the lattice topology as well, then the number of design variables grows even larger. This large number of design variables poses the main prohibitive barrier to the design and manufacture of MSTS [18].

In order to address the large quantity of design variables posed by MSTS, designers currently use synthesis methods that utilize search heuristics specializing in the optimization of a large number of design variables. Although these methods are documented to have success, they suffer from three key drawbacks:

- **Incorrect/Non-Optimal Solutions**: The large design spaces present in the design of MSTS will often contain several local minima. The presence of these local minima force the optimization problem to be highly dependent on the starting point of optimization. Since a good starting point is usually impossible to determine, optimization routines will often converge to a local solution rather than the global solution.

- **Repeatability**: Most multi-variable optimization algorithms, such as genetic algorithms, are highly stochastic. Due to the probabilistic nature of these algorithms, design methods using these algorithms will generally not return identical design results, even when provided the exact same initial design conditions. In industries where consistency is desired, these methods will not only reduce the repeatability of design results, but may reduce their performance as well.

- **High Computational Complexity/Long Design Times**: The design time

of multi-variable optimization routines often scale exponentially with the number of design variables. For truss structures with struts numbering in the hundreds, these optimizations may converge, but will be the main bottleneck in the design of truss structure. For structures that are larger or considerably more complex ($\geq$1000 struts), these methods will either converge within an infeasible time frame or simply not converge at all.

In order for MSTS, and deterministic cellular structures in general, to become a feasible design principle for designers, the issue of topological optimization must be thoroughly addressed.

1.3.2 The Unit-Cell Approach

Since it is known that the design of MSTS is bottlenecked by the need for topological optimization, designers have devoted much research directly into either improving these optimization methods or developing more efficient methods. However, these direct considerations of optimization may only alleviate some of the issues plaguing topological optimization rather than eliminate them.

In his research, Graf presented a novel, alternative approach to design of deterministic cellular structures [27]. The key feature of this method is that it attempts to completely avoid the need for any topological or shape optimization in the design of MSTS. In particular, Graf proposed a "unit-cell" approach to the design of MSTS: one that uses alternative sources of information in lieu of topological optimization.

1.3.2.1 Approach

Topological optimization of truss structures can be considered to consist of two fundamental tasks: the determination of the loading distribution of a specific loading condition in a structure and then the determination of the topology required to support this load distribution. If topological optimization is to be bypassed, then the

information required to accomplish these two functions must be derived from other sources of information.

The unit-cell approach proposes that the first function, the stress distribution, can be derived from a finite element stress analysis of the target truss structure as a solid-body. The second function, topology generation, can be accomplished by dividing the target truss structure into local, uniformly shaped regions, or "unit-cells." By looking at these regions individually and comparing them with the stress distribution from the solid body finite element analysis, a topology can be determined for that region. This localized topology is designated by scanning a library of highly optimized configurations, or "unit-cell library," selecting the configuration best-suited for the given stress condition, and then assigning that configuration to the region. Once all the regions are mapped, a topology can be developed. It is important to note that lattice topologies generated using the unit-cell approach are normalized such that diameters in the lattice are valued between zero and one. In order for the normalized topologies to be specialized for a particular loading or boundary condition, real diameter values must be assigned to these topologies based on the loading and boundary conditions of the truss structure. In particular, two specific diameter values need to be determined in order for all remaining diameters to be assigned: the smallest diameter in the structure, D_{min}, and the largest diameter in the structure, D_{max}. Once these values are determined, the remaining diameters in the topology can be appropriately sized and the truss structure will be completed.

1.3.2.2 Implementation

In his work, Graf developed a rough design method, termed the "Size, Matching, and Scaling," or SMS, method for the design of mesoscale truss structures. This method utilized the unit-cell approach to develop lattice topologies and implemented post-processing steps to assign real diameter values against the supplied boundary

conditions [27]. A more detailed description of the method and its results is provided in Chapter 2.

1.3.2.3 Drawbacks

Graf's SMS method was highly successful in generating topologies for MSTS. However, the implementation of this method contained two key design issues that limited its use. Both these issues must be addressed in order for the unit-cell approach to be a viable alternative for designers.

The first critical issue with the unit-cell approach is the utilization of the lattice topology after it has been generated, particularly in regards to the determination of diameter values. Graf's SMS method lacked a systematic step for assigning optimal diameter values to lattice topologies. In order to avoid the need for optimization, he used a critical, untested assumption to simplify the diameter determination process. He then performed a manual search of the design space to determine the correct diameter values.

The second issue revolves around the use and implementation of the library of pre-configured unit-cells, or "unit-cell library." In particular, Graf's implementation contains only one unit-cell configuration. With just one entry in the library, Graf was able to prove that the unit-cell approach is effective in generating topologies. However, without at least one other entry in the library, the unit-cell approach cannot compare entries to determine the best possible solution. This lack of depth not only limits the potential of the unit-cell approach, but also over-simplifies the topological mapping and selection of unit-cells to the truss structure.

1.4 Research Questions and Hypotheses

The original SMS method was developed specifically to remove the need for optimization in the design of MSTS. However, because optimization was avoided, the method

could not generate optimal values of D_{min} and D_{max} without performing an exhaustive, manual search of both D_{min} and D_{max}. This brute force search of the design space proved to be the principal drawback in the SMS method. This drawback forms the basis of the first research question:

Research Question 1: Can an optimization method for the design of mesoscale truss structures be developed to determine strut diameters for topologies designed using the unit-cell approach?

It is believed that optimization of diameter values cannot be entirely avoided in the design of MSTS. If, however, the main advantages of the unit-cell approach are used in *conjunction* with optimization rather than in *competition* with it, then it may be possible to develop a truly systematic design method that can generate MSTS topologies without the need for the optimization of several thousand strut diameter values. Instead, only two critical diameter values need be optimized in order for all remaining diameters to be assigned: D_{min} and D_{max}. Such a method will not only be significantly less computationally complex than current optimization methods, but will also be able to generate MSTS without the need for a manual search of diameter values. This concept gives rise to the proposed answer to the first research question:

Hypothesis 1: By utilizing the unit-cell approach and combining it with a constrained optimization of two diameter values: a minimum allowable diameter and a maximum allowable diameter, against volume and stiffness constraints, a systematic design method can be developed for the design of mesoscale truss structures. By exploring various optimization approaches and selecting the best method, design time can be minimized and structural performance can be maximized.

In order to properly test and validate Hypothesis 1, the following tasks will be completed:

- A modified Size, Matching, and Scaling (SMS) method will be developed combining the unit-cell approach with optimization methods. The first portion of the SMS method will utilize the primary driving concepts of the unit-cell approach to generate a normalized topology for MSTS. The second portion of the SMS method will utilize optimization routines to determine the minimum and maximum diameter values necessary to optimize structure volume and stiffness. In particular, an additional step will be added to the SMS method. In this step, the critical diameters values will be determined using different two-variable optimization methods.

- The modified SMS method will be tested using example problems of varying size and complexity in order to validate the method in two and three dimensions. Two of the example problems will be repeated examples from the previous iteration of the SMS method. The results from these two examples will be compared to results from previous research in order to verify accuracy.

- For each example problem, different optimization approaches will be used to determine the minimum and maximum diameter values for the target structure. The results from these methods will be compared to determine the approach with the best performance.

- In addition to the proposed optimization methods, a manual grid-search will be performed similar to the method that was used originally in the previous SMS method. The results from this grid-search will be compared to results from the proposed optimizations to determine the difference in both design time and structural performance

With the proposed Size, Matching, and Scaling method, large-scale optimization can effectively be reduced into an optimization of just two variables. However, the possibility of further reducing the optimization problem may exist. In previous research, Graf used an untested assumption in order to simplify the diameter determination process. While performing an exhaustive search of all possible D_{min} and D_{max} for a simple MSTS example, Graf noted that, for a specific target volume, a truss structure designed using the unit-cell approach would have the highest structural stiffness when the minimum diameter value was roughly 28% of the maximum diameter value. When repeated with other target volumes, this 28% value appeared to hold true. Graf therefore used the assumption that the best structural performance of a MSTS designed using the unit-cell approach has the property,

$$D_{min} = 0.28 \times D_{max} \tag{1}$$

The consequence of this assumption was that the minimum and maximum diameters were no longer independent of one another. Therefore, instead of determining two diameters, only one diameter, D_{max}, need be determined. Since only one design variable was necessary, Graf simply performed an exhaustive, iterative search of all possible values of D_{max}, selecting manually the value that would best satisfy the desired volume while maintaining the highest possible structural stiffness.

Although very useful in implementation, the assumption suffered from one major flaw: it was made without proper verification. The assumption was tested on a very small subset of design problems and was not compared to any optimization routines to determine whether the values returned were indeed the best possible solutions. Therefore, until the assumption is verified, it should not be used. However, the discovery made by Graf does present the possibility of a relationship existing between the minimum and maximum diameters. In particular, the research question can be asked:

Research Question 2: Can the two-variable optimization proposed in Hypothesis 1 be simplified in order to decrease analysis time?

It is believed that Equation (1) can be validated against optimization and that a relationship can be found between D_{min} and D_{max} at or near the 28% value discovered by Graf. This assumption can then be extended to any truss structure designed using the SMS method and can simplify and subsequently speed up the diameter determination process. This belief is the key component of the answer to the second research question:

Hypothesis 2: By exploring and analyzing the optimal minimum and maximum diameter values for meso-scale truss structures designed using the Size, Matching, and Scaling method, a direct relationship between these two values can be determined and exploited. This relationship will allow for one of the two diameter values to be expressed as a function of the other. Consequently, the two-variable minimizations outlined in Hypothesis 1 can be simplified to a one-variable minimization problem, thereby reducing overall design time.

To validate this second hypothesis, both the one-variable optimization and the two-variable optimizations proposed in Hypothesis 1 must be tested and then compared. The following tasks will be completed:

- For each of the example problems used to test the SMS method, the two-variable optimization routines outlined in Hypothesis 1 will be tested. The design times and resultant diameter values will be recorded.
- Concurrent with the two-variable optimizations, a one-variable optimization will be conducted using the 28% value assumed by Graf in order to measure the design time using this method and the accuracy of its results.

- The values of the minimum and maximum diameters returned by both the 28% assumption and the two-variable optimizations will be compared to determine whether a relationship between them exists and whether this relationship is at or near the 28% estimated by Graf.

- The design times of the 28% assumption will be compared with those of the two-variable optimizations in order to assess if there is a reduced design time and whether the reduction is significant.

The final research question is related to the unit-cell library. In the original SMS method, the unit-cell library that was used contained only one optimized unit-cell entry and provided the bare minimum required for the unit-cell approach to successfully generate a topology.

However, in order for the unit-cell library to be fully utilized, it must contain several unit-cell configurations. The SMS method can then scan these entries and select the best possible configuration for a given stress concentration. This larger selection profile should ultimately improve the performance of structures designed using the SMS method. However, it is possible that the SMS method may select the same unit-cell configuration regardless of the unit-cell library entries. Furthermore, a larger unit-cell library may result in slower design times. For each additional entry in the unit-cell library, the SMS method must scan this extra entry once for each unit-cell region in a truss structure. Therefore, the design time can grow exponentially for both large design problems and a large unit-cell library. Therefore, it is unknown whether an expanded library will have an overall positive or negative impact on the methodology. This uncertainty brings about the third research question:

Research Question 3: Will the expansion of the unit-cell library to include additional unit-cell configurations improve the performance of structures designed using the SMS method? If so, will the added benefit justify an increased overall design time?

It is believed that the true strength of the unit-cell library arises from a methodology's ability to compare multiple unit-cell configurations from the library and select the best possible configuration. Therefore, in general, a larger unit-cell library should allow the SMS method to locate better unit-cells for any given design scenario. Although a larger library and more expansive mapping algorithm will result in an increased design time, it is believed that the additional design time will be outweighed by the added benefit conferred by the addition of unit-cell configurations, particularly configurations that are well-documented and thoroughly tested. This idea is the basis for the third and final hypothesis:

Hypothesis 3: The addition of unit-cell configurations, such as the Cantley and octet configurations, will provide the SMS method with more options for the generation of the lattice topology. This, in turn, will allow for the placement of unit-cell structures that are better-suited for specific loading conditions, thereby improving structural stiffness. Although the design time will be slightly increased for a larger library, this increased time will be outweighed but the benefit conferred by improved structural performance.

Hypothesis 3 will be tested in the following manner:

- Two versions of the unit-cell library will be created. The first unit-cell library will be identical to the library used by the unit-cell approach and will contain

just one unit-cell configuration. The second unit-cell library will be filled with additional unit-cell configurations, particularly those that are well-documented in literature, such as the Cantley and octet trusses.

- Examples will be explored using the first iteration of the unit-cell library. The topologies generated using this library will only have one unit-cell type and will thus have a fairly homogeneous topology.

- The same examples will then be solved using the larger library. The topologies generated using this second library will be investigated to determine whether there is a topological difference. If there is a difference in the topologies of the structures, both the design time and structural performance of the two resultant topologies will be compared and assessed to determine whether there is an improvement in performance.

The three research questions and hypothesis outlined above compose the main arguments of this thesis and provide the framework for this research; This thesis is written with the mindset of answering these research questions.

1.5 Thesis Organization

1.5.1 Thesis Chapters

The remaining chapters of this thesis are organized to best present the research conducted. They are summarized below:

- In Chapter 2, a literature survey will be performed covering all research relevant to the SMS method. This survey will include a review of previous research in the design and analysis of cellular structures. It will also include a review of some topological optimization algorithms. Finally, it will review the driving research behind the SMS method and the unit-cell approach. After the review has been completed, a gap analysis will be conducted on the existing research.

- In Chapter 3, the modified SMS method will be presented in its entirety. This includes a problem formulation for the method and a detail presentation of each of the steps of method. Additionally, the primary deliverables of each of these steps and the assumptions taken in each step will provided. A comparison of the modified method and the original method will also be provided, including limitations and guidelines for use.

- In Chapter 4, the modified unit-cell library will be outlined. This will include a presentation of each entry in the library, a description of the mapping and selection process for the new library, and an outline of the optimization process for the unit-cell configurations in the unit-cell library.

- In Chapter 5, the SMS method will be tested against 2-D and 3-D examples of varying complexity in order validate the method and compare design results. These examples will attempt to validate or refute the three hypotheses proposed in this chapter.

- In Chapter 6, the research results will be summarized and conclusions will be drawn. Future work for the method will be outlined.

1.5.2 Connection Between Thesis Chapters and Research Questions

Table 1 presents the research questions and their relation to the remaining chapters of the thesis. As can be seen from Table 1, the bulk of the research questions will be answered in Chapter 5: Design Examples.

Table 1: Correlation between research questions and thesis chapters

	Chapter 2: Literature Review	**Chapter 3: The Modified SMS Method**	**Chapter 4: The Modified Unit-Cell Library**	**Chapter 5: Example Problems**	**Chapter 6: Discussion and Conclusions**
Hypothesis 1: The optimal minimum and maximum diameters in truss structures designed using can be determined systematically using constrained, multivariable optimization.		✓		✓	
Hypothesis 2: A direct relationship between the minimum and maximum diameters can be determined. Exploiting this relationship can reduce the design time for the SMS method.		✓		✓	
Hypothesis 3: The expansion of the unit-cell library will provide the SMS method with more options for topology generation and, consequently, will improve structural performance.			✓	✓	

CHAPTER II

LITERATURE REVIEW

In this chapter, a literature review of research relevant to the SMS method will be conducted. The review is divided into six separate categories. Section 2.1 outlines methods for analyzing cellular, and in particular, truss structures. Section 2.2 outlines current approaches to lattice design in cellular structures. Section 2.3 outlines some of the algorithms used in the design methods of Section 2.2. This review will set the groundwork for the material in Section 2.4: the original SMS method and 2.5 a description of some documented unit-cells to be utilized in the unit-cell library. Finally, in Section 2.6, gaps in the original SMS method will be outlined.

2.1 Methods for Lattice Structure Analysis

The critical task in the analysis of cellular structures is the determination of the assumptions and limitations that can be utilized in order to develop accurate models of these cellular structures. Current analysis methods for cellular structures are developed for the specific analysis of certain types of cellular structures. For instance, Wang and McDowell have developed a comprehensive review of the analytical modelling, mechanics, and characteristics of metal honeycombs [51]. Asbhy et al. have performed extensive research on the analysis and design of metal foams [10]. However, the methods presented in this section focus primarily on the analysis of truss structures as a subset of cellular structures. A portion of these analyses are provided.

The analysis of truss structures initially used the assumption that struts in a lattice structure only undergo axial loading and that joints are pin-pin joints. In their work, Wallach and Gibson use this assumption to theoretically analyze sheets of lattices under axial loading conditions [50]. When compared with experimental

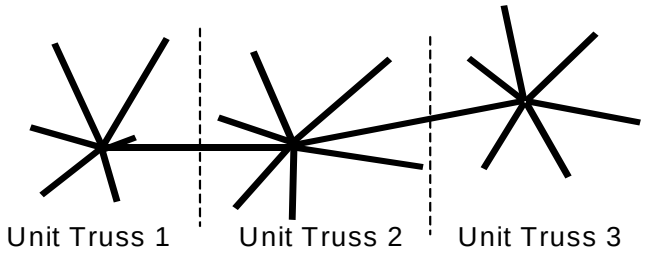

Figure 5: The unit-cell approach to lattice analysis

results, this theoretical framework returned comparable results, with percent errors ranging from between 3% and 27%. Chiras et al. have extended this assumption to lattice sheets undergoing bending and shear loading [17].

In their research, Johnston et al. propose a more general analytical model of lattice behavior by considering an assumption of beam-like characteristics for lattice struts. The model uses vertices and the set of half-struts connecting these vertices and lumps them together into discrete "unit-trusses" [31]. These elements are then analyzed using a method similar to the finite-element approach. Wang et al. have applied this unit-truss approach successfully to lattice design [52, 55]. The unit-truss representation is shown in Figure 5.

2.2 Methods for Lattice Design

In this section, an overview of current synthesis methods for cellular structures is provided.

2.2.1 Size, Shape, and Topological Design

Design synthesis methods for cellular materials can be divided into three different types of optimization tasks: shape, size, and topological optimization. Before these three optimizations are discussed, it should be noted that these terms can have different definitions depending on the research and context in question. It is also important to note that the three terms are becoming increasingly hard to decipher in research

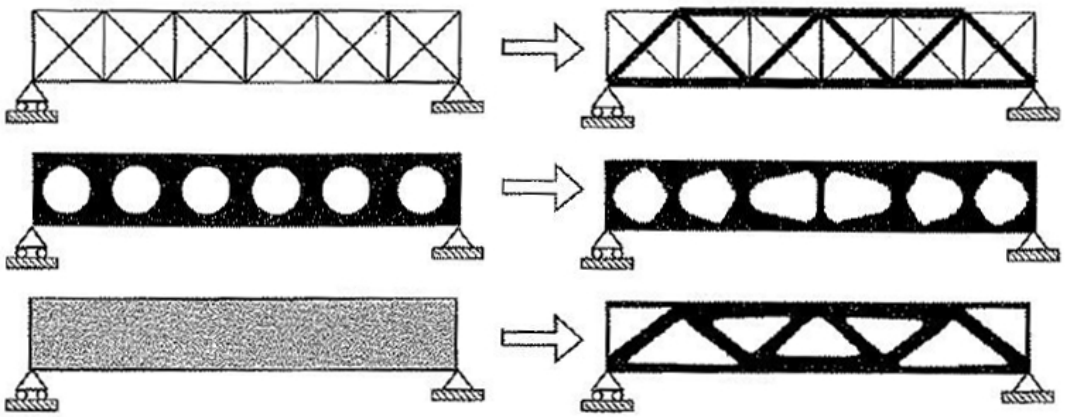

Figure 6: An interpretation of size (top), shape (middle), and topology (bottom) optimization [13].

[7]. The definitions that this research uses follow those from Bendsøe and Sigmund [13].

Shape optimization can be defined as the development of the geometric dimensions of a body [38, 9]. Methods for shape optimization are generally performed using the same process: through the use of control vertices of parameteric curves and surfaces. Size optimization, on the other hand, can be the defined as the determination of individual cross-sectional areas of struts [11]. Like shape optimizationn, Size optimization is performed using the same basic method, with feature dimensions as design variables. Topological optimization, as defined by Rozvany, can be defined as the determination of the spatial sequence or connectivity of members [43]. It contains both elements of both size and shape optimization. In this research, size and shape optimization will not be discussed in detail. Instead "topological optimization" will be the primary term used for the design and optimization of mesoscale lattice structures. Figure 6 shows Bendsøe and Sigmund's interpretation of size, shape, and topology optimization [13].

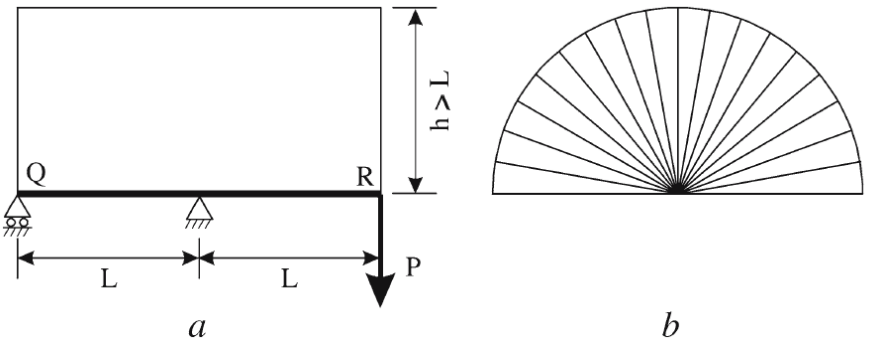

Figure 7: A truss designed using the Michell approach.

2.2.2 The Michell Analytical Approach

Topological design methods for cellular structures date as far back as 1904, when George Michell theorized the existence of an analytically optimum truss structure for any given loading condition [35]. An example of a Michell truss is shown in Figure 7.

The Michell analytical formulation became the base for nearly all analytical approaches to truss design. Since then, several extensions of the Michell truss have been developed, including those encompassing multi-material design, non-linear behavior, and for structures containing pre-defined lattices [22, 47, 44]. However, the Michell approach to truss design does not lend itself to well to manufacture and is generally restricted to two-dimensional scenarios [61]. It is therefore very limited in application.

2.2.3 Optimization Approaches

Since the development of the Michell approach to truss design, two broad topological optimization approaches have been introduced: the homogenization (continuum) approach and ground truss (discrete) approach. It is important to note that topology optimization is intrinsically a discrete optimization problem [49]. However, because discrete optimization can be highly unstable, both approaches use continuous design variables to characterize the discrete problem [60].

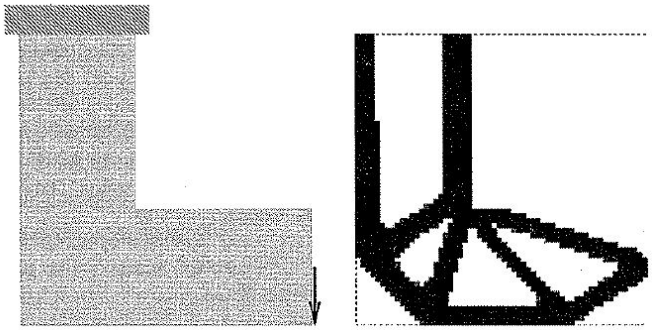

Figure 8: An example of the homogenization approach to lattice design [13].

2.2.3.1 The Homogenization Approach

The homogenization approach uses a continuum mechanics approach to topology design [12]. In the homogenization approach, a representation based on composite materials is used. A material density function, ρ, models an infinite number of periodically distributed microstructures with small holes, or voids. From the macroscopic perspective these voids allow any point in a structure to be fully occupied, partially occupied, or unoccupied by a material; areas in the structure that have densities at or near a value of 1 are filled with material while areas with densities near zero contain no material. Other microstructure representations have been developed as well, including the micro-microstructure, rank laminate composite, and free mixture representations [12]. An example of the homogenization approach is shown in Figure 8.

2.2.3.2 The Ground-Truss Approach

In the ground truss approach, the optimum topology is a subset of a ground truss: a complete graph of all the struts among all the nodes in a cellular structure. Here, the cross-sections of the truss members become the design variables of the optimization problem. These cross-sections are sized against the specific loading conditions of the structure. Cross-sections that tend toward values of zero are removed from the structure to obtain the optimum [23]. It is important to note that the ground-truss

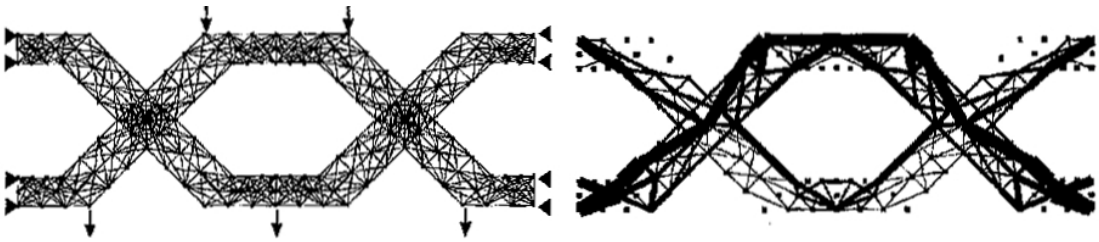

Figure 9: An example of the ground truss approach to lattice design [13].

approach is inherently a sizing optimization problem. However, the problem becomes a topological optimization problem when struts are removed from the structure [14]. For the ground truss approach, the design problem for a typical single load situation is formulated as minimizing compliance and volume subject to static equilibrium and stress constraints [9]. Further research has gone into expanding the ground-truss approach to include the nodes of the ground structure as design variables in addition to the cross-sectional areas of the struts [7, 59]. This is done to reduce the dependency of the ground-truss approach on the initial lattice configuration [7]. An example of the ground truss approach is shown in Figure 9.

2.2.3.3 Comparison Between the Ground-Truss and Homogenization Approaches

Both approaches to topology design have their own sets of advantages and disadvantages. For instance, the homogenization approach allows for true topology optimization without the need to remesh the finite-element model [12]. Furthermore, implementation of optimization routines may be simpler [48]. However, because the homogenization approach is a continuum approach and topology optimization is discrete problem, ambiguities can arise in the definition of material allocation. Research has been conducted to alleviate this issue, but the problem has not been completely solved [28, 62].

The ground structure approach, on the other hand, is a more discrete approach and does not suffer from the ambiguity problems of the homogenization approach. However, the ground structure approach is highly dependent on the starting lattice

topology of the structure [7]. As a result, this approach is generally faster than the homogenization approach, but cannot generate results as accurate as the homogenization method [53].

2.3 Multi-variable Optimization Algorithms

Regardless of whether a continuum or discrete approach is used for the design of cellular structures, an optimization still must be conducted. Optimization algorithms vary widely depending on the type of design problem and task. For instance, Rao recently divided optimization techniques into three categories: *mathematical programming techniques*, *stochastic process techniques*, and *statistical methods* [40]. However, Rao also recognizes that new optimization techniques cannot be classified cleanly into any of these three categories and has specified a new class of techniques: modern and *non-traditional optimization techniques*. This classification incorporates algorithms such as genetic algorithms, particle swarm optimization, and neural networks [40]. However, the optimization algorithms that are of particular interest in the topological optimization of truss structures are those that are specialized to solve design spaces that are nonlinear and constrained. These optimization algorithms can be classified into two broad categories: indirect methods and direct methods [16, 45]. Direct methods, such as mathematical programming, generally require some form of gradient calculation. Although these methods are fairly robust, they can also be time-consuming because the gradient calculation is inherently complex [45]. Indirect methods, on the other hand, do not use gradients to determine optimality. Instead, the use other criteria to guide optimization. For instance, a typical indirect approach may use "penalty-functions" that make the objective function less optimal as the solution approaches a constraint [16]. The Michell truss, which requires that all struts in compression and tension have identical stress, is also an example of an indirect optimality criterion [61]. In many cases, these indirect optimality criterion, such as

uniform stress, are equivalent to more direct criterion, such as compliance, and as such provide the same solution [38].

In this research, three particular optimization algorithms are either discussed or utilized: Particle Swarm Optimization (PSO), Least-Squares Minimization, and Active-set programming.

2.3.1 Particle Swarm Optimization

Particle swarm optimization (PSO) is a stochastic optimization method that can be either an indirect or direct method, depending on the problem definition. It is an extension of genetic algorithms (GA) that specifically performs parametric and limited topological optimization of structures and compliant mechanisms. The driving concept of PSO is the movement of birds in a flock, where individuals adjust their movement according to their experience and other individuals' experiences in the flock during search for food [32]. The optimization is considered stochastic because the behavior of the swarm is governed by psuedo-random numbers used to create initial values for the swarm. It combines local search with global search, and enables cooperative behavior among individuals, as well as the competition modelled in GA. Hence, PSO often converges more quickly than GA and is less sensitive to local minima [53].It is important to note that PSO was not used directly in this research, but was used in previous research regarding the SMS method [27].

2.3.2 Least-Squares Minimization

In least-squares minimization the achievement of target values of goals can be formulated as a regression problem, which has similarities to formulations in inverse design and parameter estimation [36]. For cellular material design, the number of design variables far exceeds the number of objectives, which is similar to fitting a low order polynomial model to a large data set. In particular, some iterative methods have been developed to solve nonlinear problems, such as the Gauss-Newton and

Levenburg-Marquardt methods [39]. In this research, the Levenburg-Marquardt (LM) is used because of its robustness and reliability in non-linear problems. In this research, the MATLAB nonlinear least-squares solver *lsqnonlin* is used as the primary least-squares solver.

2.3.3 Active-Set

The active-set algorithm is a mathematical programming algorithm that is particularly well-suited for the optimization of large-scale optimization problems [26]. As the name suggests, active-set methods aim to predict which of the inequality constraints are active in a given minimization function. By determining which set of constraints are active and which are not, this algorithm can reduce complexity and, subsequently, optimization time. In this research, the MATLAB function, *fmincon* is used as the active-set solver. In particular, the implementation of the active-set method in MATLAB is coupled with Sequential Quadratic Programming (SQP) methods, which are highly efficient non-linear programming methods, to solve the quadratic programming problem at every iteration [6]. The implementation also uses solutions to the Karush-Kuhn-Tucker (KKT) equations in order to enforce active constraints.

2.3.4 Other Topological Optimization Algorithms

In addition to the three algorithms listed above, other synthesis methods have been explored. Recently, an exploratory framework was developed that can minimize the risk of structural failure by integrating a topology optimization method and a reliability assessment technique [37]. In this method, a Genetic Algorithm (GA) method is used as the optimization routine and Latin hypercube sampling is conducted for the estimation of reliability constraints. In general, GA's have become more widely used in the synthesis of structural components because their evolutionary nature is well suited for exploring complex design spaces typical to cellular materials [56].

2.4 The Original SMS Method

Although the algorithms used in the design of the mesoscale truss structures differ greatly, these methods all share a common similarity: they all perform some form of a multivariable, topological optimization. Depending on the size and complexity of the structure and the design parameters, the number of design variables used in the topological optimization can be prohibitively large. For instance, it is not uncommon for structures designed using the ground truss approach to have design variables numbering in the hundreds of thousands. Consequently, these topological optimizations can be computationally expensive and time-consuming and are generally the primary bottleneck in the design of truss structures. These optimizations provide the primary motivation for the development of the SMS method. In particular, the SMS method attempted to answer the research question: *Can a design method for mesoscale truss structures be developed that does not require a time-consuming, global optimization of diameter values?*

2.4.1 Approach

The original Size, Matching, and Scaling method attempted to remove the need for topological optimization by combining information from two different sources: a finite-element analysis and a library of truss configurations specialized for specific loading conditions, termed the "unit-cell library." From the solid-body FEA, the SMS method would find the relative stress distribution throughout the structure. Using this stress distribution values, the method would then use the unit-cell library to assign a lattice topology. The original SMS methodology is shown in Figure 10.

The library that was used in this iteration of the SMS method contained only one entry: a cube containing struts along each edge and diagonal trusses connecting the corners of each face of the cube. This unit-cell configuration is shown in Figure 11. The configuration shown in Figure 11 was then optimized intuitively by Graf for 6

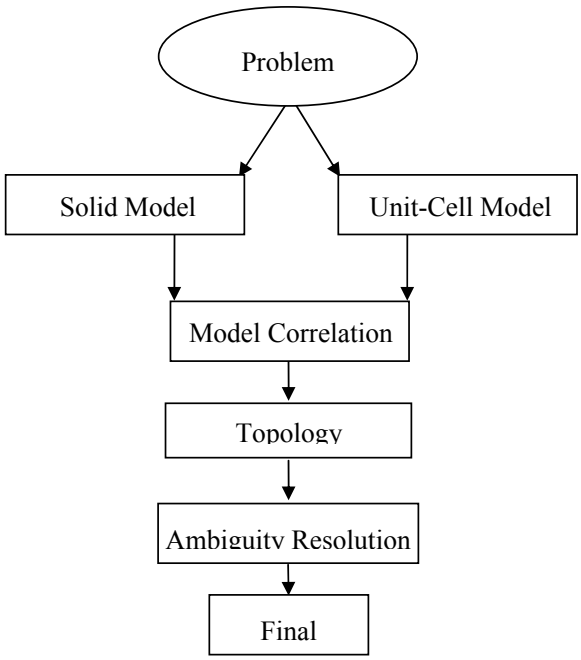

Figure 10: The original SMS method [27].

stress directions and placed into the unit-cell library. The original unit-cell library that was used is shown in Figure 12.

2.4.2 Results

This original implementation was validated against two multi-variable topological optimization routines utilizing the ground truss approach: particle swarm optimization (PSO) and least-squares minimization (LM) [27]. When compared to the PSO and LM optimization routines, the SMS method was able to formulate a design considerably faster than either of the optimization methods. When the performance results between the PSO, LM, and SMS methods were compared, the results were highly comparable. This research was ultimately able to validate the SMS method as a viable alternative to optimization.

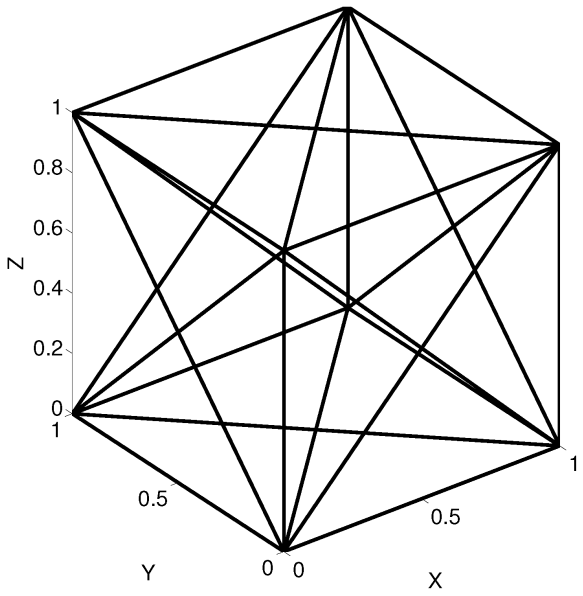

Figure 11: The crossed configuration used in the original unit-cell library [27].

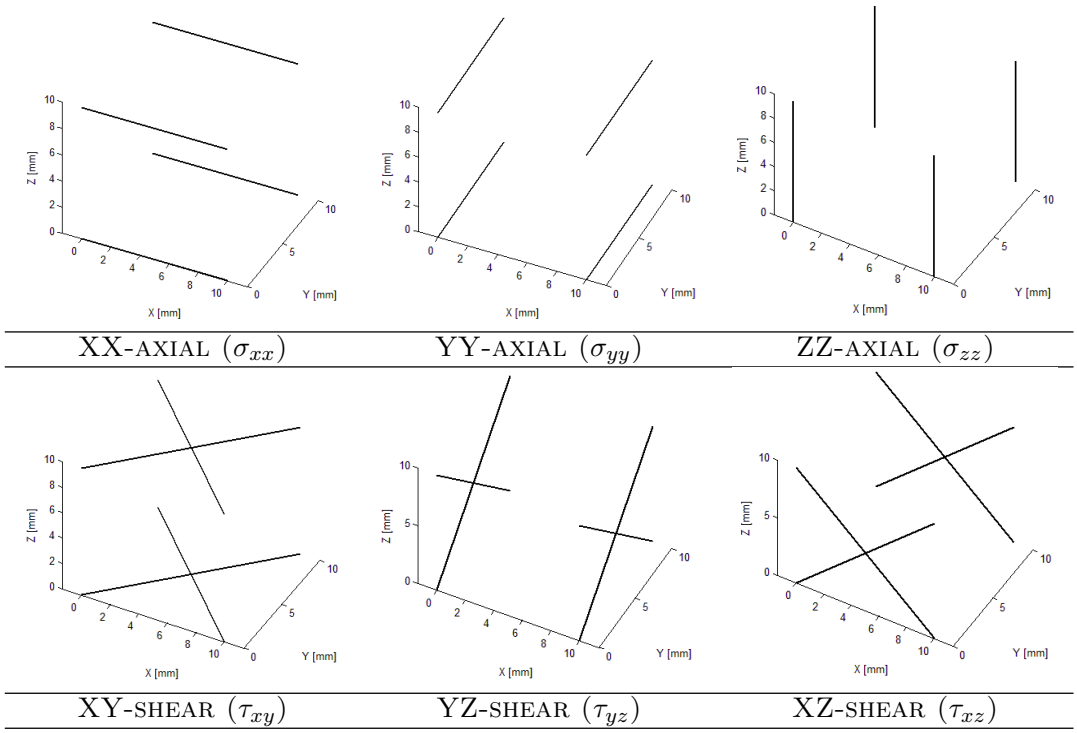

Figure 12: The original unit-cell library [27].

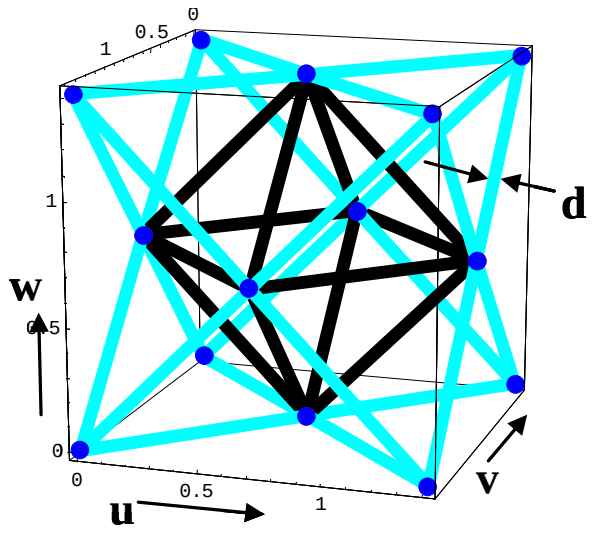

Figure 13: The octet configuration.

2.5 Unit-Cells

In addition to the "crossed" unit-cell configuration outlined by Graf, other unit-cell configurations have been researched. These configurations are outlined in this section.

2.5.1 The Octet Configuration

The octet configuration, shown in Figure 13, is a configuration that attempts to prevent the elastic buckling of struts. By eliminating failure due to bending, the structure can then allow the strength and structure of the truss to be stretching-dominated. Analytical and FE results have indicated that this structure performs favorably against metallic foams [20].

2.5.2 The Cantley Configuration

The Cantley configuration, developed by Richard Cantley, is "a molded plastic truss work includ[ing] an upper grid and a lower grid, with a plurality of interconnecting members interconnecting the grids." The configuration, shown in Figure 14, is specifically designed to be created in a two-part plastic mold [15]. In particular, the Cantley

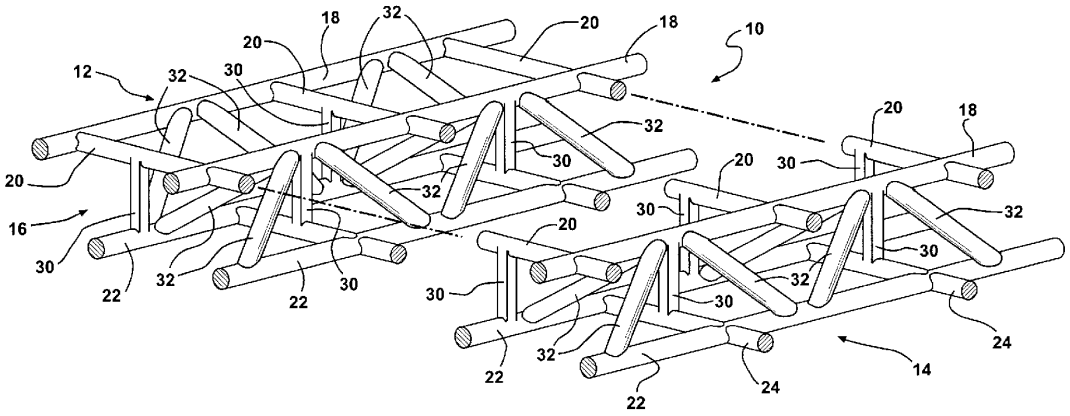

Figure 14: The Cantley configuration.

features a single configuration that can be repeated to create a lattice sheet.

2.6 Gap Analysis

Although the SMS approach to truss design was very promising, the actual method developed was highly conceptual and suffered from gaps in implementation. In particular, two key issues needed to be further explored:

1. The SMS method lacked a true systematic methodology. In particular, the allocation of diameter values to lattice topologies lacked a robust and repeatable implementation. Additionally, the assumptions driving the allocation of diameter values were not sufficiently explored.

2. The unit-cell library utilized by the method contained only one unit-cell configuration. In order to maximize usage of the unit-cell library, more than one entry must exist in the library. Furthermore, the unit-cell selection process must be re-evaluated in order to select the best configuration for a given stress condition.

These two issues form the primary motivation for the modification and improvement of the SMS method. In order for the method to be a viable alternative for the design of truss structures, these issues must be addressed.

2.7 Summary

In this chapter, research related to the design of mesoscale truss structures and the Size, Matching, and Scaling method was presented. Through this review, it can be seen that the problem of design and optimization cellular structures is not a new problem: much research has been conducted on the issue as far back as the turn of the last century. Several approaches, both analytical and optimization-based, have been presented and heavily studied. Several individual algorithms well-suited for the optimization of the large design-spaces present in the design of mesoscale lattice structures have been presented. These algorithms can range from traditional mathematical programming methods such as least-squares minimization and active-set optimization, to modern, non-traditional means, such as particle swarm optimization and genetic algorithms.

However, regardless of the optimization method or approach used, optimization is still required. It can be seen that this optimization is by far the most time-consuming and complex part of the design process. In his research, Graf attempted to circumvent the need for optimization by using a novel approach, the "unit-cell approach," for the design of mesoscale lattice structures. The method that was developed, the original "Size, Matching, and Scaling" method, showed highly promising results: stiffness and strength characteristics were comparable while design time was drastically reduced.

However, the method suffered from key drawbacks relating to the implementation of the method. In particular, the determination of diameter values lacked a reliable and systematic method. Furthermore, the library that was utilized in the generation of lattice topologies was not sufficiently explored. In order for the Size, Matching, and Scaling method to become a viable alternative for designers, these issues must be addressed. As a result, these issues form the key components of the research questions outlined in Chapter 1. In order to address these issues, both the SMS method and the unit-cell library must be modified. In the following Chapters 3 and 4, the method

and library will be modified and tested in order to address the research questions outlined in Chapter 1.

CHAPTER III

THE MODIFIED SMS METHOD

In this section, the improved Size, Matching, and Scaling Method will be presented. The modified method attempts to resolve technical and conceptual issues that arose during the first implementation of the method. In particular, this design method attempts to utilize the unique features of the unit-cell approach to generate a normalized structural topology. By combining this topology with an optimization of the minimum and maximum diameter values of the structure, the SMS method will be able to design successfully an MSTS without the need for a rigorous, global topological optimization.

3.1 Problem Formulation

In order to develop the SMS method, the inputs, outputs, constraints, and objectives must all be properly elicited. However, before this process can occur, the general design problem for mesoscale truss structures must first be formulated. This formulation can then be adapted for the specific characteristics of the SMS method.

3.1.1 General Problem Formulation

In the design of meso-scale truss structures, each design problem will differ depending on the loading conditions, geometric properties, and desired performance. However, these problems have core similarities and can thus be characterized by a general problem formulation. This formulation can be approached as a multi-objective design problem with elements of both size and topological optimization. In order to clearly formulate the design problem at hand, the Compromise Decision Support Problem (cDSP) method is used [46]. The general qualitative formulation for the design and

Table 2: Qualitative formulation of the meso-scale truss structure design problem.

Given:	Starting optimization ground structure, loading and boundary conditions
Find:	Strut diameter sizes
Satisfy:	Upper and lower diameter bounds, maximum volume constraint, maximum stress constraint
Minimize:	Compliance, deviation from target volume

Table 3: Mathematical cDSP formulation of the meso-scale truss structure design problem.

Given:	p^{BG}, p^{F}, p^{M}, i	
Find:	$D_i \in \{0, [D_{LB}, D_{UB}]\}$	(a)
Satisfy:	$\sigma_i \leq \sigma_{max}$	(b)
	$V \leq V_{max}$	(c)
Minimize:	$Z = (W_d \times d)^2 + (W_V \times V)^2$	(d)

optimization of MSTS using the ground structure approach is provided in Table 2. The mathematical equivalent of Table 2 is provided in Table 3.

In Table 3, the symbols p^{BG}, p^{F} and p^{M} represent the initial geometric, loading, and material properties, respectively. The symbol D_i represents the diameter value of each of the i struts in the truss structure. D_{LB} and D_{UB} represent the lower and upper bounds for D_i, respectively. The symbol σ_i represents the axial stress value in each i strut. The symbols V and d represent the volume and deformation of the structure and W_d and W_V represent weighting variables for d and V in the minimization function, Z.

As can be seen in Tables 2 and 3, the ground structure problem formulation requires that there be a starting topology in order to perform optimization. The topology of this structure is generally provided by the designer and contains a large number of struts, each with the same starting diameter value. These diameter values must be optimized in order to generate the optimal structure topology. As can be seen in (a) of Table 3, the diameter values can either be within the specified upper and lower diameter bounds, or zero. If all diameter values remain within the diameter bounds,

then the optimization problem becomes a size optimization problem. However, in most cases, diameter values will drop below the specified lower bounds. In this case, the diameter values become zero and the strut is essentially deleted from the structure. This scenario changes the optimization from a size optimization problem to a topological optimization problem as well, since the actual topology of the structure has changed. In the minimization function, (d) of Table 3, the volume, V, is calculated simply as the sum of the volumes of all the struts in the structures, which are assumed to be cylinders:

$$V = \sum \pi \times \frac{D_i^2}{4} \times l_i \tag{2}$$

Here, l_i represents the length of each of the i struts in the structure. It is important to note that there may be overlapping volumes in locations where struts meet that are not subtracted from the overall volume. In order to simplify the design problem, it is assumed that these overlapping regions have a negligible contribution to the net volume of the structure.

Although the volume of the structure can be determined directly using Equation 2, the deformation, d, does not have a set equation. This lack of an equation occurs because the deformation does not represent a specific metric, but instead represents any value that is directly proportional to the stiffness of the structure. In most cases, d is represented by the net displacement of the structure or the displacement of a particular point on the structure. However, d can also be represented by other values directly proportional to stiffness, such as compliance, strain energy, or work.

3.1.2 SMS Problem Formulation

Tables 2 and 3 are formulations for design methods that require a global optimization of strut diameter sizes in order to perform size or topological optimization. Because the SMS method is also a size/topological design problem, it will have a problem

Table 4: Qualitative cDSP formulation for the SMS design problem.

Given:	Bounding dimensions and unit-cell distribution within the bounding dimensions, loading and boundary conditions, material properties, unit-cell library configurations
Find:	Lattice topology in each unit-cell region, strut diameter values
Satisfy:	Upper and lower diameter bounds, target volume, maximum stress constraint
Minimize:	Compliance

Table 5: Mathematical cDSP formulation for the SMS problem.

Given:	p^{BG}, p^{F}, p^{M}, p^{UC}, $S^{L}_{j,k}$, i, k	
Find:	$D_{i,k} = [S^{u}_{i,j} \times S^{L}_{j,k} \times (D_{max} - D_{min})] + D_{min}$	(a)
	D_{min}, D_{max}	(b)
	$S^{u}_{i,j} = \frac{\sum \sigma_n - \sigma^{min}_{i,j}}{\sigma^{max}_{i,j} - \sigma i,j^{min}}$	(c)
Satisfy:	$D_{LB} \leq D_{min} \leq D_{max} \leq D_{UB}$	(d)
	$\sigma_i \leq \sigma_{max}$	(e)
Minimize:	$Z = (W_d \times d)^2 + \left(W_V \times \frac{V - V_t}{V_t}\right)^2$	(f)

formulation similar to the general formulations. However, the SMS method uses the unit-cell approach for topology generation and does not require a global optimization. Therefore, the problem formulations presented in Figures 2 and 3 must be modified to reflect the unique characteristics of the SMS method. The modified qualitative formulation is presented in Table 4. The modified quantitative formulation is presented in Table 5.

In Table 5, the symbols i, j, and k represent each unit-cell region in the structure, each unit-cell configuration in the unit-cell library, and the strut number in each of the j configurations in the library, respectively; n symbolizes the nodes from the solid-body analysis.

As seen in Tables 4 and 5, the SMS formulation contains key differences from the general formulation. Firstly, it can be seen that more information is provided initially to the SMS method. The general optimization problem only requires a starting

topology and loading conditions; the SMS method, on the other hand, requires additional sources of information, particularly from the unit-cell library and finite-element analysis. Secondly, instead of starting topology, the SMS method requires only the bounding dimensions of the structure and information regarding the distribution of unit-cell regions across the structure. The most significant change, however, is shown in (a) of Table 5. Here, the determination of the strut diameters, $D_{i,k}$, differs considerably. It can be seen that four values must be known before $D_{i,k}$ can be determined: minimum and maximum diameter values, D_{min} and D_{max}, a stress scaling factor, $S^u_{i,j}$, and a unit-cell scaling factor, $S^L_{j,k}$. Furthermore, it can be seen that the two scaling factors, $S^L_{j,k}$ and $S^u_{i,j}$, are provided by external sources of information: the unit-cell library and the solid-body stress analysis. Therefore, only two-values, D_{min} and D_{max}, need to be determined through optimization.

The optimization of D_{min} and D_{max} is performed using the minimization function, Z, shown in (f) of Table 5. The equation has two contributing components, the structural deflection, d, and the structural volume, V, of the truss structure. In particular, the minimization function is formulated to minimize the deflection of the structure and the deviation of the structural volume from a target volume, V_t. Both components also have a weighting value associated with them, W_d and W_V, in order to adjust the relative importance of each component. Both these components are formulated in a least-squares format.

In order to successfully optimize both D_{min} and D_{max}, both the deflection, volume, and associated stresses must be calculated at any given time for any value of D_{min} and D_{max}. These values are calculated using a finite-element analysis of the truss structure. In implementation, the finite-element package that was utilized was developed in MATLAB by Honqqing Vincent Wang in satisfaction of his doctoral dissertation [54]. The finite-element package assumes that each truss element in the truss structure has beam-like behavior.

When compared with the general problem formulation in Table 3, the principal advantage of the SMS method becomes apparent. Whereas the formulation for the SMS indicates that only D_{min} and D_{max} need to be determined, the general formulation requires that every diameter be determined individually through optimization.

3.2 SMS Method Overview

With the design problem formulated, the SMS method can be developed. This method can be divided into seven discrete tasks that are completed in six individual steps. These steps are summarized in Figure 15.

For each step outlined in Figure 15, there exists a specific output, or deliverable, from that step, shown in the hexagonal boxes under each step. The deliverable from each step is used in the subsequent step as the primary input. The only exception to this rule occurs in Step (3). This step requires two inputs from both Steps (2a) and (2b). In addition, it can be seen that the unit-cell library is utilized in the fourth step of the SMS method. The unit-cell library is explained in more detail in Chapeter 4.

3.3 Detailed Description of Each Step of the SMS Method

In the following sections, each step of the SMS method will be outlined. The description of the steps of the SMS method will be provided in the following format:

- **Detailed description of the step**: In this section, the actual step will be discussed in detail.
- **Primary deliverable of the step**: The ultimate deliverable, or result, of the step will be discussed.
- **Additional information**: Any notable information about the step that does not describe the actual proceedings of the step will be discussed. This section can include information such as assumptions made in the step, limitations of the step, and the storage format of data.

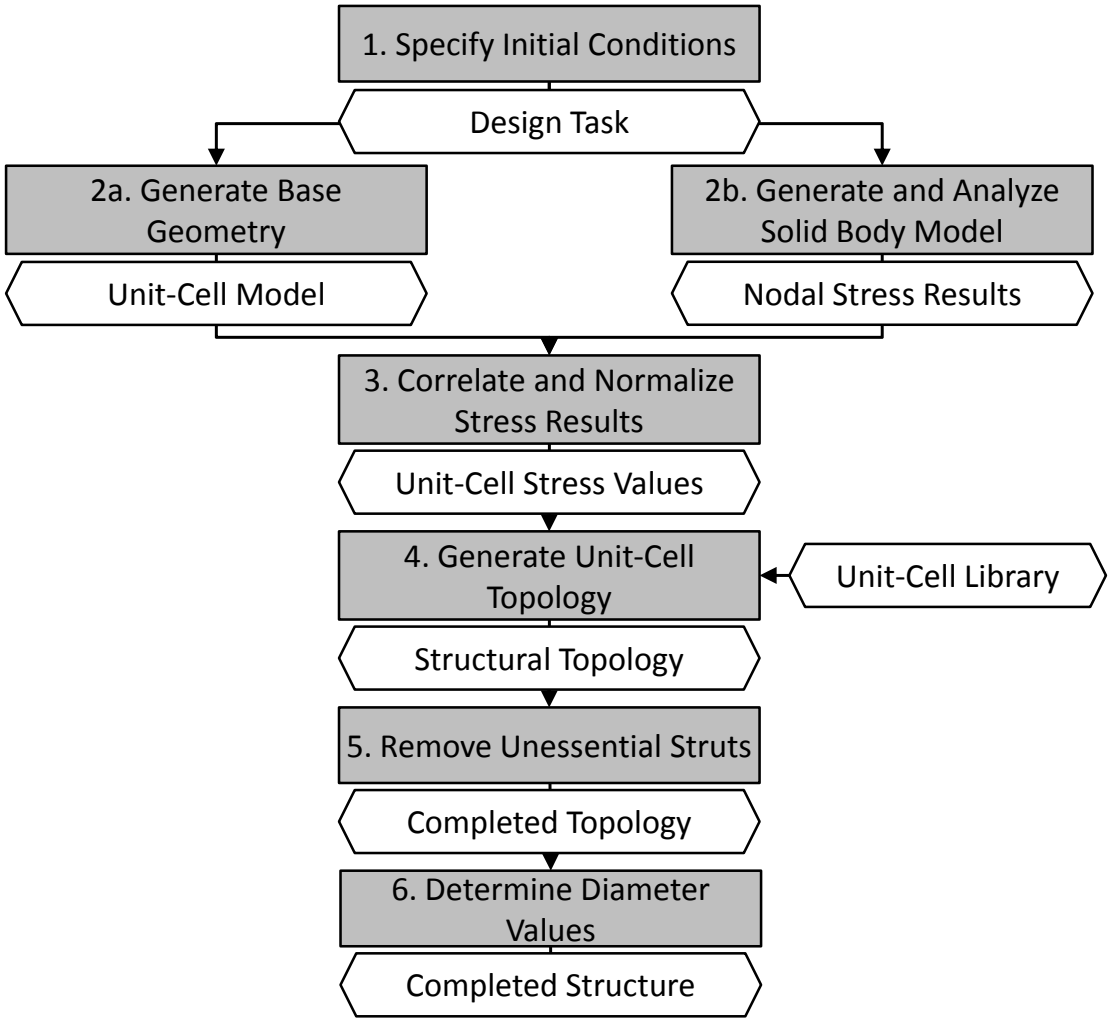

Figure 15: Summary of the SMS design methodology

3.4 Step 1: Specification of Initial Conditions

3.4.1 Method

In the first step of the SMS method, all initial properties are specified for the target truss structure. These properties encompass a large number of parameters and depend uniquely on the design task. Generally, the larger and more complex the design task is, the more initial parameters are required to fully characterize the design problem. All initial conditions fall broadly into two categories: *geometric properties* and *analytic properties*. Geometric properties are all values and characteristics relating to the dimensions of the target structure and unit-cells. Analytic properties encompass all values that are needed to perform stress analysis.

3.4.1.1 Geometric Properties

The geometric properties for the design problem include all parameters that characterize the size and shape of the target truss structure. Specifically, they relate to all values that specify either the *bounding geometry* or the *unit-cell characteristics* of the target structure. Depending on the complexity of the component in consideration, there can be a high variability in the number of these parameters. For simple and highly symmetric structures, such as beams or columns, only a small number of parameters, such as the length and cross-sectional shape, need to be specified. More complex and specialized structures will require the actual component to be designed manually, with each dimension of the part clearly defined.

Specification of the unit-cell properties requires definition of the size, shape, and distribution of the unit-cells composing the target structure. These properties are based largely on the designer's preferences and are generally not independent of one another. For instance, specifying a larger unit-cell size will result in a lattice structure with fewer and longer struts, but will also result in fewer unit-cells distributed across

the structure. It is also important to note that there are restrictions in the specification of unit-cell properties. For example, only one unit-cell size can be determined for the entire structure. Also, unit-cells can only maintain a rectangular prism shape. Components with more complex or curved geometries, such as cylinders and spheres, must be approximated using these rectangular prisms.

3.4.1.2 Analytical Properties

The analytical properties of the truss structure relate to the specification of all parameters that will be needed in the finite element analysis of the truss structure. These values include material properties, such as the Poisson's ratio and Young's Modulus of Elasticity, as well as the necessary loading and boundary conditions. The properties specified here will be used in the structural analysis of both the truss structure and the solid-body representation.

3.4.2 Primary Deliverable

The primary deliverable in this step of the SMS method is a compilation of all geometric dimensions, material properties, and loading conditions of the structure. Ultimately, at the end of this step, the design problem should be clearly and unambiguously defined. The values defined in this step will be used throughout the remaining steps of the SMS method. After the primary deliverables have been defined, the SMS method should be able to run autonomously without intervention from the designer.

The actual data storage format for the deliverable of this step currently is a series of variables stored in files that can be accessed by any of the steps in the SMS method. As mentioned in the step, the number and type of variables differs greatly with the type of design problem. However, there will always be variables that are commonly defined for any design problem, such as loading and fixity conditions and material properties.

3.4.3 Additional Information

This first step of the SMS method is ideally the only step where the designer must input design values. Therefore, the method assumes that the structural values are clearly, correctly, and unambiguously defined. An incorrect value will either cause the SMS method to incorrectly design the truss structure or result in a failure of the method. The first step can alternatively be thought of as the "problem definition" task of the design process and can be considered external to the actual SMS method itself, as no work is actually done in this step save for the definition of several variables and values.

3.5 Step 2a: Generation of a Ground Structure

3.5.1 Method

For this step of the design methodology, the ground, or base, structure of the meso-scale truss structure is created. The ground structure is simply the bounding geometry of the truss structure with the unit-cell divisions clearly defined. The structure does not contain any struts or material, but instead represents a hypothetical space containing the bounding dimensions of the target structure. This space is divided into several identically sized, cuboid, meso-scale regions. By dividing the structure in this way, each cuboid region can be isolated and analyzed independently from other regions. These regions are delimited by nodes at the vertices of each region. Furthermore, these nodes also serve as the end and starting points for struts when the base structure is filled with struts.

3.5.2 Primary Deliverable

At the end of this step, the ground structure should be successfully generated. This includes not only each and every node number and coordinate in the geometry, but also the set of nodes associated with each unit-cell region in the structure. Because

the unit-regions are cuboid in shape, there must exist eight nodes for each of the unit-cell regions. Furthermore, these nodes must be defined in a certain manner such that the orientation of the local coordinate system of the region is known relative to the global coordinate system of the structure. More information is provided in Chapter 4.

3.5.3 Additional Information

The determination of the ground geometry should ideally be an autonomous step where the geometric and unit-cell information entered in the first step is converted seamlessly into a geometry. However, in its current implementation, the SMS method is unable to generate a base geometry without manual guidance. This is because the generation of a base geometry is inherently a difficult one. The process for determining the base geometry is very similar to the mapped meshing process in the finite element method. Because the shapes of the unit-cell regions must be hexahedral, a free mesh using tetrahedrons is insufficient and a mapped mesh is required. This mapped mesh generally requires manual involvement in defining mesh sizes. As a result, the meshing (and the base geometry generation process) is usually one of the most time-consuming aspects of the finite-element approach [34]. Much work has been developed attempting a free mesh-approach for the development of truss structures [24]. However, this approach was not implemented in this work and a manual, 3-D mapped approach was used for all design problems.

The ability to define the size of unit-cell regions in the ground geometry brings about the possibility of there being and "optimal" unit-cell size and distribution: one that will maximize the performance of the truss structure. Because the generation of base lattices is entirely manual at this stage of research, it is not possible to optimize the unit-cell size. However, it is believe that the unit-cell size will have an impact on structural performance. This concept will be a topic of future work.

It should also be noted that, because the ground structure requires that the structure be divided into uniformly-sized hexahedral regions, any structure with shapes that cannot be divided cleanly into these regions, such as tetrahedrons and highly curved surfaces, must be approximated using hexahedra. Furthermore, the completed structure must not have any overlapping regions or nodes. The existence of these overlapping regions or nodes will not necessarily halt the SMS method, but will cause the method to return a truss structure design that has an undesired performance due to unknown interactions between the adjacent unit-cell regions.

3.6 Step 2b: Solid Body Analysis

3.6.1 Method

In this step, a stress analysis must be performed on a solid-body structure of the bounding dimensions of target structure using the loading and fixity conditions specified in Step 1. The ultimate goal of this step is to obtain the relative stress distribution across the solid-body structure and extrapolate this knowledge to determine the relative stress distribution of the truss structure. The solid-body analysis is performed using a finite-element analysis program. Once the analysis is complete, the von Mises stress distribution of the structure is obtained. The primary deliverables from this analysis are stress values of all the FEA nodes in the FEA program. In particular, the stress values in the axial and shear directions are taken for each node.

It is important to note that stress might not be the only metric that can be used to determine the relative material distribution throughout the truss structure. Other components, such as strain or strain energy, are directly proportional to the stress distribution and could also be feasibly used to determine lattice topology. An example of the stress distributions, strain energy distribution, and strain are shown for a cantilever beam problem In Figure 16. As can be seen, the distribution is very similar for all the different metrics. Therefore, these could all be potentially used.

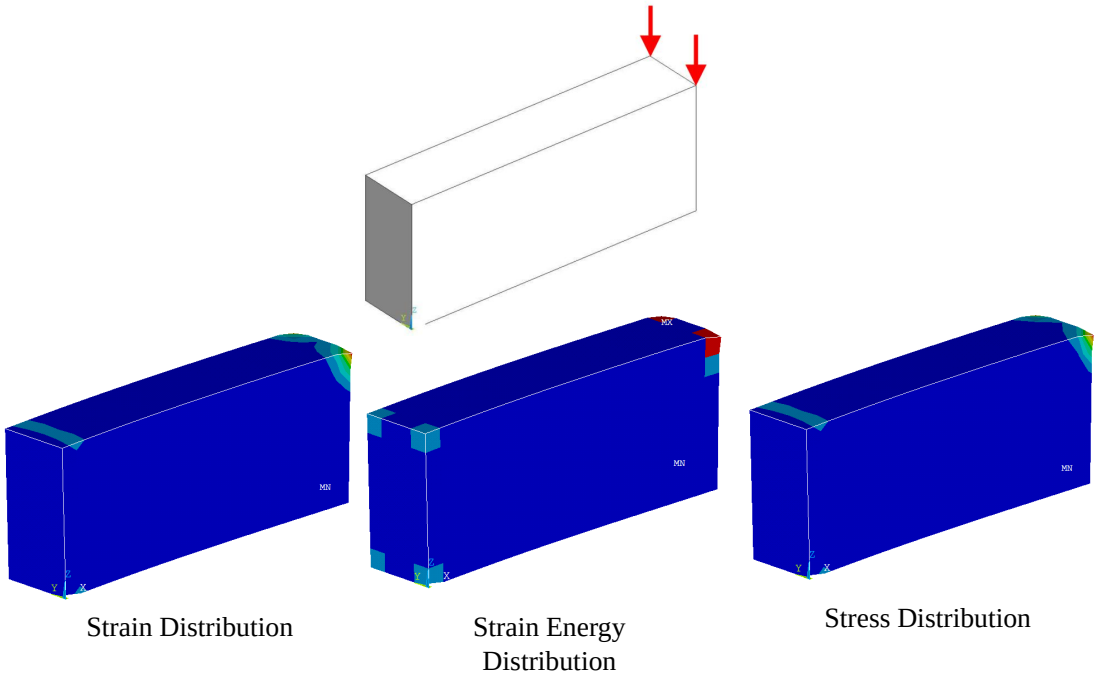

Figure 16: Comparison of the finite-element strain, strain energy, and stress distributions for a 3-D cantilever beam.

However, it is important to note that, currently, the method takes values for each of the stress directions, $\sigma_{xx}, \sigma_{yy}, \sigma_{zz}, \tau_{xy}, \tau_{xz}, \tau_{yz}$. Because strain energy is element-specific and does not have a direction, there is only one value of strain energy per element. Therefore, the library as it is cannot be used because each topology is optimized for a certain stress direction and strain energy does not have directional components. Furthermore, because von Mises stress is a nodal value and strain energy is an element value, a finer mesh might be required to use strain energy, because there are roughly 8 times as many nodes as there are elements in the cantilever beam. On the other hand, strain alone can most likely be used interchangeably with stress because it can be broken into six directional components and it is node-specific as opposed to element-specific.

Table 6: Example of the nodal coordinates from a solid-body FEA.

NODE	X	Y	Z
1	0.00000000000	0.00000000000	0.00000000000
2	50.0000000000	0.00000000000	0.00000000000
3	2.50000000000	0.00000000000	0.00000000000
4	5.00000000000	0.00000000000	0.00000000000
5	7.50000000000	0.00000000000	0.00000000000
6	10.0000000000	0.00000000000	0.00000000000
7	12.5000000000	0.00000000000	0.00000000000
8	15.0000000000	0.00000000000	0.00000000000
9	17.5000000000	0.00000000000	0.00000000000
10	20.0000000000	0.00000000000	0.00000000000

Table 7: Example of the stress values from a solid-body FEA.

NODE	SX	SY	SZ	SXY	SYZ	SXZ
1	-1.8124	-0.69913	-0.63678	-0.18155	-0.93638E-02	-0.13439
2	-0.27010E-02	-0.51930E-02	-0.30358E-02	-0.24652E-03	0.31510E-03	-0.44166E-02
3	-1.5162	0.31273E-01	0.63280E-01	-0.83728E-01	0.11385E-01	-0.76378E-01
4	-1.2550	-0.25043E-01	-0.24116E-01	0.11092E-01	-0.60209E-02	-0.27931E-01
5	-1.2287	0.13232E-01	0.12453E-01	0.10636E-01	0.13295E-02	-0.34261E-01
6	-1.1853	0.22893E-02	0.78830E-03	0.68094E-02	-0.60613E-04	-0.35813E-01
7	-1.1219	0.12600E-02	0.12287E-02	0.38301E-02	0.10793E-03	-0.36752E-01
8	-1.0501	0.47512E-04	0.95568E-04	0.30708E-02	0.91482E-05	-0.37088E-01
9	-0.97568	-0.29720E-04	0.78344E-04	0.30126E-02	0.97315E-05	-0.37298E-01
10	-0.90080	-0.24599E-04	0.37313E-04	0.30852E-02	0.11869E-04	-0.37451E-01

3.6.2 Primary Deliverable

The primary deliverable resulting from the solid body analysis should be the Cartesian coordinates and stress values in the three axial and three shear directions for each finite-element node in the solid-body. An example of the data returned from an ANSYS 11 analysis is shown in Tables 6 and 7.

As can be seen in Table 7, six stress values are of particular interest for use in the SMS method: three axial stresses, $\sigma_{xx}, \sigma_{yy}, \sigma_{zz}$, and three shear stresses, $\tau_{xy}, \tau_{xz}, \tau_{yz}$.

3.6.3 Additional Information

In order for the solid-body analysis to be appropriate for usage for this step, several criteria must be satisfied:

- The bounding dimensions and shape of the structure must be identical to the ground structure.
- The loading and fixity conditions must be identical to the ground structure.

- The number of finite-element nodes in the structure must be equal to or greater than the number of unit-cell regions in the target structure. In general, the more finite-element nodes that are present in the structure (i.e. the finer the meshing of the finite element structure), the better the approximation of the average stress in the structure. However, a finer mesh will result in a longer analysis and design time, so a trade-off must be made.

3.7 Step 3: Stress Normalization and Matching

3.7.1 Method

In this step of the design method, the deliverables from Steps 2a and 2b are combined determine the stress concentrations in each of the unit-cell regions composing the base geometry. Specifically, three sequential operations are performed on the nodal results in sequential order: unit-cell correlation, averaging, and finally normalization. These three operations are explained below.

3.7.1.1 Unit-Cell Correlation

In order to utilize the solid-body results to create the truss-structure, the stress results must be correlated, or "mapped," to the appropriate unit-cell region of the base geometry. Essentially, the solid-body nodes are checked to find which unit-cell region they fall into. If one of these nodes falls into the region enclosed by a unit-cell region, then the stress values of that node are included in the calculation of the stresses in the unit-cell region.

Once the mapping process is complete, then each unit-cell region will contain an array of FEA nodes that will be included in the calculation of the stress distribution in the unit-cell. If, for some reason, a unit-cell region contains no FEA nodes, then it is assumed that that particular region has zero stress in all directions. Also, if there is a scenario where a FEA node exists on the border between multiple unit-cells, it will be included in each of these respective unit-cells.

3.7.1.2 Averaging

Once the correlation procedure is completed, each unit-cell region will contain a set of FEA nodes. In order to determine the overall stress in each unit-cell region, the stress values of all the FEA nodes in the array will be averaged. As seen in Table 7, each node contains six stress values. Each of these six stress values is averaged for all nodes present in the unit-cell region. It is important to note that only the absolute value of the stresses are averaged since only the magnitude, not the direction of these stress values is important for determining the overall stress of the unit-cell region.

3.7.1.3 Normalization

The final operation is the normalization of the stress results to between zero and one. The exact stress values returned by the nodal FEA solution are relevant only for a solid-body structure. The exact value therefore cannot be used in the SMS method because they will not match the stress values in an equivalent truss structure. Instead, it is more important to know the relative distribution of stresses in the solid-body analysis than the stress values themselves. Since the actual values are not necessary, they are normalized to between zero and one. This normalization is performed for two reasons. First, the normalization removes superfluous stress information from the analysis, allowing results to be interpreted more easily. In this case, the normalization allows the largest stress value corresponds to a value of one and the smallest stress near a value of zero. Second, the normalized values will allow the mapping of specialized unit-cells to the truss structure to be accomplished much more easily.

3.7.2 Primary Deliverable

The final result of this step of the SMS method should be the ground structure of the SMS method with each of the unit-cell regions containing the average stress values for the entire region. It is important to note that each region will contain six stress values, three axial and three shear: $\sigma_{xx}, \sigma_{yy}, \sigma_{zz}, \tau_{xy}, \tau_{xz}, \tau_{yz}$. These values are normalized to

between zero and one across the entire structure.

3.7.3 Additional Information

In order for this step to be successful, there must exist at least one FEA node per region in the structure. Thus, it is important to have a finite-element model that is finely meshed enough so there are a sufficient number of nodes for each region in the structure. If no nodes exist in the structure, then the method assumes that there is zero stress in the structure. Therefore, during the fourth step, no topology will be mapped to the structure and a blank space will exist in the region.

A critical assumption that the method makes in this step is that the average stress in the region is a good approximation of the overall stress distribution in the region. However, if there is a region where the stress varies considerably and the average stress is not representative of the local stresses, then the assumption will not be valid. To counter the possibility of this issue occurring, it is important to specify an accurate unit-cell size such that each region only encompasses small stress variations that can be accurately modelled using an average value.

3.8 Step 4: Topology Generation

3.8.1 Method

With the average, normalized stresses known for each unit-cell region, the unit-cell library can be used to map specialized unit-cells to the unit-cell region. Each region in the base structure is scanned. Then, based on the six stress values, a unit-cell configuration is selected and mapped to the region. This process continues iteratively across all the unit-cell regions until all the regions are mapped. Once this process is completed, the topology of the structure will be completed. A more detailed explanation of the selection and mapping process is provided in Chapter 4.

3.8.2 Primary Deliverable

At the completion of this step, the ground-structure will have a topology specialized for the anticipated stress distribution of the structure based on the solid-body analysis. It is important to note that because all the strut diameters lie between zero and one, the structure at this point essentially contains only topological data for a normalized loading situation. In this topology, the relative diameter sizes are known relative to each other; a strut with a diameter value of one is the thickest relative strut in the structure. Alternatively, a strut with a value at or near zero will be the thinnest relative strut in the structure; every other strut diameter is known relative to the other strut values. The normalized diameters must be associated with actual diameter values based on the loading conditions of the structure.

3.8.3 Additional Information

The success of this step is highly contingent upon the accuracy of the unit-cell library and of the base configuration. The method assumes that the unit-cell configurations are all correctly optimized and their directions are correctly oriented with the truss structure. The step also assumes that the base structure and each unit-cell region is oriented correctly. If the local coordinate system of both the unit-cell configuration and the unit-cell region are not oriented in the same direction as the global coordinate system, then the topology will be mapped incorrectly and the truss structure will perform sub optimally.

3.9 Step 5: Unessential Strut Removal

3.9.1 Method

In this step, struts that are deemed unessential for the optimal performance of the structure are removed from the structure. These struts can be classified into two types of struts: ambiguous struts and dispensable struts.

3.9.1.1 Ambiguous Struts

Ambiguous struts are those struts that should not exist within the truss structure. For instance, ambiguous struts can be multiply-defined or overlapping struts in the structure. These overlapping struts often exist because adjacent unit-cell regions often have identical struts on their shared planes. To resolve this conflict, the largest strut of the duplicate struts is kept and the smaller struts are removed. This process ensures that the remaining strut is adequately large enough to support all the stresses of both unit-cell regions. Other ambiguous struts can include struts with zero diameter sizes or that have the same beginning and ending points. The removal of such ambiguous struts can be considering a "book keeping" step, where the majority of flaws created during the first four steps are removed from the structure.

3.9.1.2 Unnecessary Struts

Unnecessary struts are those struts that have negligible contribution to the overall performance of the truss structure. These struts are removed from the structure in order to reduce the overall normalized volume of the structure. This, in turn, will improve the results of the final step of the method, when diameter values are determined for the structure.

The previous iteration of the SMS method used a simple algorithm for the removal of unnecessary struts. This method used the concept of a cutoff diameter, D_{cutoff}. D_{cutoff} can be defined as a value between D_{min} and D_{max} where all struts with diameter values below this value are removed from the structure:

$$D_{cutoff} = c \times (D_{max} - D_{min}) + D_{min} \tag{3}$$

where c is a decimal value between zero and one. In the previous SMS method, c was set as 2.5%, or 0.025. D_{cutoff} was initially used because it is observed that some diameter values at or near D_{min} are either too small to be fabricated by AM,

or too small to provide any stiffness or strength to the truss structure. For simple problems, the implementation of D_{cutoff} was successful in reducing structure volume without significantly reducing structural performance. However, in this research, it was determined that when the use of D_{cutoff} was scaled to larger, more complex problems, critical struts for the performance of the structure were removed because the method did not take into account interactions between these struts and adjacent struts. Furthermore, the method tended to leave "floating struts" that did not have any function. Based on these results, it was determined that a "cutoff" approach to strut removal was ineffective for all problems. However, a sufficient method has not been determined yet for the removal of dispensable diameters to replace this approach.

3.9.2 Primary Deliverable

The primary resultant deliverable of this step is the normalized topology with all ambiguous and dispensable struts removed from the structure. The removal of all these struts will ensure not only an accurate determination of the volume and deflection of the truss structure, but the elimination of errors involving overlapping struts during the final step of the SMS method.

3.10 Step 6: Diameter Sizing

3.10.1 Method

In the previous step, the topology of the truss structure was successfully defined. However, before the structure can be successfully manufactured, the normalized diameter values must be correlated to real diameter values. This assignment of diameter values is done here in Step 6. Since the topology is already known, then the diameter values relative to each other are also already known. Therefore, only a few key diameter values are required to determine all other diameter values in the SMS structure. In particular, as seen in the problem formulation in Figure 5, two key diameter values must be determined: a maximum allowable diameter, D_{max}, and a minimum

allowable diameter, D_{min}. The maximum diameter value corresponds to the thickest diameter in the structure and the minimum diameter corresponds to the thinnest strut in the truss-structure. Once the minimum and maximum diameters are found, then the remaining diameters can be determined using Equation 4 below:

$$D_{i,k} = [S^u_{i,j} \times S^L_{j,k} \times (D_{max} - D_{min})] + D_{min} \tag{4}$$

where $S^u_{i,j}$ is a scaling factor taken from the unit-cell library, $S^L_{j,k}$ is a scaling factor associated with the solid-body finite element analysis, and D_{min} and D_{max} are the minimum and maximum diameters respectively. The two scaling terms, $S^u_{i,j}$ and $S^L_{j,k}$, are already found previous to this step. Therefore, in order for this step to be completed, only D_{min} and D_{max} need be determined. Therefore, the design problem becomes a two-variable design problem with D_{min} and D_{max} as the primary design variables.

3.10.1.1 Determination of D_{min} and D_{max}

To determine the values of D_{min} and D_{max} in the structure, the problem formulation provided earlier must be utilized. As the problem formulation states, the target truss-structure must satisfy a maximum volume constraint while attempting to minimize compliance. These two goals will have contrasting effects. The volume constraint will attempt to drive the volume, and thus the strut diameter values, down. Conversely, the compliance constraint will drive the volume up. By using these constraints with the current normalized geometry, optimal values of D_{min} and D_{max} can be found. The objective function, (e) in Figure 5 can be rewritten as a function of D_{min} and D_{max} in Equation 5,

$$F(D_{min}, D_{max}) = (W_d \times d(D_{min}, D_{max}))^2 + \left(W_V \times \frac{V(D_{min}, D_{max}) - V_t}{V_t}\right)^2, \tag{5}$$

where the volume, $V(D_{min}, D_{max})$, and the deformation, $d(D_{min}, D_{max})$, are functions of D_{min} and D_{max} only. It is important to reiterate that deformation, d, does not correlate to a specific metric, but instead represents any unit of measure directly proportional to structure compliance, such as tip deflection or work. It is also important to note that there is no target deflection variable as there is a target volume variable, V_t, because the target deflection is always set at zero, $d_t = 0$.

With an objective function provided, D_{min} and D_{max} can be determined by performing a two-variable minimization. Because of the nature of the design problem, the optimization of D_{min} and D_{max} is a non-linear, constrained, optimization problem. In this research, two optimization approaches will be taken to determine D_{min} and D_{max}: the Levenburg-Marquardt least squares regression approach and a constrained minimization approach using the active-set algorithm discussed in Chapter 2. The Levenburg-Marquardt approach was utilized because it already had documented success in previous research on the optimization and design meso-scale truss structures [18]. The second algorithm, the active-set algorithm, was utilized because it is an algorithm that is documented to have success in the optimization of multivariable, non-linear, constrained optimization problems [6]. These two algorithms use different approaches in the optimization of the design problem and will be compared in order to determine if there is a difference in design performance when different algorithms are used.

3.10.1.2 A One-Variable Approach to Determining D_{min} and D_{max}

In previous research, it was determined that a possible relationship could exist between D_{min} and D_{max}. In his research, Graf noted that, for a specific target volume, any structure designed using the SMS method had the highest strength when an approximate D_{min}/D_{max} ratio of 28% was achieved. When the target volume was varied, this assumption appeared to hold true within a tolerance of $\pm 2\%$. Figure

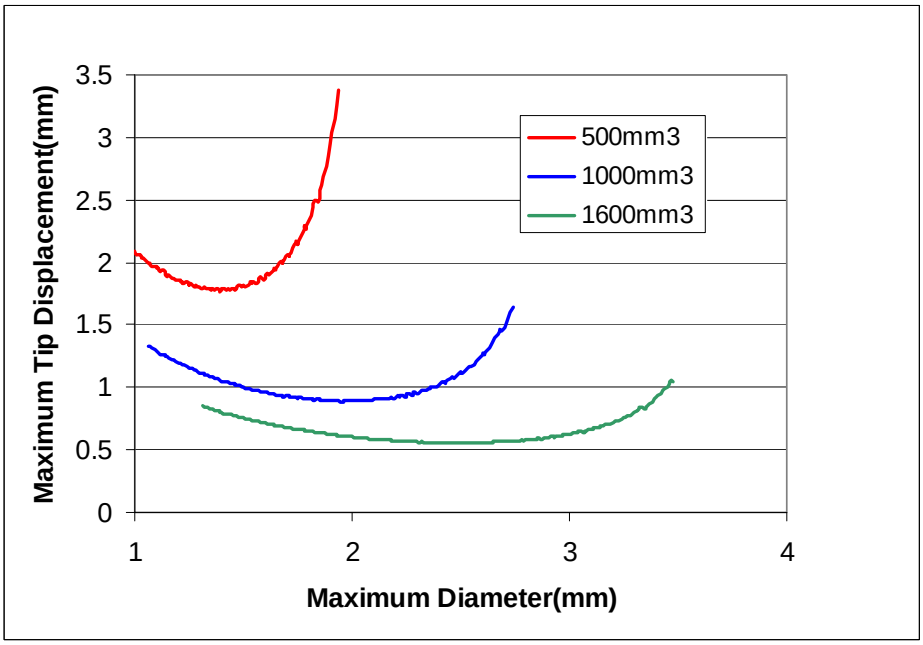

Figure 17: A survey of the relationship between D_{min} and D_{max} [27].

17 shows this correlation for a cantilever truss structure designed using the SMS approach. Here, for a constant D_{min} value, the D_{max} was varied and the tip displacement was recorded. For a specific volume, the lowest tip placement occurred when the D_{min}/D_{max} value reached 28%. The discovery of this relationship had a significant effect. Using this assumption, the minimum diameter could be expressed as a function of the maximum diameter:

$$D_{min} = 0.28 \times D_{max} \tag{6}$$

When Equation 6 is plugged into the diameter determination equation, Equation 4, the equation becomes,

$$D_{i,k} = [0.72(S^u_{i,j} \times S^L_{j,k}) + 0.28] \times D_{max}. \tag{7}$$

Thus, the diameter determination equation can be reduced from a two-variable equation to a one-variable equation and only D_{max} needs to be determined. Since only

one diameter value needs to be determined, the optimization problem is dramatically simplified and should significantly reduce the overall design time for the SMS method.

Although the potential benefits of this approach are great, the issue is that it was not fully explored before it was used. The assumption was not sufficiently tested and was not compared against actual optimization routines in order to assess it's validity. In this research, the "28% Assumption" will be tested for both stiffness and design time. In other words, the assumption will be tested to determine under what circumstances it will be valid and how the assumption will affect the overall process.

3.10.2 Primary Deliverables of the Step

At the completion of this step, the SMS method should be completed. The final truss structure with correct diameter sizing should be returned.

3.10.3 Additional Information

This sixth and final step is generally the most time-consuming step of the entire method, generally taking around 90% of the overall design time. The principal assumption that takes place in the determination of diameters is that the struts in the structure are cylinders. If this assumption is used, the cross-sectional area can be parameterized using only one value: the diameter value. If the cross-section of the struts are not cylinders, then this assumption will not be valid.

The optimizations that were performed utilized finite-element analysis software developed internally and implemented in MATLAB. In the analysis of the truss structure, this code makes the assumption that all the trusses have beam-like behavior. Therefore, the struts in the structure can experience bending stresses. This element-type is in contrast to truss elements that can only experience axial and shear stresses.

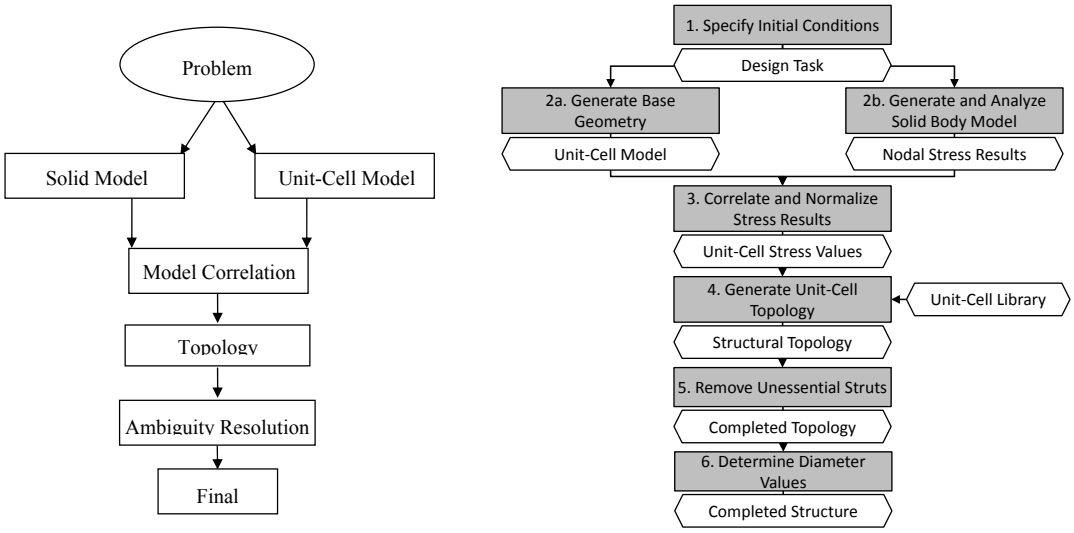

Figure 18: A comparison of the original SMS method (left) and the modified SMS methods (right).

3.11 Comparison Between the Original and Modified SMS Method

Figure 18 shows the overview of both the original and modified SMS methods. The major changes between the original and modified SMS method are summarized below:

- As can be seen, the first four steps of the methods are fairly similar: the problem is defined and the unit-cell approach and unit-cell library are utilized in these steps. The key differences between the original method and the modified method lie primarily in the creation of a sixth separate step for determination of D_{min} and D_{max}. The original method does not discern between the generation of topology and the determination of diameter values. Furthermore, the ambiguity resolution step occurs after the determination of diameters rather than before. This lack of a sixth step occurs because the original method lacks a systematic method for the determination of D_{min} and D_{max}. Instead, a brute-force approach was taken with the 28% assumption. Although this approach was somewhat successful in determining the optimal D_{min} and D_{max} values, the method was time-consuming and required manual intervention.

- The cutoff diameter, D_{cutoff}, is identified as an area of future work for the SMS method. For the purposes of this thesis, it will still be used. However, it will be used only in problems where it does not negatively affect structural performance.
- Various technical issues are addressed in the implementation of the method, improving both robustness and repeatability of the method.

3.12 Research Questions Revisited

The modified method addresses two of the three research questions discussed in Chapter 1. The hypotheses for the research questions are repeated below:

Hypothesis 1: By utilizing the unit-cell approach and combining it with a constrained optimization of two diameter values: a minimum allowable diameter and a maximum allowable diameter, against volume and stiffness constraints, a systematic design method can be developed for the design of mesoscale truss structures. By exploring various optimization approaches and selecting the best method, analysis time can be minimized and structural performance can be maximized.

Hypothesis 2: By exploring and analyzing the optimal minimum and maximum diameter values for meso-scale truss structures designed using the Size, Matching, and Scaling method, a direct relationship between these two values can be determined and exploited. This relationship will allow for one of the two diameter values to be expressed as a function of the other. Consequently, the two-variable minimizations outlined in Hypothesis 1 can be simplified to a one-variable minimization problem, thereby reducing overall design time.

It can be seen that both of these hypotheses are addressed in particular by the addition of a sixth and final step of the SMS method: a diameter determination step for D_{min} and D_{max}. By isolating the determination of diameters from the designation of lattice topology, both hypotheses can be addressed in detail. To validate the first hypothesis, the diameter determination step will be converted from a brute-force approach into an optimization approach. In continuation with the first hypothesis, two different optimization algorithms, an active-set and least-squares minimization algorithm, will be utilized to characterize the effect of the optimization algorithm on the diameter determination step.

The second hypothesis, on the other hand, will be addressed by the simultaneous exploration of the optimal minimum and maximum diameter values returned by two-variable optimization and the 28% assumption determined by Graf. By looking at the results of the both the two-variable and one-variable results, the validity of a one-variable approach will be assessed.

3.13 Summary

In this chapter, the modified Size, Matching, and Scaling method was presented. Each of the steps of the method, including the process and the deliverables, were presented. When compared to the original method proposed by Graf, it can be seen that the first four steps are similar because they utilize the core features of the unit-cell approach. It can also be seen that the unit-cell library, the key tool in topology generation, is utilized directly in the fourth step. The key differences, however, occur after the topology is generated. In particular, the determination of diameter values for the normalized topology proposed in the revised method is different. Instead of a manual search of D_{min} and D_{max} proposed by Graf, an optimization approach is used. This optimization is in direct contrast with Graf's conception for the SMS method: to avoid optimization entirely. The driving concept for this method, on the other hand,

is to utilize optimization in conjunction with the unit-cell approach rather than in spite of it.

The modified SMS method, and in particular the sixth step, will address research questions 1 and 2 and will determine whether an optimization approach to determining D_{min} and D_{max} is valid, and whether this optimization can be reduced from a two-variable optimization to one-variable. The modified method will be thoroughly tested in Chapter 5.

CHAPTER IV

THE MODIFIED UNIT-CELL LIBRARY

In this chapter, the modified unit-cell library will be presented. The unit-cell library serves as the primary tool used by the SMS method in the generation of lattice topologies. It is a collection of lattice configurations that have their topologies optimized for specific stress conditions. These lattice configurations conform to a set of guidelines that allow them to be connected to one another to form more complex lattices. The original unit-cell library contained one configuration, specialized for one of six stress conditions. In total, there were six entries in the library. The new library attempts to expand the unit-cell library to include additional entries. The following sections will outline not only the current library, but the mapping and selection process utilized for the library and the optimization process for the entries in the library themselves.

4.1 The Optimization Process for Unit-Cell Configurations

Before a certain unit-cell configuration can be entered in the unit-cell library, it must first undergo an optimization process to cater its performance for six separate loading conditions. Each of these loading conditions is representative of the six stress values utilized in the SMS method and solid-body stress analysis: the σ_{xx}, σ_{yy}, and σ_{zz} axial stresses and the τ_{xy}, τ_{yz}, and τ_{xz} shear stresses.

4.1.1 Problem Formulation

The optimization of unit-cell configurations can be considered its own unique design problem, separate from the SMS method. As a result, a second problem formulation must be utilized for the optimization of unit-cells. The cDSP problem formulation for the optimization of unit-cells is shown in Table 8.

Table 8: Qualitative cDSP formulation for the optimization of unit-cells.

Given:	Loading and Fixity Conditions, Starting Lattice Topology	
Find:	Truss Diameters/Lattice Topology	(a)
Satisfy:	Target Strain Energy	(b)
	Maximum Stress Value	(c)
Minimize:	Volume	(d)

As Table 8 shows, the problem formulation for the optimization of unit-cells is very similar to the problem formulation for that of the ground structure approach to lattice design. Much like for the ground structure approach, both the loading conditions and starting topology are provided. Furthermore, the truss diameters are the main design variables. However, there is one key difference between the formulation for the ground structure approach and the formulation for unit-cell optimization. For unit-cell optimization, rather than the minimizing both stiffness and volume, only volume is minimized. Stiffness is no longer a minimization target, but is instead a constraint. The primary reason that stiffness is set as a constraint instead of an objective is to force the performance of all optimized unit-cells to be equal. Thus, the only differing factor between the unit-cell configurations will be the actual volume of the configurations themselves. This will, in turn, allow the selection process of unit-cells to be simplified. For the optimization of unit-cells, strain energy is used as the primary determinant for stiffness. Strain energy can be defined as the potential energy stored in an element due to deformation. The strain energy, $\triangle U$, is calculated as,

$$\triangle U = \frac{\triangle F}{2} d \tag{8}$$

where $\frac{\triangle F}{2}$ is the average force magnitude of the load and d is the overall displacement of the structure [29]. Strain energy is used as the primary metric for unit-cell

optimization because it is directly proportional to strain, and therefore the compliance/stiffness of the structure. It is widely used in objective problem formulations for topological optimization problems [8]. It is preferred over stress, because microscopic stress values may exist in a truss structure that differ from the macroscopic whole. These microscopic deviations are not represented in the macroscopic stress values but can negatively influence the performance of the structure. Therefore, stress may not be as indicative of the overall structural performance of truss structures as strain energy. Furthermore, strain energy may be easier to implement in finite element analysis because of FEA's heavy reliance on elastic energy principles such as Hamilton's Principle and the principle of minimum total potential energy [41].

4.1.2 Process Overview

With the unit-cell optimization problem formulated, the design method can be presented. An overview of the method is shown in Figure 19. As Figure 19 shows, the optimization process contains five individual steps. These steps will be summarized in more detail in the following sections. An example of the unit-cell optimization process is shown in Appendix A for the Cantley configuration.

4.1.3 Step 1: Insert Initial Unit-Cell Configuration

In the first step, the initial unit-cell configuration must be defined. This includes definition of all nodes, elements and diameters in the structure. Additionally, starting diameter values must be specified. For this optimization, a uniform starting value of "1" was used for all diameters. Although many unique lattice configurations can be utilized by the SMS method, not all configurations are supported. Theoretically, unit-cell regions can be any shape and size, as long as the shape can successfully compose the bounding geometry. However, for the purposes of this research, cuboid regions were used because division of a structure into these regions can be performed more easily and because most documented configurations, such as the Cantley truss and

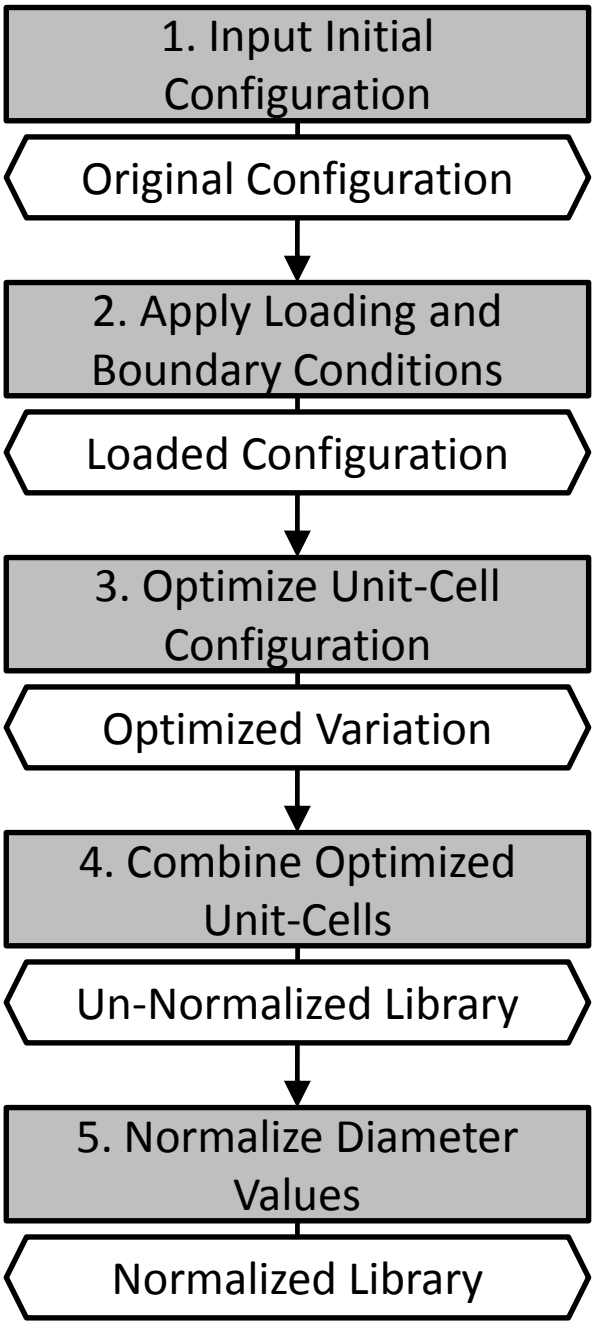

Figure 19: An overview of the unit-cell optimization process.

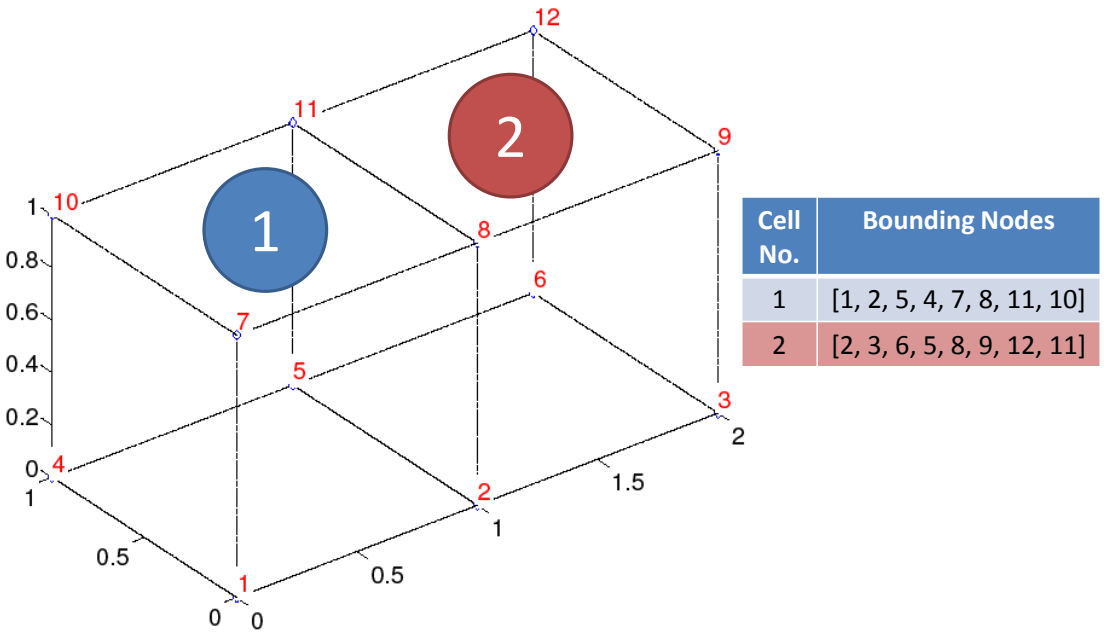

Figure 20: Typical unit-cell regions.

the octet truss, conform easily to the cuboid shape. Two adjacent unit-cell regions are shown in Figure 20.

As can be seen in Figure 20, each region is characterized by 8 nodes in each of the corners of the cube. In order for configurations to be capable of being placed into the unit-cell library, they must conform to such regions. These configurations are mainly limited in their shape by their interaction with adjacent configurations in the mesoscale structure. In order to prevent potentially negative interaction between elements in the mesoscale structure and ensure correct optimization of configurations, the following set of guidelines should be satisfied:

1. There must be a nodal connection at each of the eight corners of the cuboid unit-cell region. This constraint will ensure that all unit-cells are connected to adjacent unit-cell regions via these eight common nodes.

2. The unit-cell configurations cannot be loaded or fixed at any other nodal position than the eight corners of the cuboid region. This once again ensures that

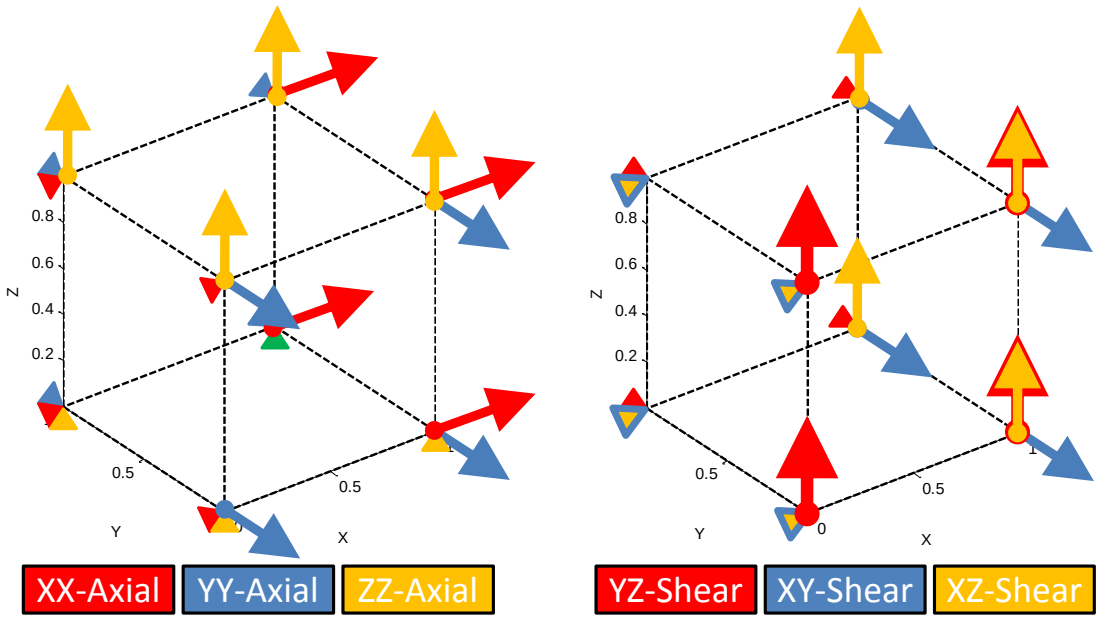

Figure 21: The loading conditions for unit-cell optimization.

interaction between adjacent unit-cell regions remains consistent.

3. No nodes or elements should be defined outside the bounding dimensions of the cuboid unit-cell region. This constraint is not a strict guideline as it may not affect the performance of the mesoscale truss structure. However, the interaction between adjacent unit-cells may be affected by the intersection or overlap of elements or nodes.

4.1.4 Step 2: Apply Loading Conditions

In the next step, the unit-cell is loaded. For the optimization, there exist six pre-defined loading conditions, each approximating a particular stress direction. The loading and fixity conditions are summarized in Figure 21.

It should be noted that these loading conditions must be applied in multiple directions, especially for the shear cases. For instance, the loading condition for the τ_{xy} scenario is only applicable for the positive XY shear direction. However, it is known that $\tau_{xy} = \tau_{yx} = -\tau_{xy} = -\tau_{yx}$. In order for the unit-cell to be properly optimized

Table 9: Optimization parameters for unit-cell optimization in ANSYS.

Strain Energy Constraint (mJ)	50
Poisson Ratio	0.3
Elastic Modulus $(N/cm)^2$	1960
Loading Magnitude (N)	10
Element Type	BEAM4

for all shear conditions in the XY plane, it must be optimized individually for the loading conditions simulating each of the these shear directions. These separately optimized unit-cells must then be combined to form the final optimized unit-cell for that direction.

4.1.5 Step 3: Optimize Unit Cell

After both the loading conditions and topology have been defined, the structure can be optimized. As can be seen in the problem formulation in Table 8, the volume is minimized subject to strain energy and maximum stress constraints. In order to avoid exceeding a maximum stress, a small force magnitude of 10 N was applied. The strain energy constraint was set at 0.5 mJ, a value that can be achieved by any of the configurations in the unit-cell library regardless of the loading condition. The analysis and optimization of the unit-cells were performed in the software package, ANSYS 13.0. Table 9 summarizes the numerical constraints and material properties used in the optimization.

4.1.6 Step 4: Combine Optimized Unit-Cells

As mentioned in Step 2, each stress condition is approximated using loading conditions. Therefore, an optimization must be performed for each of the loading conditions. The results of these optimizations must then be combined to form the final topology. For instance, for the τ_{xy} condition, four separately optimized unit-cells are returned from optimization and must be combined. The combination of the resultant configurations is fairly simple: for each strut in the configuration, the strut with the

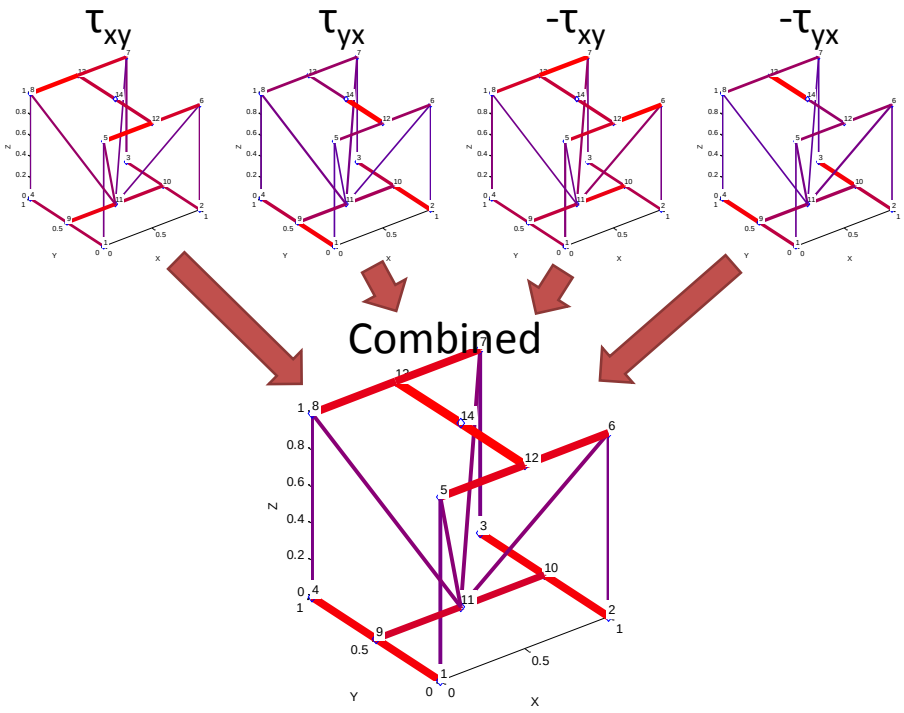

Figure 22: Example of the combination of optimized unit-cells for the τ_{xy} direction for the Cantley configuration.

largest diameter is retained and the other diameters are discarded. An example of this process is shown in Figure 22.

4.1.7 Step 5: Normalize Unit-Cells

After all the unit-cell configurations have been optimized, the diameters must be normalized to between 0 and 1:

$$D_{j,k,l}^{norm} = D_{j,k,l}/D_{l}^{max} \tag{9}$$

where j represents each strut for each of the k^{th} configurations for each of the l stress directions. As can be seen from Equation 9, the unit-cell configurations are normalized to the largest diameter value existing in each of the six stress directions. This ensures that all the unit-cell configurations maintain the same stiffness characteristics relative to one another. Therefore, it is important to note that every time a new entry is added to the unit-cell library, the entire library must be re-normalized.

Once all the entries have been optimized, the entries can be stored in a library. The unit-cell library is currently stored in a list format. For each unit-cell configuration, there are three specific data structures to store: the nodal coordinates, the elements within the structure, and the diameter values of each element in the structure.

4.1.8 Element-Type Variation for the Crossed Configuration

For the optimization of unit-cells in ANSYS, it was noted that for the crossed configuration, the beam element type, BEAM4, did not return optimal results. Here, the optimization tended to overemphasize bending in the structure and returned apparently sub-optimal results for the shear loading cases. In order to adjust for these results, the element type was replaced with the truss element, LINK188, in order to ensure that optimization did not skew the results toward bending. This element type does not recognize bending stress. However, because it does not account for bending, it cannot be used for all the configurations in the library, as the problem becomes underconstrained when bending is not considered. The results for the crossed configuration using bar elements were combined with the results from the beam optimization from the other configuration.

4.2 Unit-Cell Library Overview

In this section, the modified unit-cell library is presented. The current library contains seven separate entries, each entry with six optimized configurations. In total, there are 42 entries in the library. In the following sections, each entry in the unit-cell library will be detailed, including a description of the configuration and the presentation of the optimized versions of each unit cell.

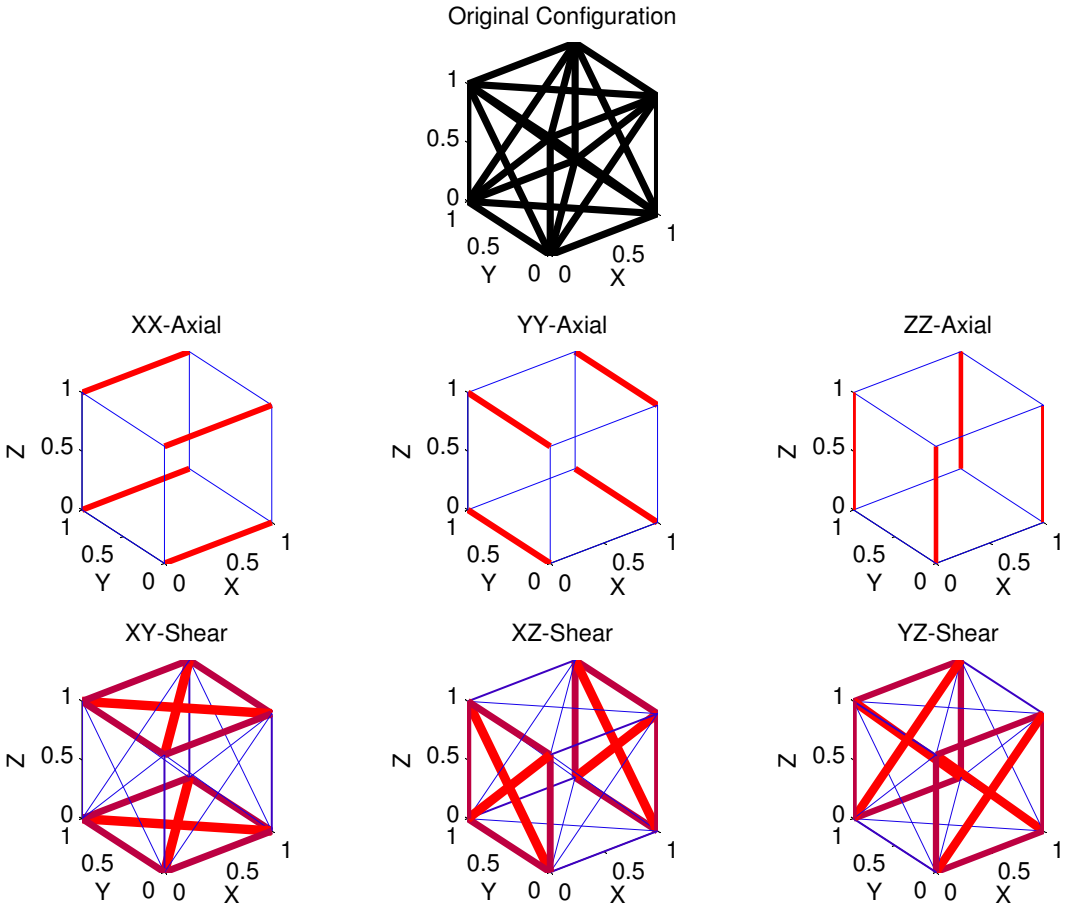

Figure 23: Summary of the crossed unit-cell configuration.

4.2.1 Crossed

The crossed configuration is the configuration retained from the first unit-cell library utilized in the SMS method. This configuration features struts along each of the edges of the unit-cell region. In addition to these struts, there are diagonal struts connecting the corners of each face of the cube. In total, there are 24 struts in the structure. The original unit-cell and the optimized configurations are shown in Figure 23.

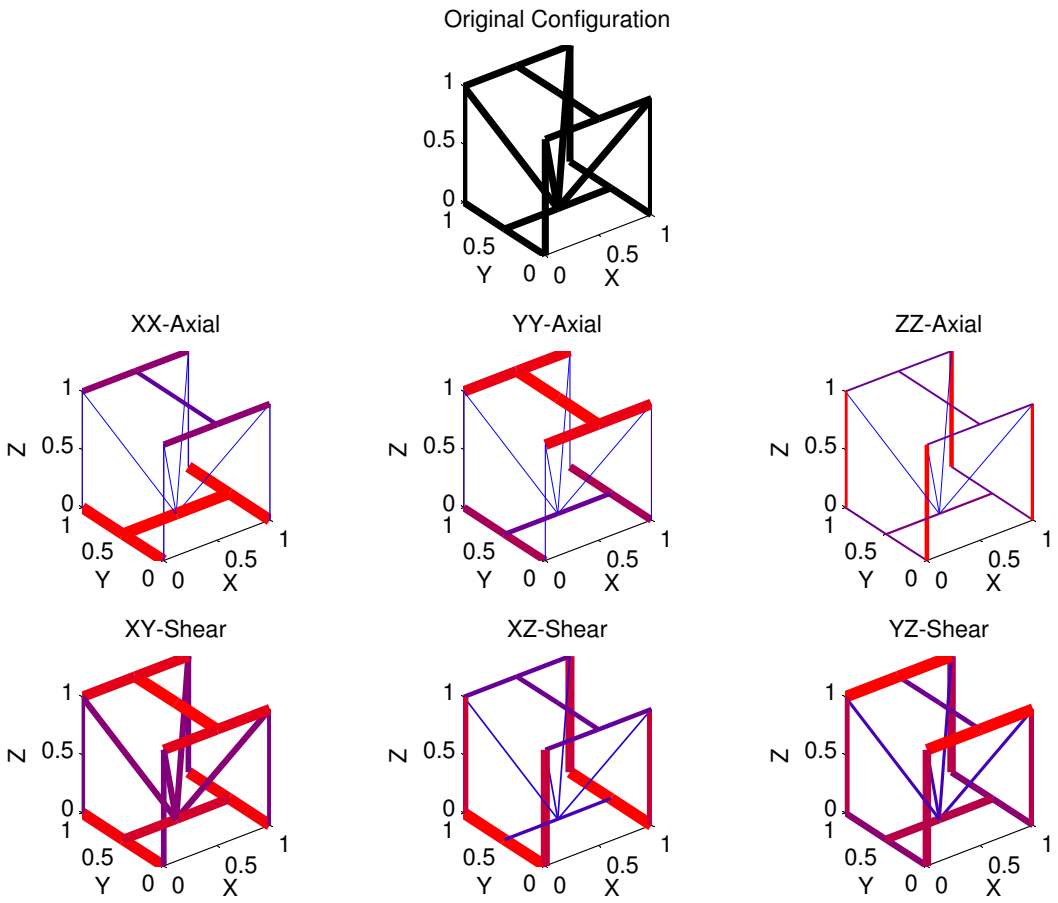

Figure 24: Summary of the Cantley unit-cell configuration.

4.2.2 Cantley

The Cantley configuration, as mentioned in Chapter 2, was developed with the intention of developing a lattice structure that can be developed using a two-part mold for injection molding. However, this structure is also conducive to manufacturing using AM processes. The Cantley configuration features two parallel struts extending along the top surface of the unit-cell. A third and fourth strut run along the middle of the bottom and top of the unit-cell. Diagonal struts connect the top four corners to the middle of the bottom face of the region. The structure also contains four vertical struts along the edges of the unit-cell. In total, there are 14 struts in this configuration. The original and optimized configurations are shown in Figure 24.

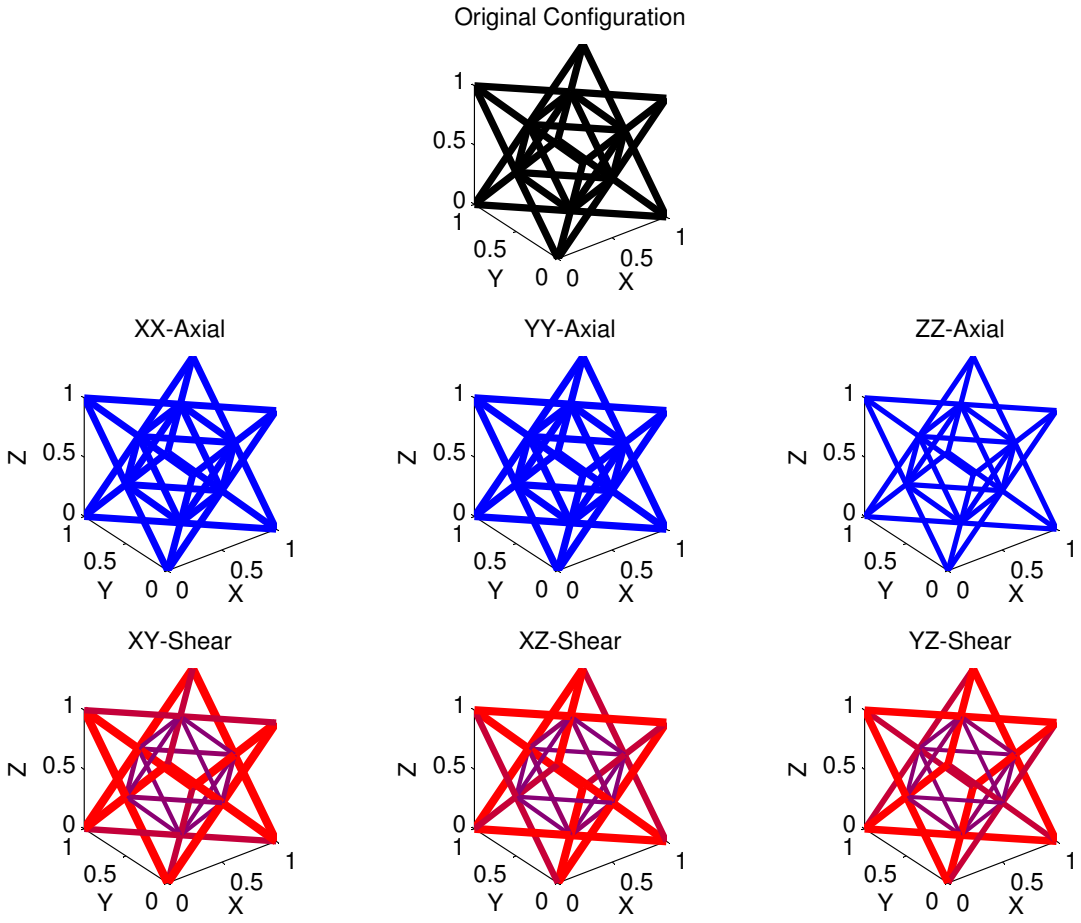

Figure 25: Summary of the octet unit-cell configuration.

4.2.3 Octet

The Octet configuration was developed to minimize bending throughout the mesostructure, allowing the stress and stiffness in the structure to be stretching dominated. It features eight tetrahedrons connected such that one face from each of the tetrahedron also composes one of the faces of an octahedron at the center of the structure. The octet configuration contains a total of 36 struts. The original unit-cell and the optimized configurations are shown in Figure 25.

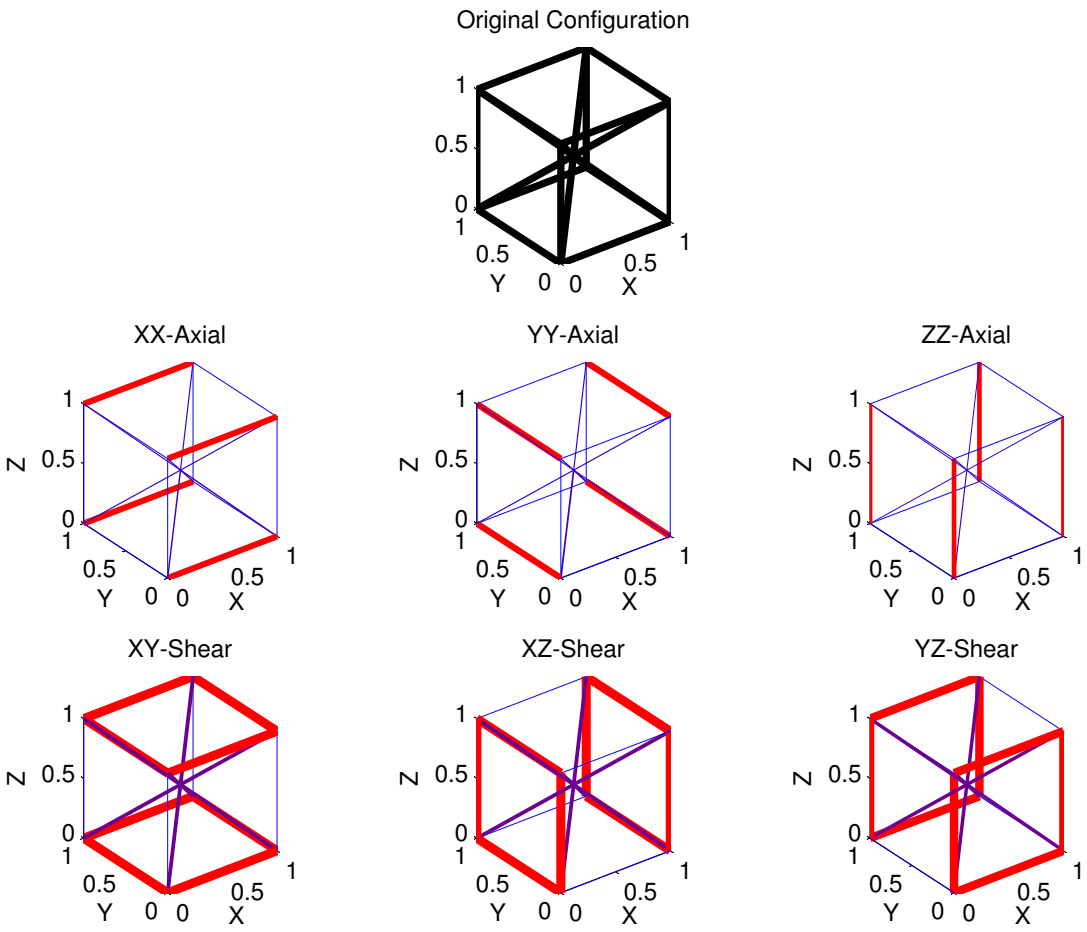

Figure 26: Summary of the diagonal unit-cell configuration.

4.2.4 Diagonal

The diagonal configuration is a configuration inspired by the performance of the crossed configuration. Like the crossed configuration, the diagonal configuration contains struts along each of the edges of the unit-cell region. However, instead of diagonal struts crossing along each face of the cube, only four diagonal members extend through the interior of the unit-cell. The diagonal configuration contains 14 struts. The original unit-cell and the optimized configurations are shown in Figure 26.

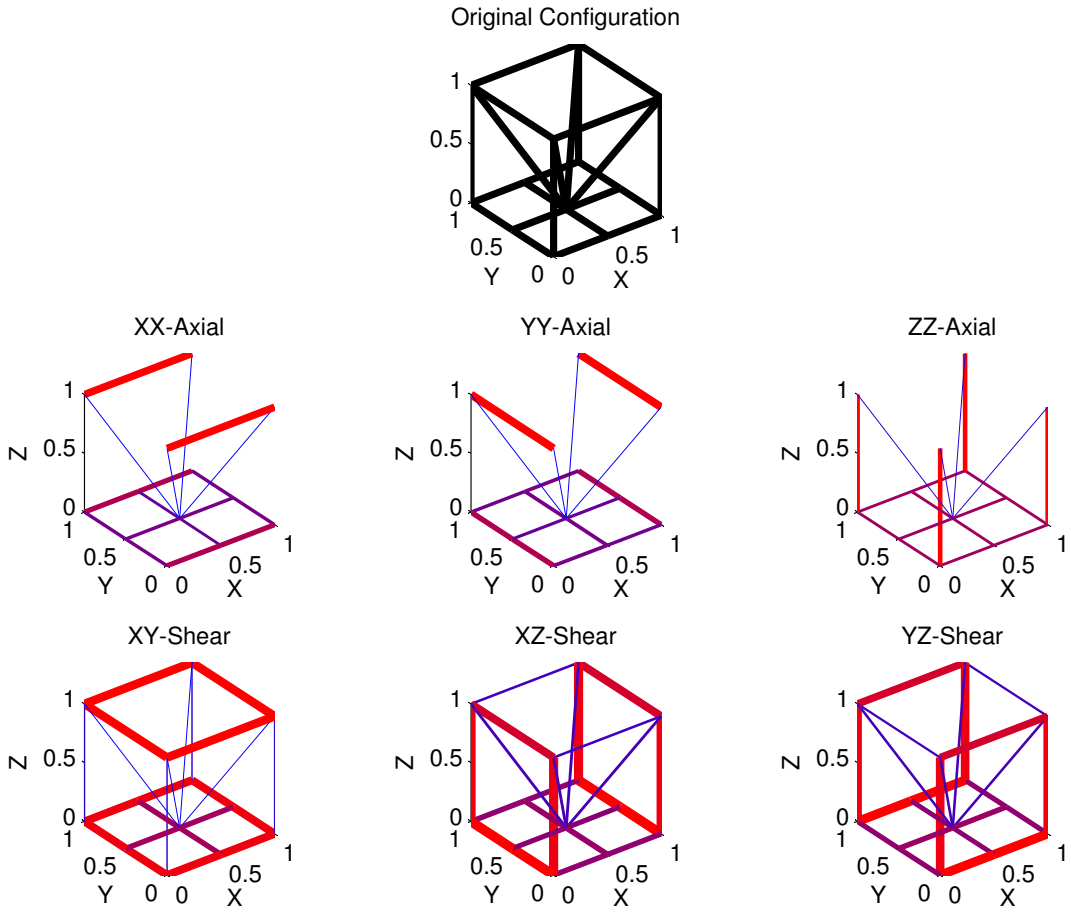

Figure 27: Summary of the first Paramount unit-cell configuration.

4.2.5 Paramount 1 and 2

Both paramount structures are derivative of the Cantley structure and attempt to strengthen various aspects of the Cantley structure. Both configurations still contain the same diagonal struts connecting the top four corners with the midpoint of the bottom face as the Cantley. The first paramount structure, however, contains struts along each each of the region and two struts connecting the midpoints of the bottom edges of the structure. This configuration has a total of 18 individual struts.

The second paramount structure, on the other hand, does not contain any struts on any of the edges of the unit-cell region. Furthermore, rather than a cross at the bottom face, two diagonal beams crossing on the bottom face of the unit-cell. This

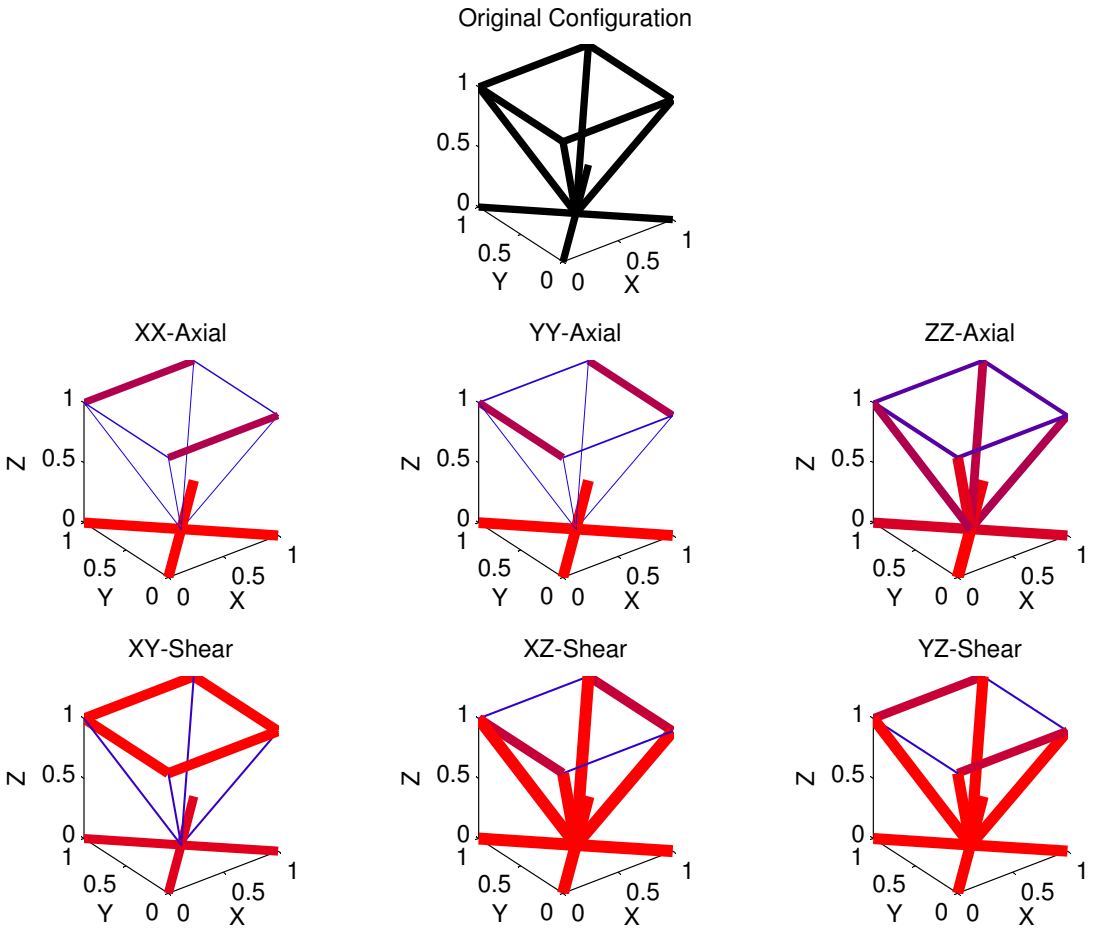

Figure 28: Summary of the second Paramount unit-cell configuration.

configuration has a total of 12 struts.

Both Paramount configurations are shown in Figures 27 and 28, respectively.

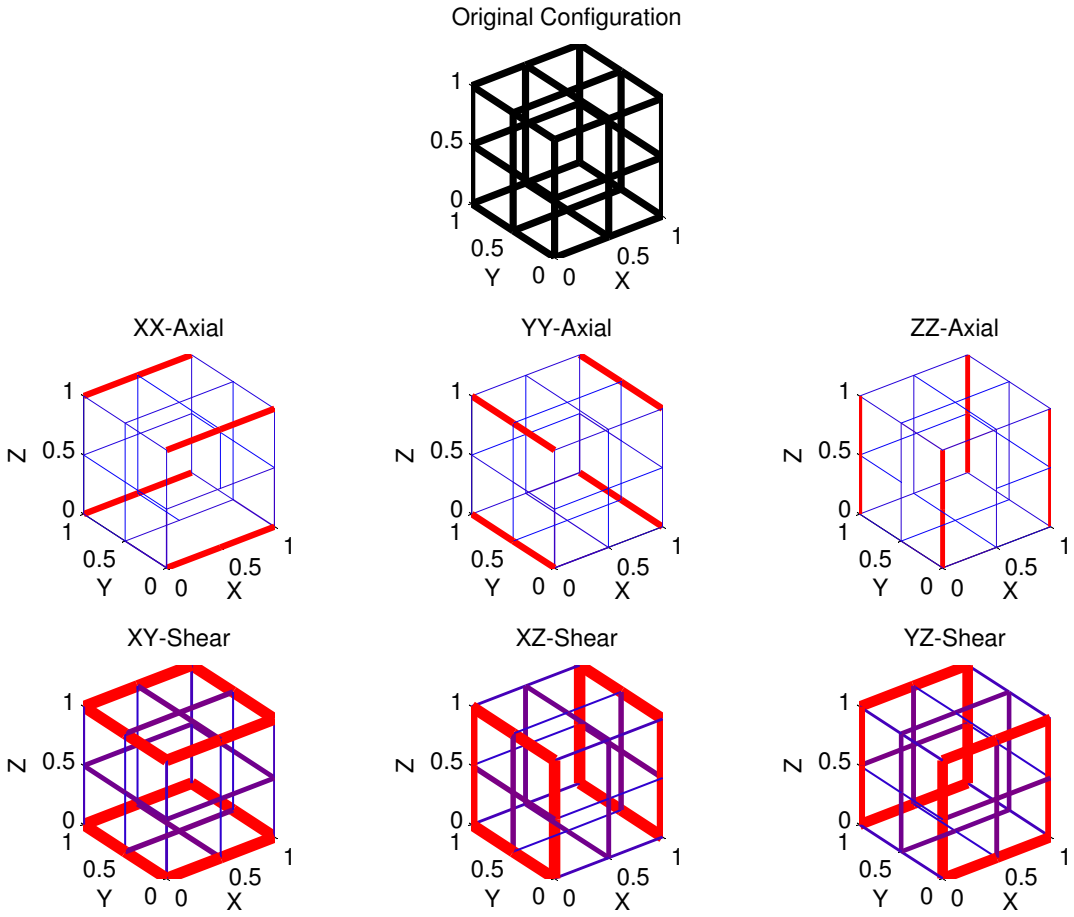

Figure 29: Summary of the midpoint unit-cell configuration.

4.2.6 Midpoint

The midpoint configuration is motivated by the performance of the first paramount structure under shear loading conditions. In particular, the bottom face of the paramount structure was used as the basis for the midpoint structure. In this structure, the midpoints of all the edges of the unit-cell are connected to form crosses on each face of the unit-cell. There are a total of 24 struts in the structure. The original unit-cell and the optimized configurations are shown in Figure 29.

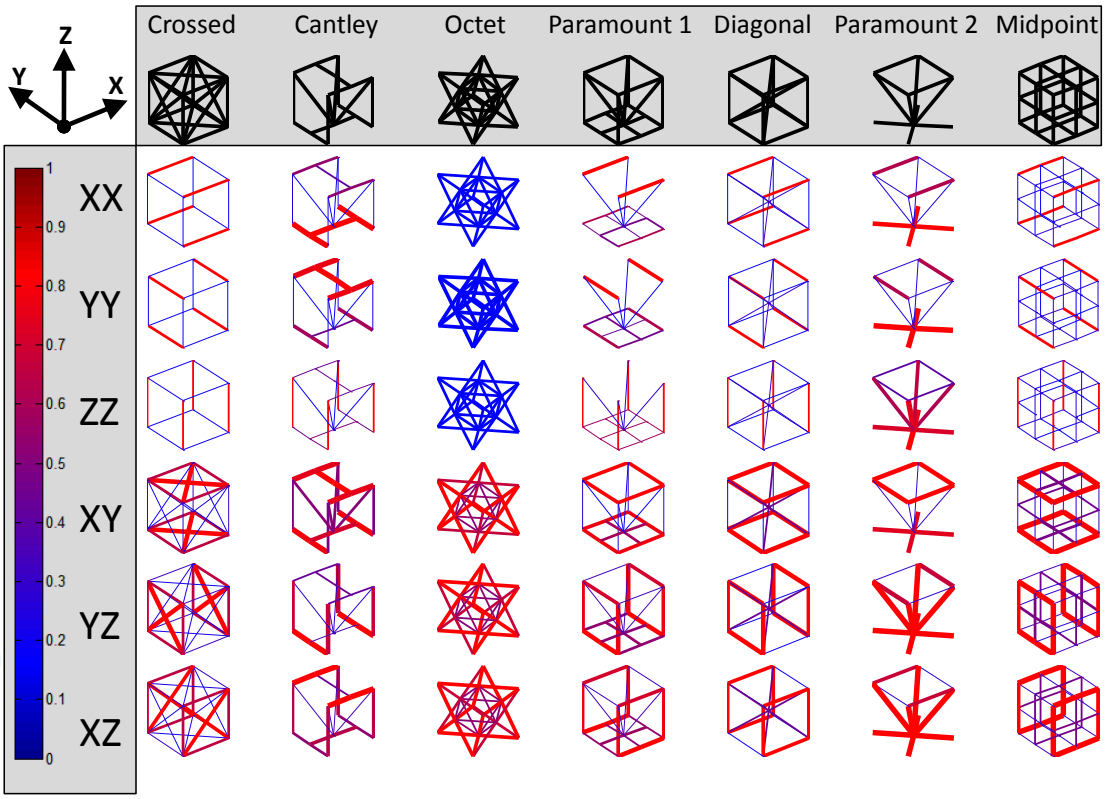

Figure 30: The modified unit-cell library.

4.3 Comparison with the Old Unit-Cell Library

The complete unit-cell library is summarized in Figure 30. The entries in this library form the components of all topologies designed using the SMS method. The original unit-cell library utilized by Graf is shown in Figure 31.

As can be seen from Figures 30 and 31, the modified library is a far more extensive selection than the original library. Another difference between the two libraries is in the optimization process itself. The original library lacked a true methodology for determining strut diameters. It is unknown what optimization was used and what loading conditions were applied. However, the results from this library do not match the results returned using optimization and finite element analysis. Furthermore, the approach seems to only utilize a binary approach to diameter determination: strut values are either 1 or 0, no diameter values exist in between these two values. The

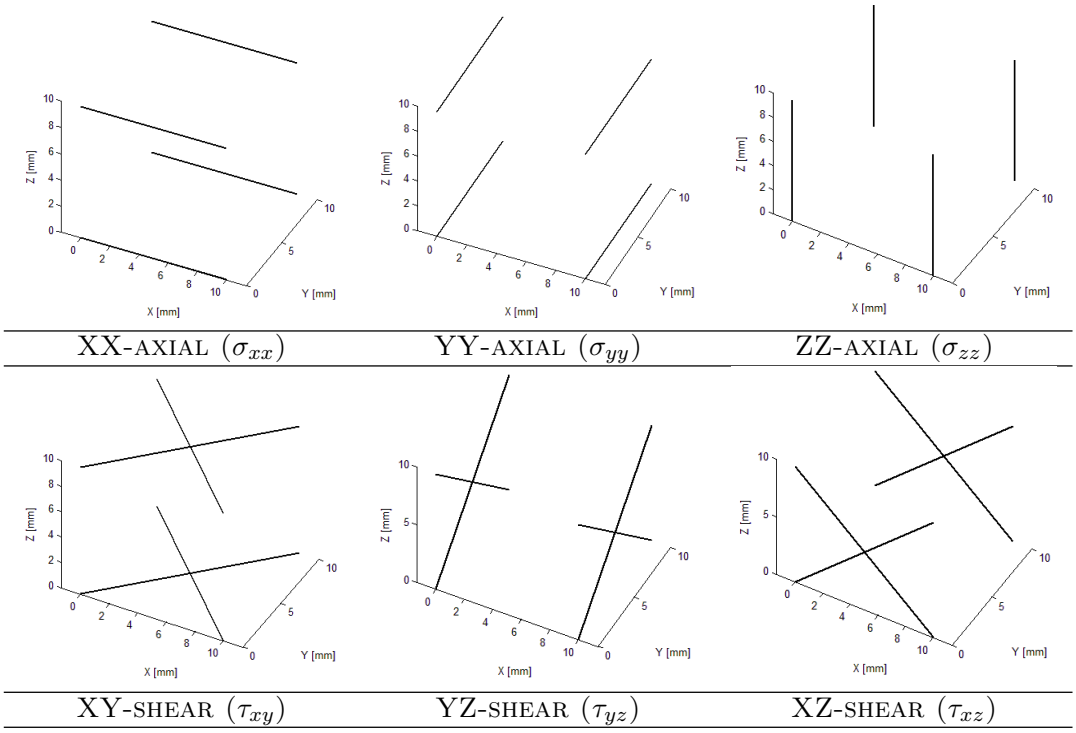

Figure 31: The original unit-cell library.

current library utilizes a more robust and systematic approach for optimizing lattice diameters.

4.4 Topology Generation Using the Unit-Cell Library

Because the original unit-cell library contained only one unique entry, the "crossed" configuration, the topology generation process was relatively straightforward and a selection method was not required. However, because the current library contains more than one entry in the unit-cell library, a selection process must be developed to determine which of the current entries is best suited for selection. For the modified SMS method, the generation of topological configurations is divided into two sequential tasks. First, a unit-cell configuration must be selected. Then, this configuration must be mapped to the unit-cell region of the base lattice. The two tasks are described in the following sections.

4.4.1 Unit-Cell Selection

Because several entries exist in the unit-cell library, a selection criterion must be implemented to estimate the best combination of configurations to maximize the stiffness of the structure. The only way to assess with certainty the best topology for a structure is to iteratively test every possible combination of configurations. For any given unit-cell library, there are:

$$M^N \tag{10}$$

number of possible combinations of configurations, where M is the number of configurations in the unit-cell library and N is the number of unit-cell regions in the structure. Therefore, for a design problem with just 10 unit-cell regions, there are $7^{10} = 282475249$ unique topologies that can be generated. Therefore, it is computationally inefficient to generate topologies in this manner. Instead, a selection heuristic is developed that will attempt to predict the best predict topology of a design problem given using information from different sources.

The original selection equation was based purely on the results from the unit-cell optimization. As mentioned in Section 4.1.1, all configurations were optimized based on a target stiffness constraint. Therefore, all the optimized configurations were assumed to perform identically. The only differing component, therefore, between the configurations was the volume. The structure with the smallest normalized volume would be selected. Consequently, this smaller normalized volume would then allow for more freedom in the diameter determination step of the SMS process. This larger design freedom will ultimately result in a better overall stiffness of the structure. Selection was performed using Equation 11,

$$r = \sum V_\sigma = V_{xx} + V_{yy} + V_{zz} + V_{xy} + V_{xz} + V_{yz} \tag{11}$$

where the rating, r, is determined as the sum of each of the volumes of the six specialized variants of each configuration after they are scaled against the stress values from the solid-body analysis. The configuration with the lowest rating was selected.

When Equation 11 was actually implemented, topologies were successfully generated. However, further investigation determined that these topologies were not actually the best topologies because the selection method was biased toward one particular configuration: the diagonal configuration. Furthermore, this selection method did not take into account the fact that the crossed configuration was not optimized using the same element types as the other configurations or that overlapping struts are not counted in the volume of the structure once the six variants are combined. Therefore, heuristics needed to be added to the rating equation in order to adjust for these observations. This modified selection equation is shown in Equation 12:

$$r = W_v \times (\sum V_\sigma) + W_{vn} \times (V_{net}) + W_p \times (\sum P) \tag{12}$$

where V_σ, V_{net}, and $\sum P$ are all values calculated by the SMS method and W_v, W_{vn}, and W_p are all weighting values that are manually set to vary the importance of $\sum V_\sigma$, V_{net}, and $\sum P$. In particular, two heuristics were added to the rating equation from Equation 11. The first added heuristic, V_{net}, is the net volume of the unit-cells after all six specialized variants are merged and overlapping struts are removed. The second heuristic, $\sum P$, is a value that attempts to estimate the performance of multiple instances of a configuration. The optimization of unit-cells discussed in Section 4.1.2 only characterized the performance of a single instance of a configuration under certain axial and shear loading conditions. However, the configurations in the unit-cell library were observed to behave differently when multiple instances of the configuration are placed alongside one another. The parameter, $\sum P$, attempts to predict the relative performance of these configurations for multiple adjacent instances.

The value for the heuristic, $\sum P$, is determined using values shown in Table 10.

Table 10: The performance table used for selection of unit-cell configurations.

	XX Axial	YY Axial	ZZ Axial	XY Axial	YZ Axial	XZ Axial
Crossed	0.0745	0.0693	0.0375	0.0810	0.0747	0.0752
Cantley	0.5399	0.4885	0.0539	0.5418	0.5353	0.2626
Octet	0.2281	0.2023	0.1050	0.1004	0.0891	0.0863
Paramount 1	0.0917	0.0907	0.0500	0.9865	0.3904	0.3734
Diagonal	0.0743	0.0704	0.0390	0.1166	0.0881	0.0956
Paramount 2	1.0000	1.0000	1.0000	0.6043	0.5569	0.5462
Midpoint	0.1058	0.0955	0.0507	1.0000	1.0000	1.0000

The values in this table, dubbed the "Performance Table," were determined by using empirical results from a design example. This design example is provided in Example 2 of Chapter 5. In this example, a cube with a length of 15 cm was divided into $3 \times 3 \times 3$ unit-cell regions. This cube was then loaded with all six loading conditions simulating the 6 stress values used in the SMS method: σ_{xx}, σ_{yy}, σ_{zz}, τ_{xy}, τ_{yz}, and τ_{xz}. These boundary conditions are equivalent to those in Figure 21. Then, for each loading condition, the SMS method was utilized to generate topologies. However, instead of using a selection metric to select configurations for the structure, each of configuration in the unit-cell library was allocated to the cube. Therefore, 6 loading conditions $\times$ 7 configurations = 42 unique topologies were generated for this problem. The strain energy values from the method were then calculated for each of the topologies. These values were normalized to between 0 and 1 and placed in the performance table. A more detailed explanation of the example problem is provided in Example 2 of Chapter 5.

The value, $\sum P$, is calculated using values from Table 10. For a particular configuration, $\sum P$ is calculated as:

$$\sum P = P_{xx} + P_{yy} + P_{zz} + P_{xy} + P_{xz} + P_{yz} \tag{13}$$

As with Equation 11, the configuration with the lowest rating in Equation 12 is the configuration that is selected. It is important to note that each of the three components of Equation 12 are normalized in order to ensure that one component

does not dominate the equation. The three weighting values, W_v, W_{vn}, and W_p, also ensure that this does not happen. A detailed example of the use of the selection equation is provided in Appendix B.

4.4.2 Mapping

Once the best possible configuration is determined, it is mapped to the current region. This process is completed first by adding nodes from the unit-cell configuration that do not already exist in the unit-cell region. These nodes are added using a 3-D linear interpolation method. Once the nodes have been added to the structure, the elements from the unit-cell configuration are copied to the region by matching the nodes from the configuration with the corresponding nodes in the unit-cell region.

It is important to note that the normalized stress values will only determine the relative size of the struts for each unit-cell configuration in the library. For example, a normalized axial stress of 0.75 will correspond to a normalized strut diameter value of 0.75. Therefore, after the unit-cell mapping is complete, all struts in the structure will have diameter values between zero and one. A diameter value of 1 implies that that particular strut is the thickest in the structure; a value near zero implies that the strut will be very thin or non-existent.

4.5 Research Questions Revisited

The modified unit-cell library addresses the third and final research question presented in Chapter 1. Hypothesis 3 is repeated below:

Hypothesis 3: The addition of unit-cell configurations, such as the Cantley and octet configurations, will provide the SMS method with more options for the generation of the lattice topology. This, in turn, will allow for the placement of unit-cell structures that are better-suited for specific loading conditions, thereby improving structural stiffness. Although the design time will be slightly increased for a larger library, this increased time will be outweighed but the benefit conferred by improved structural performance.

The modified unit-cell library and selection process allow for Hypothesis 3 to be tested by allowing for more than entry to be selected and mapped in the SMS method. In order to test Hypothesis 3, design examples must be pursued using both the original library and the modified library. If Hypothesis 3 is indeed correct, the second library and selection process should result in topologies with superior stiffness characteristics. This hypothesis will be tested in Chapter 5.

4.6 Summary

In this chapter, the modified unit-cell library was formulated and presented. The library, as shown in Figure 30, contains seven unique configurations with each configuration containing six "variations" for each of the six stress values from the solid-body stress analysis for a total of 42 entries. The seven configurations are composed of some well-documented configurations, such as the octet and Cantley configurations, and several newly developed configurations, such as the Paramount variations and the "Crossed" configuration. In addition to the presentation of the current unit-cell library, the systematic optimization process for optimizing these configurations was also formulated and outlined. Using this process, any unit-cell configuration that conforms to certain guidelines can be added to the unit-cell library.

Along with the expansion of the unit-cell library, the selection and mapping process of the unit-cells was modified. Because the original library contained only one configuration, the tasks of mapping unit-cell configurations was relatively simple. However, in order to determine which configuration is best-suited for a specific region, a selection process was developed using three different selection criteria.

In the following section, both the modified SMS method and unit-cell library will be validated against various design examples.

CHAPTER V

DESIGN EXAMPLES

In order to validate the modified SMS design methodology, it will be applied toward design examples of varying complexity. The first example is a 2-D simply-loaded beam, which is a modified version of an example presented in Graf's thesis. This example is primarily utilized to test the modified SMS method and compare it to the results from the first SMS method. The second example, a simple 3-D cube, will attempt to test the various entries in the unit-cell library in order to gauge and predict the performance of the various entries of the library. The results from this example will actually be used in the selection process for both examples 3 and 4. The third example, also a modified version of an example problem from Graf's work, is a 3-D cantilever beam. In this example, both the modified SMS method and unit-cell library will be tested. The fourth and final example, a modified L-bracket, will combine both the modified method and unit-cell library to a design problem that is too complex to be solved using optimization. For each example, each step of the SMS method will be applied and the results of each step will be discussed. Of particular note is that for each example, the sixth step will be completed using three different methods: the 28% Assumption as noted by Graf [27], the nonlinear, constrained minimization optimization approach using the active-set algorithm, and the least-squares minimization method using the Levenburg-Marquardt algorithm. These three methods will be evaluated in two ways: level of ability in satisfying constraints, and overall analysis time. Ultimately, the goal is to determine which method is most efficient method for sizing diameter values in the truss structure and determine under what conditions each method can be best utilized. In addition, a

manual grid search will be performed on D_{min} and D_{max} for Examples 1, 3, and 4 in order to simulate the approach taken by the original SMS method if the 28% assumption were not used. The results from this grid search will be compared to the three proposed optimizations in order to assess whether optimization is indeed a better approach than the original grid-search. Furthermore, results from Example 1 and 3 will be compared to results from the previous version of the SMS method [27]. All examples are implemented using the ANSYS finite-element analysis tool and the MATLAB technical computing software distribution.

Another important issue to mention is in the fifth step of the SMS method. As mentioned in Chapter 3, the removal of unessential struts in topologies lacks a consistent and robust method for unessential strut removal. In previous work, Graf mentioned used the concept of a "cutoff" diameter to accomplish this task. After the struts in the structure had been sized, a final sub-step was implemented that removes small diameters that contribute little to structural performance. To accomplish this topology alteration, a third diameter was introduced: D_{cutoff}. D_{cutoff} is a diameter between D_{min} and D_{max} such that any struts that fall below this diameter value are discarded. In this work, D_{cutoff} is set as,

$$0.025 \times (D_{max} - D_{min}) + D_{min}, \tag{14}$$

or the lower 2.5% of values between D_{min} and D_{max}. The D_{cutoff} method utilized by Graf proved to be effective for simpler structures. However, as will be seen in Example 4, it will not be sufficient for more complex examples. The D_{cutoff} method will be utilized in all the example problems except Example 4.

Table 11 shows each example problem and its intended relationship with the three research questions.

Table 11: Correlation between the example problems and the research questions.

	RQ1: Can a systematic, non-iterative method for the design mesoscale truss structures be developed to determine strut diameters for topologies designed using the unit-cell approach?	**RQ2: Can the two-variable optimization proposed in Hypothesis 1 be simplified in order to decrease analysis time?**	**RQ3: Will the expansion of the unit-cell library to include additional unit-cell configurations improve the performance of structures designed using the SMS method? If so, will the added benefit justify an increased overall design time?**
EX1: 2-D Simply-Loaded Beam	●	●	✕
EX2: 3-D Cube	✕	✕	●
EX3: 3-D Cantilever Beam	●	●	●
EX4: 3-D L-Bracket	●	●	●

● - Addressed

✕ - Not Addressed

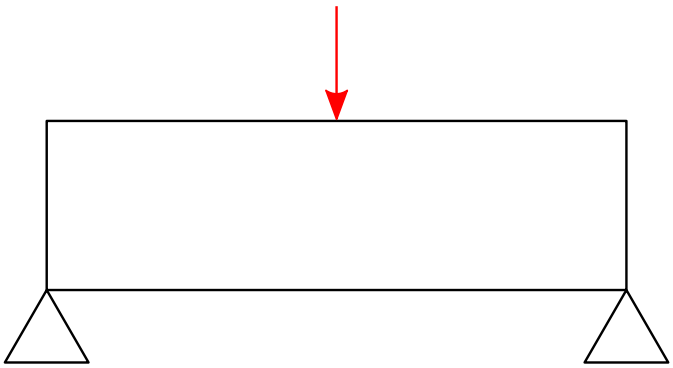

Figure 32: Problem representation of the 2-D simply-loaded beam design problem.

Table 12: Initial properties for the 2-D simply-loaded beam.

Length (m)	6	Unit-Cells Along Length	24
Height (m)	1	Unit-Cells Along Height	4
Loading Magnitude (kN)	200	Total Unit-Cell Count	96
Elastic Modulus (N/m)	2×10^{11}	Target Volume (m^2)	0.02

5.1 Example 1: 2-D Simply-Loaded Beam

5.1.1 Problem Description

The first example is a 2-D example: a simply-loaded beam. This example is an extension of a design problem proposed by Graf. The premise of this example is to reduce the weight of the structure as much as possible without sacrificing stiffness at the central point load of 200 kN. The beam is 6 m long and 1 m in height. As seen in Table 11, this example problem exclusively addresses the first and second research questions related to the determination of diameter values. The definition of the problem is shown in Figure 32. Table 12 summarizes all the initial geometric and analytical conditions for the design problem.

5.1.2 Ground Geometry and Solid-Body Analysis

The beam in Figure 32 is divided into the desired number of unit-cells specified in Table 12. An image of the beam split into the appropriate number of unit cells is shown in Figure 33. The solid-body stress results for the simply-loaded beam are shown in Figure 34.

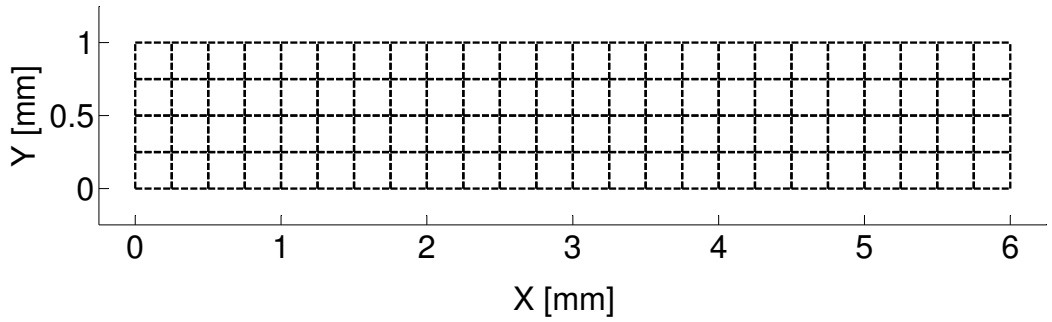

Figure 33: Ground geometry of the 2-D simply-loaded beam.

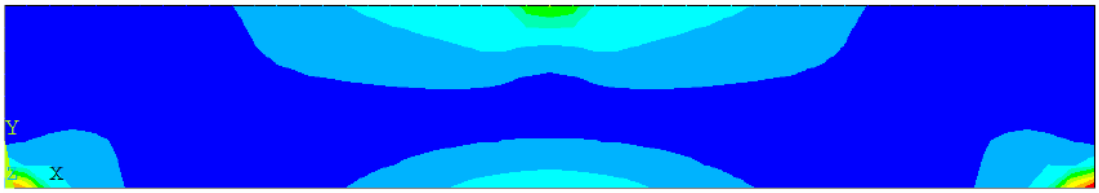

Figure 34: Solid-body analysis of the 2-D simply-loaded beam.

5.1.3 Topology Generation

Figures 35 and 36 show the topologies generated by the SMS method before and after the cutoff diameter is implemented. From Fig. 35 it can be seen that the completed topology closely matches intuitive understanding of the design problem. Firstly, the truss structure is symmetric across the beam. Secondly, the struts are thickest at the loading point, the center of the structure, and at the bottom corners of the structure; struts are thinnest at the top corners and at the mid-lower portions of the beam. Additionally, the effect of the cutoff diameter can be seen here: the struts at the top corners of the beam have been removed.

5.1.4 Diameter Determination

For this problem, three diameter determination problems were explored: the 28% assumption, 1-variable optimization, a two-variable, non-linear, constrained optimization, and a non-linear least-squares regression approach. For each of the determination methods, five separate trials were completed. The average values for D_{min}, D_{max},

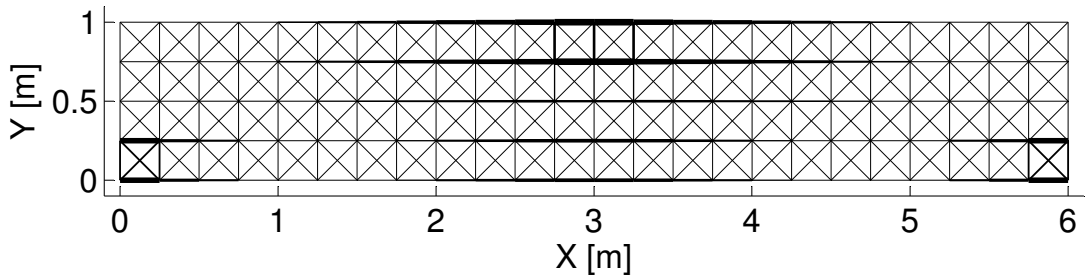

Figure 35: Topology of the 2-D simply-loaded beam before the cutoff diameter is implemented.

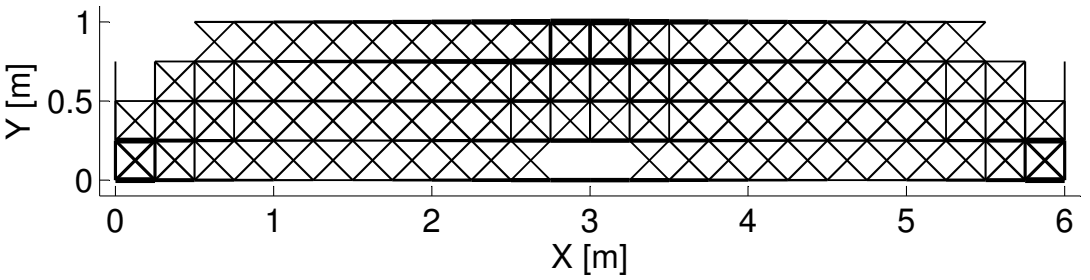

Figure 36: Completed topology for the 2-D simply-loaded beam.

D_{cutoff}, D_{min}/D_{max}, design time, volume, and stiffness were taken. For this example, the displacement of the loaded node was used as the primary metric for stiffness. For all three methods, the upper and lower bounds for D_{min} and D_{max} were set to 0.01 m and 10 m, respectively. The results from the five iterations for each of the three methods are shown in Appendix C.

In order to verify the accuracy of the three diameter sizing methods, a design space exploration/grid search was also conducted on the normalized topology. This exploration was performed by iterating both D_{min} and D_{max} from 0.01 m to 0.05 m in increments of 0.001 m. The combination that returned the smallest value of the objective function in Equation 4 was saved. It is also important to note that the increment size is set to 0.001 m, a relatively coarse value, in order to reduce analysis time. A finer increment was not necessary because the design exploration is needed only to gain a rough estimate of where optimal D_{min} and D_{max} values should lie. The results of the exploration are plotted in Figure 37. The best values from the

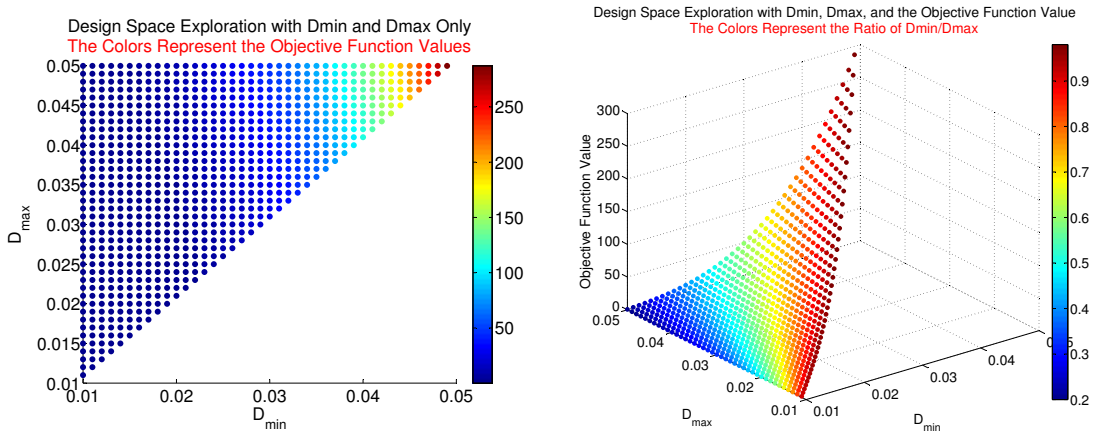

Figure 37: Plot of the design space for the 2-D simply-loaded beam.

Table 13: Optimal design space exploration for the 2-D cantilever beam.

Deflection (m)	0.0118
Volume (m^2)	0.202
Design Time (s)	468.9431
D_{min} (m)	0.0100
D_{max} (m)	0.0380
D_{cutoff} (m)	0.0107
D_{min}/D_{max}	26.32

exploration are shown in Table 13.

5.1.4.1 Results Summary

Table 14 summarizes the average values from all three sizing methods. It also includes the results of the design space exploration for comparison. Table 14 shows that all three methods are able to attain the target volume of 0.02 m^2 and return similar values for deflection (0.0119 m). These results are in-line with the results returned from the grid search and from the previous SMS method [27]. All methods also return similar values for D_{min}, D_{max}, and D_{cutoff}. Furthermore, the ratio of D_{min}/D_{max} are very close, with values ranging from 27% to 28%. The main differing component between the three sizing methods is the design times. Because only one variable needs to be determined, the 28% assumption converges the most quickly at roughly 19 seconds. This design time is less than half of the second-fastest method: the constrained

Table 14: Diameter determination results for the 2-D simply-loaded beam.

	28% Assumption	Constrained Optimization	Least-Squares Minimization	Design Space Exploration
Deflection (m)	0.0119	0.0119	0.0119	0.0118
Volume (m^2)	0.0201	0.0201	0.0201	0.202
Design Time (s)	18.9770	39.4111	107.1327	468.9431
D_{min} (m)	0.0103	0.0100	0.0100	0.0100
D_{max} (m)	0.0369	0.0378	0.0378	0.0380
D_{cutoff} (m)	0.0110	0.0107	0.0107	0.0107
D_{min}/D_{max}	28.00	26.43	26.45	26.32
Objective Function Value	0.0143	0.0143	0.0143	0.0143

optimization using the active-set algorithm. The least-squares minimization took by far the longest time to converge, with an average design time of 107 seconds. This design time is roughly 5.6 times longer than the 28% assumption and 2.7 times slower than the constrained optimization methods. Although the design space exploration is able to return nearly identical results for the objective function, it is the slowest method, taking more than four times longer than the least-squares approach and more than 24 times longer than the 28% assumption.

5.1.5 Discussion and Conclusion

The first design problem, a simple 2-D beam, was implemented to test the modified SMS for a simple, intuitive problem in two dimensions. In particular, the design problem attempted to test the final diameter determination step of the modified method for a simple design problem. From these results, several important observations can be made. They are summarized below:

- All three sizing methods are able to return nearly identical results for D_{min} and D_{max} and, consequently, are all equally capable of returning accurate results for the diameter sizes of struts developed using the SMS method.

- When compared to the design space exploration, all three optimization-based

methods are able to converge to similar results. This result confirms that optimization is a viable approach for determining the diameter values for mesoscale truss structures design using the SMS method.

- A full design-space exploration, even with a relatively coarse increment value, is a time-consuming process and is not preferred.

- Between the two-variable methods, the constrained optimization approach apparently converges more quickly than the least-squares regression approach. These results indicate that, of the two-variable approaches, this approach is superior for the SMS method in two dimensions.

- The one-variable optimization utilizing the "28% assumption" is able to converge to the same optimal values returned by two-variable optimization and an iterative search of the design space. Such a result confirms, at least initially, that this assumption is a viable option.

5.1.6 Research Questions Revisited

The results listed above can be further applied to the research questions and hypotheses presented in Chapter 1. Hypotheses 1 and 2 in particular are addressed. They are repeated below:

Hypothesis 1: By utilizing the unit-cell approach and combining it with a constrained optimization of two diameter values: a minimum allowable diameter and a maximum allowable diameter, against volume and stiffness constraints, a systematic design method can be developed for the design of mesoscale truss structures. By exploring various optimization approaches and selecting the best method, analysis time can be minimized and structural performance can be maximized.

The results from this example show that an optimization approach for D_{min} and D_{max} does, indeed, return the best diameter values for a two dimensional simply-loaded beam. The results from both constrained minimization and least squares regression returned diameter values close to the best values found by the design space exploration. Furthermore, both methods are considerably faster than design space exploration, indicating that an optimization approach is superior to an exhaustive search of all D_{min} and D_{max} values. Therefore, for the first example, Hypothesis 1 remains valid.

Hypothesis 2: By exploring and analyzing the optimal minimum and maximum diameter values for meso-scale truss structures designed using the Size, Matching, and Scaling method, a direct relationship between these two values can be determined and exploited. This relationship will allow for one of the two diameter values to be expressed as a function of the other. Consequently, the two-variable minimizations outlined in Hypothesis 1 can be simplified to a one-variable minimization problem, thereby reducing overall design time.

The results from this example show that a 28% assumption is able to return identical results to the values returned by both two-variable optimization methods as well as the design space exploration. Also, the approach is able to reduce design time significantly, with a more than two-fold decrease in optimization time. Therefore, for the 2-D simply-loaded case, it appears that a 1-variable assumption holds and is appropriate for use. Therefore, for the first example Hypothesis 2 is valid.

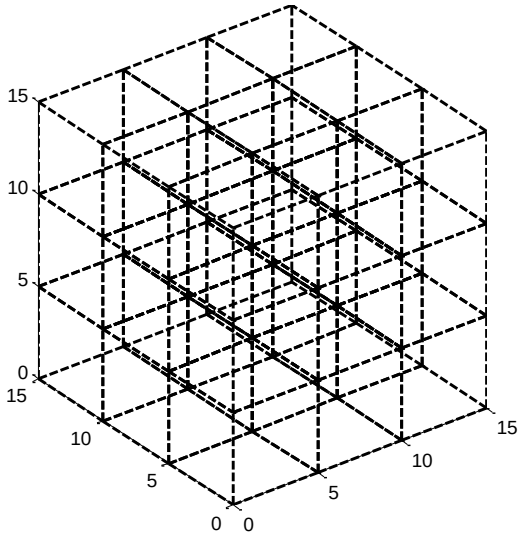

Figure 38: Base lattice for the unit-cell configuration analysis.

Table 15: Initial geometric and loading values for unit-cell configuration analysis.

Length (cm)	15
Width (cm)	15
Height (cm)	15
Elastic Modulus (N/cm)	1960
Unit-Cell Size (cm)	10
Total Unit-Cell Number	27
Target Volume (cm^3)	150

5.2 Example 2: Unit-Cell Library Analysis

5.2.1 Problem Description

The purpose of the second example problem is to utilize each of the seven unit-cell configurations in the unit-cell library and test them against general shear and axial loading conditions in order to gauge and compare their individual performances. In this problem, a 15 cm×15 cm×15 cm cube is supplied with the same general axial and shear loading cases provided for the unit-cell optimizations, shown in Figure 21. The main difference in this example, however, is that the cube is divided into a 3×3×3 configuration of unit-cells in order to test the performance of multiple instances of the same configuration. The ultimate objective of this example is to provide insight into the performance of the various configurations when multiple instances are used

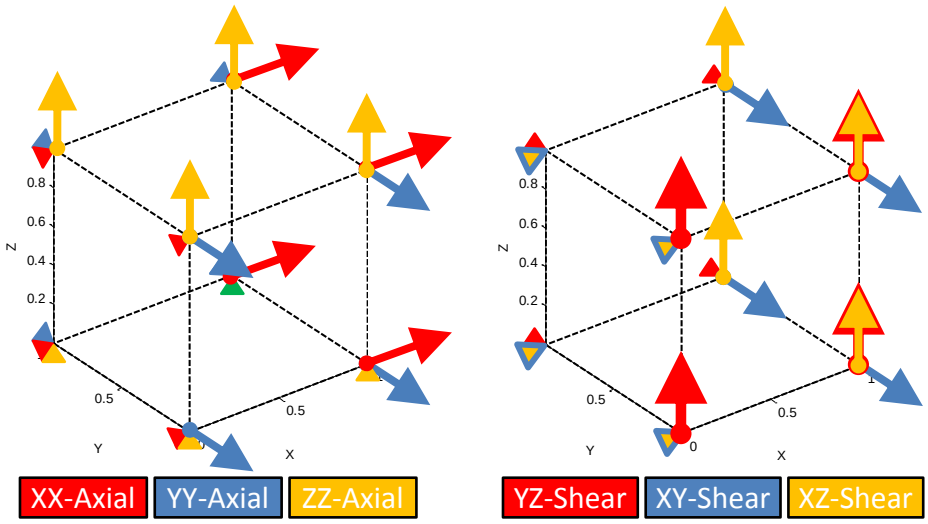

Figure 39: The loading conditions for unit-cell optimization.

and to use this information to improve the selection process for structures developed using the SMS method.

The base lattice configuration for the problem is shown in Figure 38. Table 15 summarizes the initial geometric and loading values for the problem.

For the example shown in Figure 38, there are six separate loading and boundary conditions applied to the structure. Each of these loading conditions approximates the six axial and shear stresses present in the SMS method and are identical to the loading conditions used for unit-cell optimization shown in Figure 21. These loading conditions are shown again in Figure 39.

For each of these loading conditions, all of the seven configurations in the library will be applied. Therefore, for this design example, 42 separate topologies will be generated using the SMS method. The results will then be compiled. Then, the strain energies and volumes of the resultant topologies will be compared. These results will be normalized and plugged directly into the performance table in Table 10 used in Equation 12.

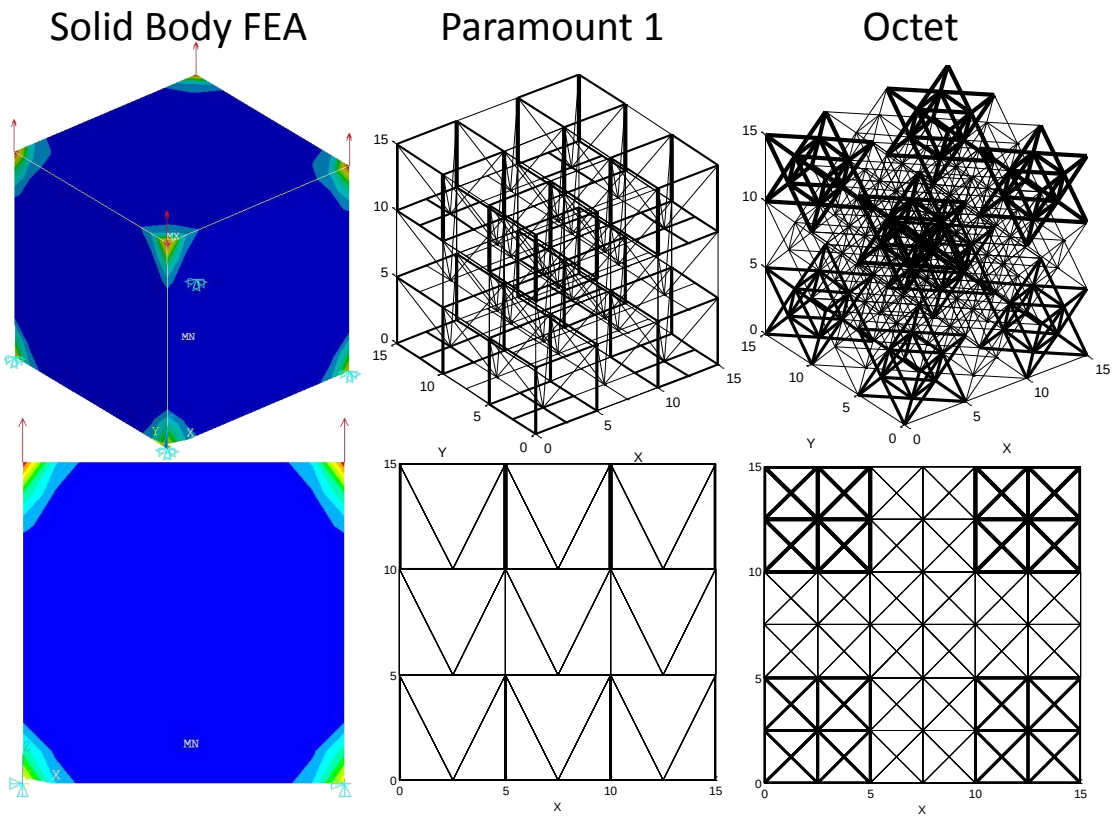

Figure 40: 3-D and side views of the paramount 1 and octet SMS topologies for the ZZ loading case.

5.2.2 Results

Because there are 42 separate topologies generated for this problem, not all of them are shown. Instead, two of the topologies are shown in Figure 40 for the ZZ axial loading case. After the SMS method was completed for each of the 42 examples, these 42 topologies were then imported into the ANSYS finite element package and analyzed for strain energy and volume. The volumes and strain energies were then taken for each of these values. The resultant values are shown in Tables 16 and 17.

From Table 17, it can be seen that all configurations were able to achieve the target volumes within the range of 150 cm^3 to 160 cm^3. However, as Table 16 shows, the resultant strain energies vary considerably. In the axial directions, the crossed, diagonal, first paramount, and midpoint configurations all perform well, with strain

Table 16: Strain energies for the various unit-cell configurations and loading scenarios.

	XX Axial	YY Axial	ZZ Axial	XY Axial	YZ Axial	XZ Axial
Crossed	7.2219	7.7939	8.2561	42.2065	43.7735	45.5494
Cantley	52.3657	54.8995	11.8527	282.3490	313.6932	159.0399
Octet	22.1299	22.7410	23.0924	52.3284	52.2103	52.2435
Paramount 1	8.8953	10.1965	11.0039	514.0857	228.7971	226.1189
Diagonal	7.2077	7.9123	8.5831	60.7725	51.6522	57.9218
Paramount 2	96.9992	112.3950	219.9493	314.9413	326.3808	330.7908
Midpoint	10.2618	10.7366	11.1471	521.1452	586.0577	605.6265

Table 17: Resultant volumes for the various unit-cell configurations and loading scenarios.

	XX Axial	YY Axial	ZZ Axial	XY Axial	YZ Axial	XZ Axial
Crossed	149.9245	149.9245	149.9245	149.9406	149.9421	149.9437
Cantley	150.3048	150.0996	149.9253	151.7035	152.3611	153.4423
Octet	149.9273	149.9273	149.9272	149.9456	149.9455	149.9453
Paramount 1	149.9248	149.9251	149.9255	155.2938	150.8447	150.8175
Diagonal	149.9244	149.9245	149.9247	149.9617	149.9524	149.9591
Paramount 2	149.9713	149.9836	160.4172	151.2174	150.7451	150.7619
Midpoint	149.9249	149.9252	149.9253	155.5136	156.9949	157.1381

energies at or below 11 cJ. On the other hand, the cantley, octet, and paramount 2 configurations all perform fairly poorly, with the second paramount performing the worst of all the configurations. In the shear directions, the results are different. This time, the crossed, octet, and diagonal configurations all perform well, with average strain energies less than 100 cJ. The remaining four configurations, the cantley, paramount 1 and 2, and the midpoint all perform poorly, with the midpoint configuration having the worst performance. If the configurations are ranked for their performance, it can be seen that the crossed configuration excels in all six directions. Therefore, given these results, the crossed configuration should be the most preferred. The only other configuration that could be any competition would be the diagonal configuration.

The strain energy results from Table 16 are normalized and used for the performance table in the second selection method discussed in Section 4.4.1.

5.2.3 Discussion and Conclusion

In this example, the modified SMS method was utilized with the new unit-cell library in order to characterize the performance of the various configurations of the unit-cell library for various axial and shear loading scenarios. From the strain energy results, conclusions about the performance of each entry in unit-cell library can be drawn:

- It appears that the crossed configuration is the superior configuration for all six loading scenarios: XX, YY, ZZ axial and XY, YZ, XZ shear.
- The Cantley configuration performs poorly in nearly all directions except the Z-axial direction. This is due to the asymmetric nature of the configuration and the lack of trusses in all directions except the Z-direction.
- The octet configuration performs well in the shear directions, surpassed only by the crossed configuration. However, the axial directions do not perform nearly as well as other configurations in the library.
- Both paramount configurations perform very poorly in the shear directions. This is most likely because the configurations are very similar to the Cantley configuration in that they contain very few struts that resist shear force. However, the first paramount configuration performs significantly better than its counterpart in the shear directions.
- The diagonal configuration performs well in both shear and axial directions. As can be seen, its performance in axial directions is nearly identical to that of the crossed configuration. However, in shear conditions, it performs slightly worse. It can therefore be seen that the diagonal configuration is the main competition for the crossed configuration.
- The midpoint configuration, like the first paramount, performs well in the axial directions but poorly in the shear directions. According to Table 16, the

midpoint configuration performs the worst of all the configurations in shear.

The strain energy results were normalized and then utilized directly in the selection process for future examples utilizing the modified unit-cell library.

5.2.4 Research Questions Revisited

This second example problem specifically addresses the third hypothesis, shown below:

> **Hypothesis 3**: The addition of unit-cell configurations, such as the Cantley and octet configurations, will provide the SMS method with more options for the generation of the lattice topology. This, in turn, will allow for the placement of unit-cell structures that are better-suited for specific loading conditions, thereby improving structural stiffness. Although the design time will be slightly increased for a larger library, this increased time will be outweighed but the benefit conferred by improved structural performance.

Although Hypothesis 3 cannot be directly addressed by this example, the strain energy energy results from Table 16 can help predict which configurations are best for selection. If axial stresses dominate the problem, then it is likely that the crossed, diagonal, paramount 1, or midpoint configurations will be selected. On the other hand, if shear stresses dominate, then the crossed, octet, and diagonal configurations are most likely to be selected. However, the crossed configuration appears to perform the best overall in all directions. Therefore, it is likely that this configuration is the only one that needs to exist in the library. If so, then Hypothesis 3 will likely be proved incorrect. More example problems must be pursued, however, to determine if this statement is true.

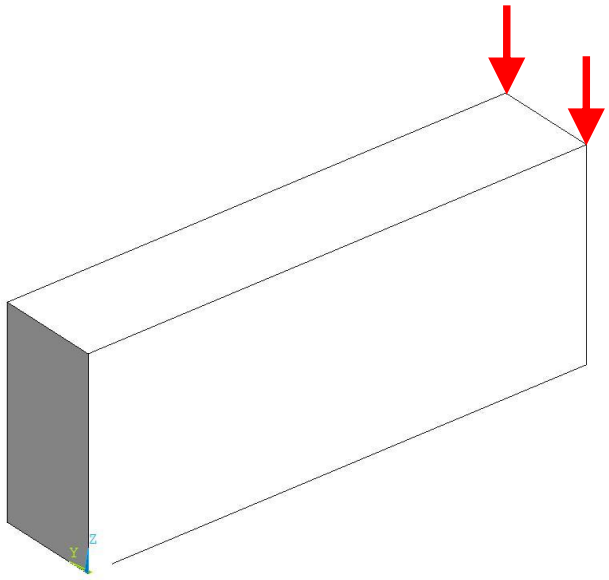

Figure 41: Problem definition of the 3-D cantilever beam example.

Table 18: Initial properties for the 3-D cantilever beam example.

Length (mm)	50	Total Unit-Cell Count	10
Width (mm)	10	Unit-Cells Along Length	5
Height (mm)	20	Unit-Cells Along Height	2
Loading Magnitude (N)	10	Unit-Cells Along Width	1
Elastic Modulus (N/mm)	1960	Target Volume (mm^3)	1600

5.3 Example 3: 3-D Cantilever Beam

5.3.1 Problem Description

The third example is a simple, three-dimensional, rectangular cantilever beam. The beam is fixed at its base and has two vertical point loads supplied on the two upper corners at the tip of the beam. A physical representation of the design problem is shown in Figure 41. Ultimately, the primary goal of the first example will be to test the functionality of the SMS methodology through the use of a simple, intuitive, example problem in three dimensions. The dimensions, loading magnitudes, and material properties of the structure are provided in Table 18. In addition to the physical properties, the truss structure is to have other target unit-cell configuration properties. These properties are also summarized in Table 18.

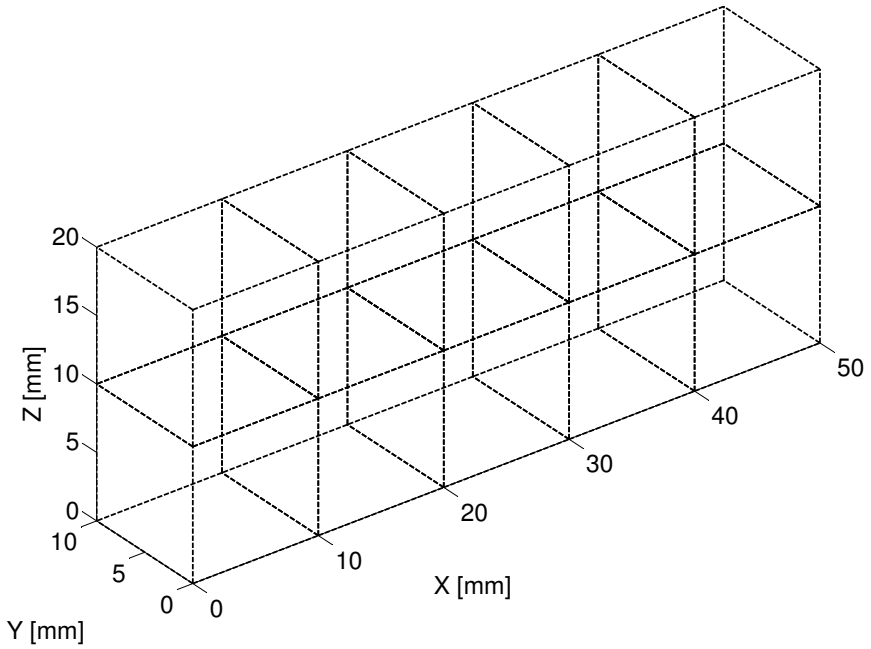

Figure 42: The 3-D cantilever beam structure divided into unit-cell regions.

5.3.2 Ground Geometry and Solid-Body Analysis

The cantilever beam is created with the desired unit-cell divisions provided in Table 18. An image of the cantilever beam split into the appropriate number of unit cells is shown in Figure 42. In addition to the base lattice generated in Figure 42, a base lattice was generated where the number of unit-cells was increased from 10 to 40 by decreasing the size of the unit-cells manually. This base lattice is shown in Figure 43. This "higher resolution" base lattice was generated in order to understand the impact of unit-cell size on the performance of the structure.

Figure 44 shows the solid-body cantilever beam created in ANSYS with the appropriate bounding and loading conditions applied. Of particular interest is the X-component (along the beam) of the the stress distribution, also shown in Figure 44.

From the solid-body analysis of the structure, some important observations can be made. First, it can be seen that highest stresses occur at both the tip of the beam where the load is applied and the upper base of the beam. In general, the stress

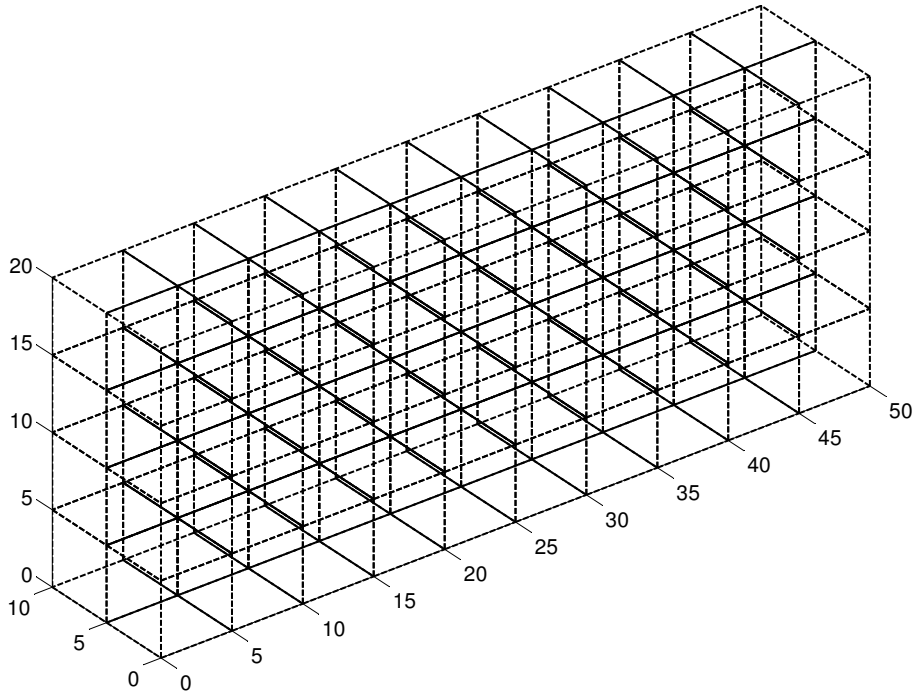

Figure 43: The base lattice of the cantilever structure with the number of unit-cells quadrupled.

values decrease moving down from the top to the bottom of the beam and along the beam from the tip to the base. It can also be seen that the stress distribution for the beam is symmetrical along the width of the beam.

From these observations, some inferences can be made about the potential shape topology of the truss structure. First, it can be expected that the largest diameter values will be along the x-axis (length) of the beam. Furthermore, the symmetrical distribution of the stress implies that the diameter values will also be symmetrical along the width of the beam. Finally, it can be expected that the struts will be thickest at the base of the beam and at the point where the load is applied; the struts should be thinnest at the lower and middle portions of the beam.

With the unit-cell regions unambiguously defined, the results from the solid-body analysis can be mapped to the structure. A total of six stress values were determined for each unit-cell, three associated with tensile stress along the X, Y, and Z directions

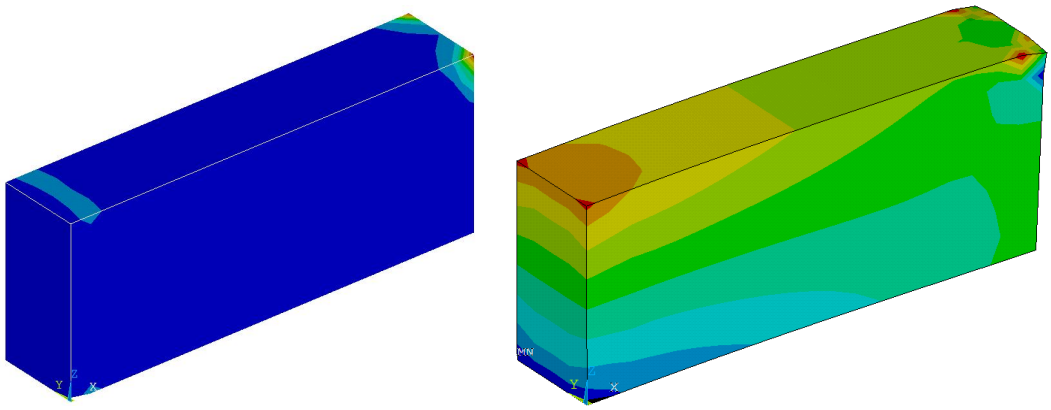

Figure 44: (Left) von Mises solid-body results for the cantilever beam. (Right) X-component results for the cantilever beam.

and three associated with shear stresses along the XY, XZ, and YZ planes. Once all the stress values are known, the unit-cell library can be used to determine the location and sizes of the struts to use in each unit-cell. For this example, both the original and modified unit-cell library are utilized to generate the topology of the structure.

5.3.3 The Original Unit-Cell Library

The topology generated by the first unit-cell library in step 4 is shown in Figure 45.

Figure 45 shows that the topology matches expectations for the structure. The thickest struts do indeed occur at the tip and base of the structure. The remaining struts are thin relative to these struts. Next, the topology in Figure 45 undergoes topology alteration in order to remove struts that are deemed overlapping or deemed to have negligible contribution to the performance of the structure. The topology after D_{cutoff} is implemented is shown in Figure 46. As can be seen from 46, the D_{cutoff} works effectively for the simple cantilever beam: no critical connective or load bearing struts are removed from the structure. The cutoff diameter is therefore valid for this example.

The diameter results from the 28% Assumption, the constrained minimization,

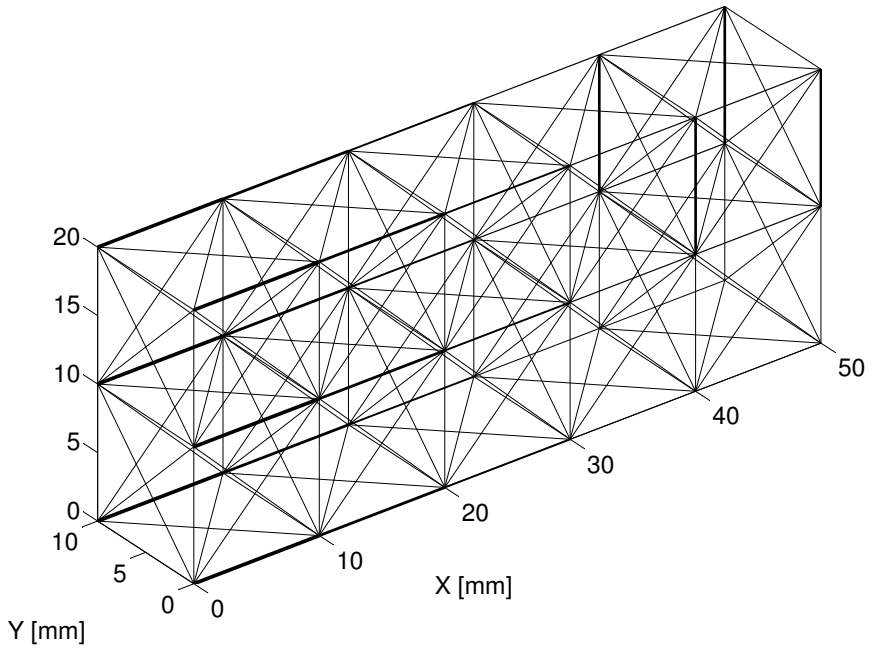

Figure 45: Topology of the cantilever beam before topology alteration.

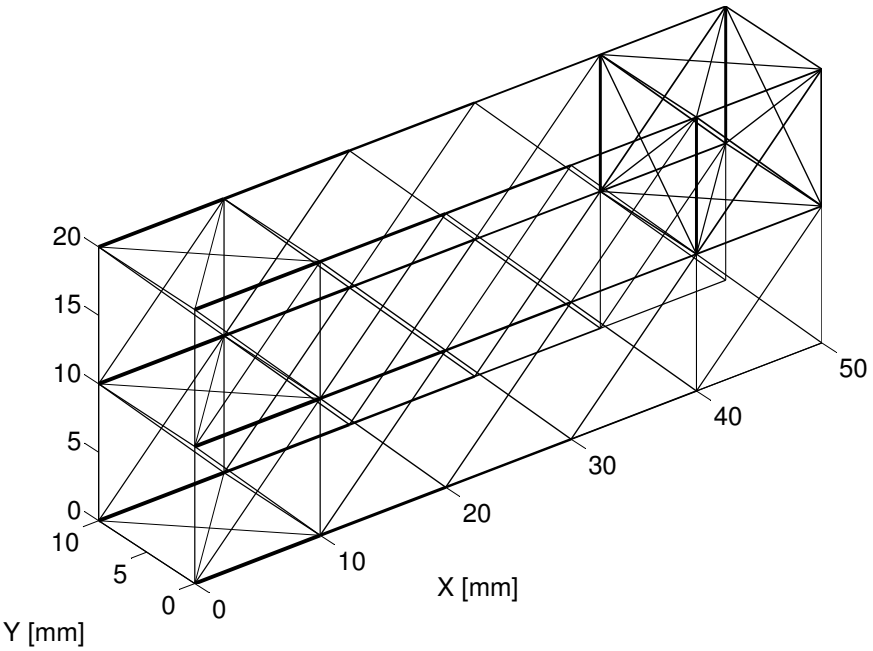

Figure 46: Topology of the cantilever beam after D_{cutoff} utilized.

and the least-squares minimization are provided. Once again, for each of the determination method, five separate trials were completed. The average values for D_{min}, D_{max}, D_{cutoff}, D_{min}/D_{max}, design time, volume, and stiffness were taken. For this example, the displacement of the loaded node was used as the primary metric for stiffness. For all three methods, the upper and lower bounds for D_{min} and D_{max} were set to 0.01 mm and 5 mm, respectively. The results from the individual trials for each of the three optimizations are shown in Appendix D.1.

5.3.3.1 Design Space Exploration/Grid Search

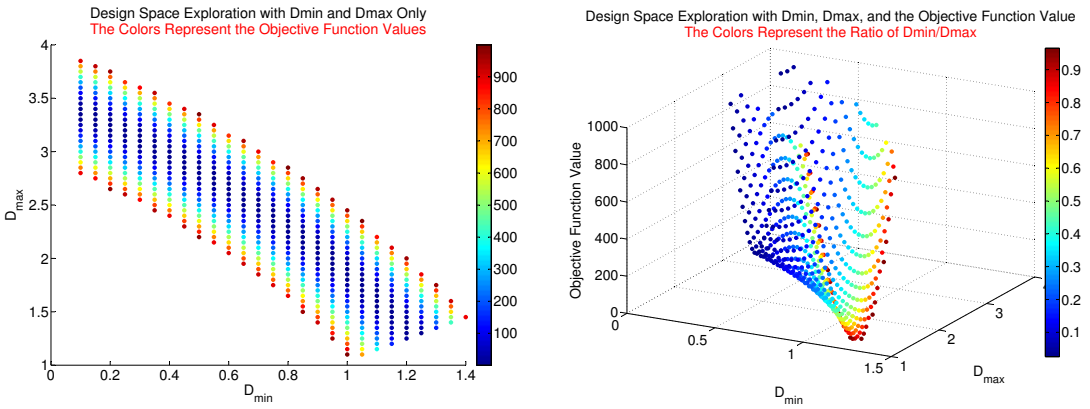

Figure 47: Plot of the design space for the 3-D cantilever beam.

Table 19: Optimal diameter values for the 3-D cantilever using design space exploration.

Deflection (mm)	0.6123
Volume (mm^3)	1589
Design Time (s)	841.35
D_{min} (mm)	0.4500
D_{max} (mm)	2.9000
D_{cutoff} (mm)	0.5112
D_{min}/D_{max}	26.32

Because computational complexity is relatively small for the cantilever beam, it is possible to conduct a design space exploration/grid search within a reasonable time

frame. The design space was explored by iterating both D_{min} and D_{max} from 0.1 mm to 5 mm and storing the values returned by the objective function Equation 4. The values of 0.1 mm and 5 mm were selected because it was determined that a diameter value smaller than 0.1 mm would be too small to be realized in AM, and a value greater than 5 mm would never be necessary in a meso-scale truss structure of this size and scale. The results of the exploration are plotted in Figure 47.

From the design space analysis, it can be seen that the objective function does have a well-defined region where the values are minimal. Also, in the design space there are no glaring local minima that could potentially skew optimization routines. The diameter values that returned the lowest objective function value are shown in Table 19. The analysis time, tip displacement, and volume are provided as well.

Based on the information in Table 19, it can be expected that the minimum and maximum diameters determined by the three sizing methods should be near 0.45 mm and 2.9 mm, respectively. It can also be expected that the final tip displacement of the structure should be at or near 0.6123 mm.

5.3.3.2 Results Comparison

Table 20 summarizes the averages values from all three sizing methods. It also includes the results of the design space exploration for comparison. From Table 20, results indicate that all three sizing methods return minimum and maximum diameters at or near 0.7 mm and 2.5 mm, respectively, and a tip displacement near 0.57 mm. Also, in general, these results correspond to the results returned by the design space exploration and by the previous SMS method [27], which returned a tip displacement of 0.5547 mm and a volume of 1615 mm^2. The small deviation of D_{min} and D_{max} in the design space exploration likely resulted because of the coarse incrementation of D_{min} and D_{max} and the rigid constraints set by the exploration. For the design exploration, a volume greater than 1600 mm^2 was a hard constraint and could not

Table 20: Diameter determination results for the 3-D cantilever beam.

	28% Assumption	Constrained Optimization	Least-Squares Minimization	Design Space Exploration
Deflection (m)	0.5724	0.5723	0.5723	0.6123
Volume (m^2)	1600	1600	1600	1589
Design Time (s)	2.7572	21.3883	17.6459	841.35
D_{min} (m)	0.6967	0.6864	0.6860	0.4500
D_{max} (m)	2.4884	2.5073	2.5080	2.9000
D_{cutoff} (m)	0.7415	0.7319	0.7316	0.5112
D_{min}/D_{max}	28.00	27.38	27.35	26.32
Objective Function Value	0.3726	0.3725	0.3725	0.8541

be violated. Because D_{min} and D_{max} were incremented with such low resolution, the achieved volume of 1589 mm^2 was the closest the design space could get to 1600 mm^2 without exceeding it. Therefore, D_{min} and D_{max} could not be changed to more optimal values without violating the volume constraint. Another comparison that can be made between the design space exploration results and the sizing methods are the ratios of D_{min} and D_{max}. As expected from the three sizing methods, the ratios are all close to 28%. However, the ratio for the design space exploration is 15.5%. This results suggests that a large range of ratios can lead to satisfactory objective function results.

The criterion that best reflects the ability of the four diameter sizing tools is the total analysis time. As can be seen, the 28% assumption converges in under three seconds and is once again the fastest of all the optimization methods. It is nearly 8 times faster than constrained optimization and roughly 6.5 faster than least-squares minimization. In contrast to the first example, the least-squares minimization converges slightly faster than the constrained optimization, with a 21% faster design time. Finally, it can be seen that a design space exploration, even for just two design variables, is a time-consuming and computationally expensive process. Such a rigorous exploration would likely be infeasible for larger, more comprehensive design problems.

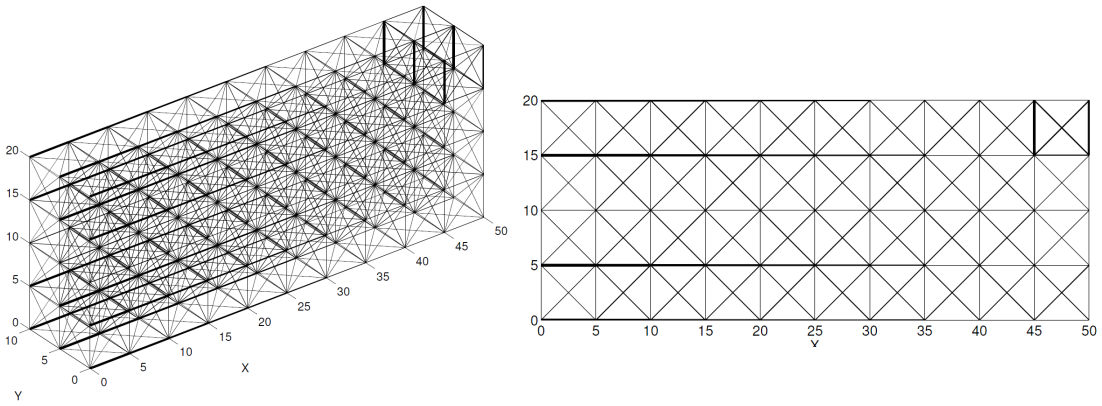

Tip Deflection (mm)	0.2159
Volume (mm^3)	1600

Figure 48: A survey of the 3-D cantilever design problem when the number of unit-cells is increased from 10 to 40.

5.3.3.3 Unit-Cell Size Exploration

As discussed in Section 5.3.2, a base lattice was generated where the number of unit-cells was quadrupled. Everything else remained unchanged. Then, the SMS method was applied to the modified design problem, as shown in Figure 48. The stiffness results and volumes were then recorded as 0.2150 mm and 1600 mm^3, respectively. As can be seen, the performance of the cantilever beam improves dramatically when the number of unit-cells is quadrupled. Therefore, it can be seen that there is, indeed, a change in the performance of the structure when unit-cell sizes are considered. This observation reveals the possibility of their being an optimal unit-cell size for a particular structure. The optimization of this unit-cell size could possibly be an area of future work for the SMS method.

5.3.3.4 Summary

In this section, the second design problem, a 3-D cantilever beam, was designed using the modified SMS approach and the original unit-cell library. Multiple diameter

determination techniques were used to determine the best diameter values for D_{min} and D_{max}. Based on these results, some key observations can be made:

- Once again, all three sizing methods are able to return identical results for D_{min} and D_{max} All three sizing methods are also able to converge to results similar to those from the design space exploration.

- A full design-space exploration for D_{min} and D_{max} is time-consuming in the 3-D case as well and is not preferred. However, results from the exploration verify the validity of the three optimization-based approaches.

- Between the two two-variable methods, the least-squares approach is able to converge slightly faster than the constrained optimization approach. These results suggest that, although the optimization approach may be better for 2-D design problems, least-squares regression may be better for 3-D examples.

- The one-variable optimization utilizing the "28% assumption" is able to converge to optimal values much faster than either of the two-variable methods. These results corroborate the idea that a one-variable assumption is both valid and beneficial for the SMS method.

- A brief exploration of the impact on unit-cell region size and structural performance revealed that there is a relationship between the two characteristics of the truss structure. Given these results, the development of an optimization method for the unit-cell region size may be an area of future work.

5.3.4 The Modified Unit-Cell Library

In this section, the modified unit-cell library and selection method are used to generate the topology for the SMS method. The weighting values in Equation 12, W_v, W_{vn}, and W_p are varied in order to generate multiple topologies for the cantilever. In total three separate topologies are generated for this example problem.

5.3.5 Selection Method 1

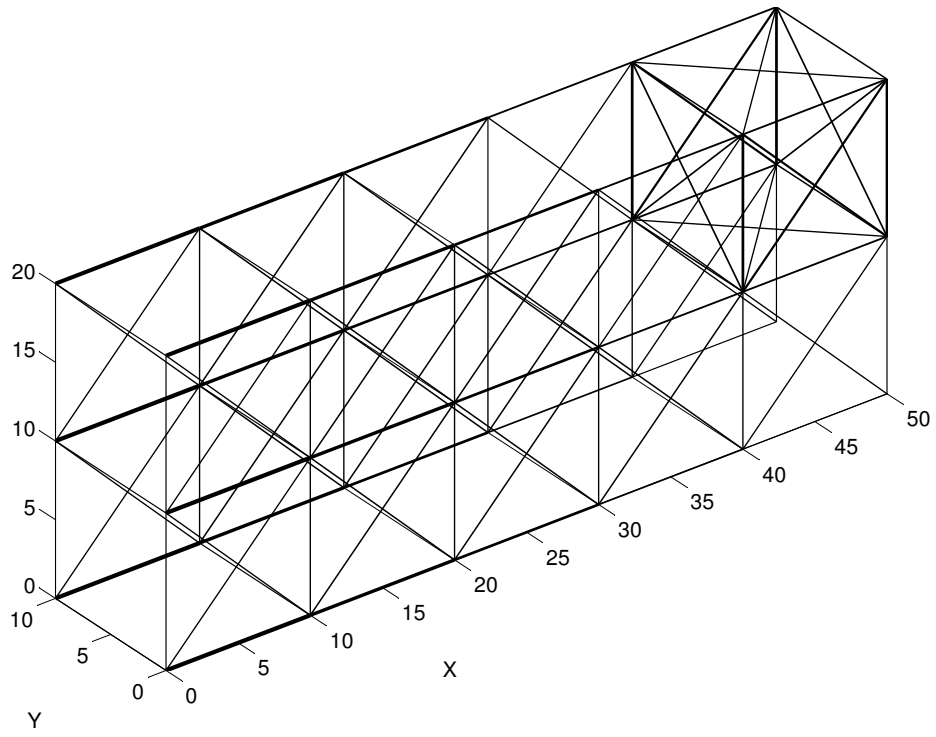

Figure 49: Topology of the first selection variant for the cantilever beam.

Table 21: Diameter determination results for the first selection variant for the cantilever beam.

	28% Assumption	Constrained Optimization	Least-Squares Minimization
Deflection (m)	0.6355	0.5687	0.5687
Volume (m^2)	1600	1600	1600
Design Time (s)	3.0109	18.8111	20.0815
D_{min} (m)	0.8548	0.5091	0.5087
D_{max} (m)	3.0529	4.5520	4.5533
D_{cutoff} (m)	0.9098	0.6101	0.6099
D_{min}/D_{max}	28.00	11.18	11.17
Objective Function Value	0.4039	0.3234	0.3234

The first topology generated using the new library is shown in Figure 49. For this topology, the weighting values for W_v, W_{vn}, and W_p were 2, 0 and 1, respectively. As

can be seen in Figure 49, the topology generated using the new library and selection method is very similar to the topology generated using the original library. This is because the new method only selects the crossed configuration for the topology; none of the other configurations are selected.

The diameter determination results for the topology in Figure 49 are shown in Table 21. It is important to note that Table 21 contains the average results for each of the determination methods based on five iterations. The values from the five trials are shown in Appendix D.2.

From Table 21 it can be seen that the 28% assumption does not return the same results as the constrained optimization or least-squares minimization. Although the convergence time is considerably less, the overall deflection values are approximately 10% greater, indicating a significant reduction in structural stiffness. Between the two-variable optimizations, the constrained optimization approach is able to converge slightly more quickly, with a 1.27 second, or 6.33% decreased optimization time. Both of these optimizations are able to converge to the same stiffness value, with equivalent D_{min} and D_{max} values. The D_{min}/D_{max} ratio returned by both optimizations is around 11%. This results indicates that the 28% assumption is not correct for this selection method or library.

5.3.6 Selection Method 2

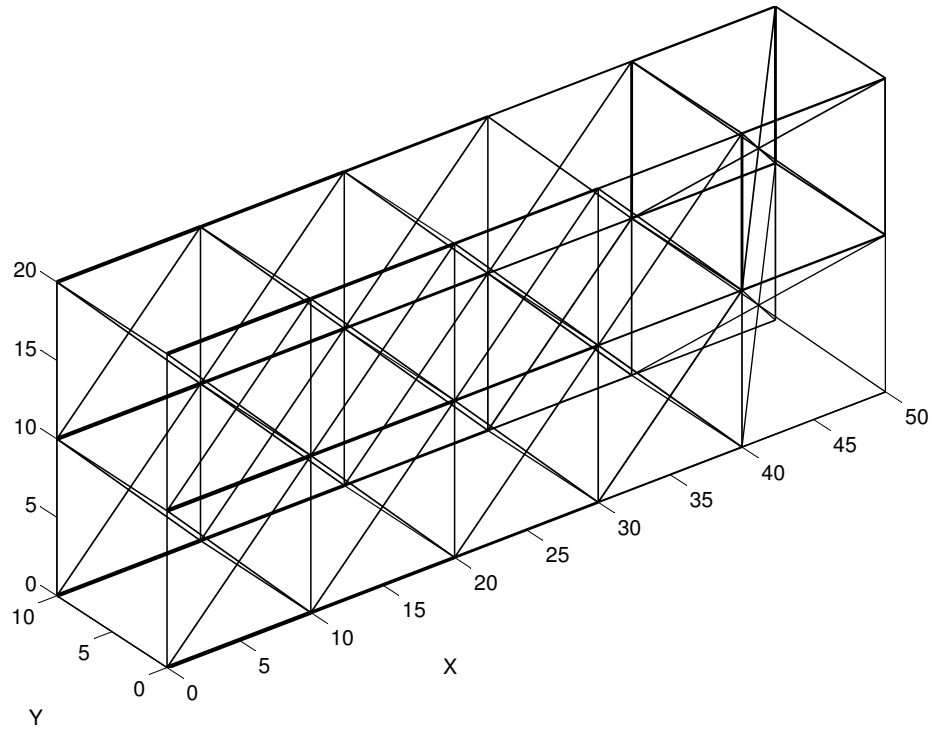

Figure 50: Topology of the second selection variant for the cantilever beam for the cantilever beam.

Table 22: Diameter determination results for the second selection variant for the cantilever beam.

	28% Assumption	Constrained Optimization	Least-Squares Minimization
Deflection (m)	0.6616	0.6328	0.6328
Volume (m^2)	1600	1600	1600
Design Time (s)	3.1136	14.7989	19.4370
D_{min} (m)	0.8898	0.6912	0.6911
D_{max} (m)	3.1777	4.0781	4.0788
D_{cutoff} (m)	0.9470	0.7759	0.7758
D_{min}/D_{max}	28.00	16.95	16.94
Objective Function Value	0.4377	0.4004	0.4004

The second topology generated using the new library is shown in Figure 50. For this topology, the weighting values for W_v, W_{vn}, and W_p were 1, 0, and 1, respectively. The topology generated using these weighting values returns a varied topology. Here, eight of the configurations are designated as the "crossed" configuration and the other two configurations are designated as the "diagonal" configuration.

The diameter determination results for the topology in Figure 50 are shown in Table 22. Table 22 contains the average results for each of the determination methods based on 5 iterations. The actual iteration values are shown in Appendix D.3.

The results from Table 22 show similar trends as the results from the first configuration. Here, it can be seen that once again, the 28% assumption returns a solution much more quickly, but is unable to return the diameter values that result in the best possible stiffness. The two-variable optimizations, on the other hand, take longer to converge but are able to return better stiffness results, with a 4.5% increase in stiffness performance. Both results are identical, but the constrained optimization is able to converge roughly 4.64 seconds, or 23.9% faster. The D_{min}/D_{max} is roughly 17%, well below the value of 28% proposed by Graf.

5.3.7 Selection Method 3

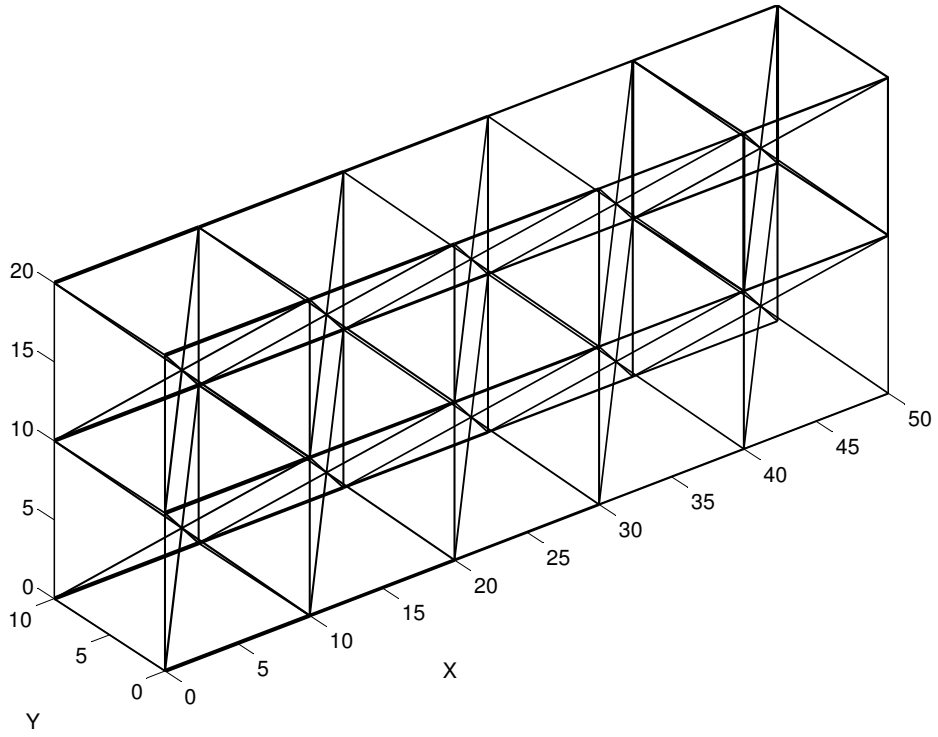

Figure 51: Topology of the third selection variant for the cantilever beam.

Table 23: Diameter determination results for the third selection variant for the cantilever beam.

	28% Assumption	Constrained Optimization	Least-Squares Minimization
Deflection (m)	0.8258	0.8202	0.8202
Volume (m^2)	1600	1600	1600
Design Time (s)	4.8155	16.3032	30.9161
D_{min} (m)	0.8884	0.8230	0.8229
D_{max} (m)	3.1727	3.4945	3.4945
D_{cutoff} (m)	0.9455	0.8897	0.8897
D_{min}/D_{max}	28.00	23.55	23.55
Objective Function Value	0.6819	0.6727	0.6727

The third selection variation utilized for this example problem is shown in Figure 51. Here, the weighting parameters, W_v and W_{vn}, and W_p were all set to 1. With these values, the cantilever beam designates 10 diagonal configurations for the topology; no other configuration is selected.

The diameter determination results for the third topology are shown in Table 23. Once again, the 28% assumption converges the most quickly, but the two-variable optimization methods return more optimal results. For this topology, the gap in stiffness results, however, is not as profound, with only a 0.68 % deviation in results. This results occurs because the optimal D_{min}/D_{max} ratio, as determined by the two-variable optimizations, is roughly 23.5%, a value that is close to the predicted value of 28%. Between the two-variable methods, the diameter and stiffness results are virtually identical, save for the optimization time. Here, the constrained optimization converges much more quickly than the least-squares minimization, with a 14.6 second reduction in design time.

5.3.8 Results Comparison

In total, there are four separate topologies have been generated for the cantilever beam using the SMS method and unit-cell libraries: one using the original library and three using the modified library. In this section, these topologies will be compared. In particular, the stiffness, design time, and D_{min}/D_{max} ratios will be compared. Table 24 shows all the stiffness results returned by the four separate topologies.

The results from Table 24 vary significantly. Firstly, it can be seen that the only time the optimization utilizing the 28% method matches the two variable optimizations is with the original library. For all the other topologies, the 28% assumption returns inferior results. This result disproves the idea that a 28% assumption is valid for all instances of topologies generated using the modified unit-cell library. However, the 28% assumption may still be valid for topologies generated using the original

Table 24: Compiled deflection results for the cantilever design problem.

	28% Assumption	Constrained Optimization	Least-Squares Minimization
Original Library	0.5724	0.5723	0.5723
Selection Variation 1 [10 crossed]	0.6355	0.5687	0.5687
Selection Variation 2 [8 crossed, 2 diagonal]	0.6616	0.6328	0.6328
Selection Variation 3 [10 diagonal]	0.8258	0.8202	0.8202

library, as the 28% remains valid for the topology generated using this assumption.

When directly comparing selection variant 1 (with all 10 unit-cells generated using the crossed configuration), it can be seen that the stiffness results are better than those returned by the original unit-cell library, with the exception of the 28% method. This result shows that the crossed configuration optimized using the new unit-cell optimization method is superior than the configuration utilizing the original procedure proposed by Graf.

The results from selection variants 2 and 3 are considerably worse than the results from selection variant 1 and, on the whole, are also worse than the results from the original library. When comparing variants 1 and 2, it can be seen that the main difference is the replacement of the crossed configuration with diagonal unit-cells. For variant 2, the two unit-cells at the tip of the cantilever are replaced. For variant 3, all the unit-cells are replaced with the diagonal unit-cell. As a result, the stiffness results for these topologies appear to be directly proportional to the number of diagonal unit-cells present in the structure; the more diagonal unit-cells present in the structure, the worse the stiffness results appear to be.

Table 25 shows the compiled design time results for all the topologies. From Table 25, some trends can be observed. First and foremost, it can be seen that for all four topologies, the 28% assumption converges much more quickly because only

Table 25: Compiled design time results for the cantilever design problem.

	28% Assumption	Constrained Optimization	Least-Squares Minimization
Original Library	2.7572	21.3883	17.6459
Selection Variation 1 [10 crossed]	3.0109	18.8111	20.0815
Selection Variation 2 [8 crossed, 2 diagonal]	3.1136	14.7989	19.4370
Selection Variation 3 [10 diagonal]	4.8155	16.3032	30.9161

one variable needs to be optimized. In addition, it can be seen that, on the whole, the constrained minimization approach returns results faster than least-squares minimization, except for when the original unit-cell library is utilized. In general, it can be seen that topologies generated using the new unit-cell library converge faster than than those generated using the original library when constrained minimization is used. Conversely, when least-squares minimization is used, optimization converges more slowly than when the original library is used. From these results, no correlation can be established between the speed of convergence and the type of unit-cell configuration used.

The compiled D_{min}/D_{max} ratios for all four topologies are shown in Table 26. The diameter ratios in Table 26 show that the only situation where the 28% assumption matches the results returned by two-variable optimization is with the original library. All the configurations generated using the new library do not converge to 28%. The closest to reach the 28% assumption is variant 3, the configuration generated using all diagonal configurations. This result is believed to be purely coincidental. When comparing the three topologies generated using the modified library, it can be seen that the D_{min}/D_{max} ratios are all different. Therefore, the optimal D_{min}/D_{max} ratio is likely related directly to the topology of the structure and, in particular, the type of unit-cell used. When the topology is composed entirely of diagonal configurations,

Table 26: Compiled diameter ratio results for the cantilever design problem.

	28% Assumption	Constrained Optimization	Least-Squares Minimization
Original Library	28.00	27.38	27.35
Selection Variation 1 [10 crossed]	28.00	11.18	11.17
Selection Variation 2 [8 crossed, 2 diagonal]	28.00	16.95	16.94
Selection Variation 3 [10 diagonal]	28.00	23.55	23.55

the D_{min}/D_{max} ratio is higher at 23.5%. When eight of the ten unit-cells are crossed, the ratio drops to 17%. When all the unit-cells are composed with the crossed configuration, the ratio is around 11%. When comparing the results from the original configuration with variant 1, it can be seen that, despite the fact that both topologies are composed entirely with the crossed configuration, the optimal diameter ratios are very different. This result shows that even the initial optimization of the unit-cells has a significant impact on the final topological makeup of the structure.

5.3.9 Summary

For the cantilever design problem, the modified unit-cell library was utilized with the selection method described in Chapter 4. Various weighting values were used to vary the topologies generated using the SMS method. The results from the diameter sizing methods were then presented and compared. From these results, several key observations and trends were recorded:

- For the cantilever problem, the selection method appears to select only either the crossed configuration or diagonal configurations for the topology of the structure. Varying the weighting parameters changes the relatively distribution between these two configurations. These results suggest that these two configurations are the best two configurations in the unit-cell library.

- The stiffness results from the modified topologies show that the topology using only the crossed configuration has the best possible stiffness results. When these configurations are replaced by the diagonal configuration, the stiffness results worsen. This implies that, in general, the diagonal configuration returns inferior results for this example problem

- Regardless of the selection method or library used, it appears that the 28% assumption will always return diameter values faster than either of the two-variable methods. However, unless the topologies are generated using the original library, these diameter values are not optimal. This indicates that the 28% assumption is not valid for structures generated using the new library. However, it may still be valid for structure generated using the original library.

- The optimal D_{min}/D_{max} ratios for topologies generated using the SMS method appear to vary based on the topology. In this case, topologies containing more diagonal entries have higher ratios, whereas structure generated using the crossed configuration have lower ratios. This trend likely occurs because the diagonal configuration generally contains fewer struts. This smaller number of struts allows for a smaller distribution of relative diameter values. This, in turn, results in larger minimum diameter values relative to the maximum diameter values and an overall higher D_{min}/D_{max} ratio.

- For the problem, the unit-cell regions in the base lattice were quadrupled in order to determine the effect, if any, on structural performance. When the SMS method was applied and stiffness results were compiled, a change in performance was, indeed, found. This leads to the idea that there could be an optimal unit-cell region size for a given SMS structure.

5.3.10 Research Questions Revisited

In this section, a simple 3-D cantilever problem was presented. For this problem, both the old and new library were utilized to generate topologies. Furthermore, all three diameter determination methods were applied to these topologies. Various important results were discovered. These results can be applied toward the three hypotheses discussed in Chapter 1:

> **Hypothesis 1**: By utilizing the unit-cell approach and combining it with a constrained optimization of two diameter values: a minimum allowable diameter and a maximum allowable diameter, against volume and stiffness constraints, a systematic design method can be developed for the design of mesoscale truss structures. By exploring various optimization approaches and selecting the best method, analysis time can be minimized and structural performance can be maximized.

The diameter determination results from the original library align well with the results from the design space exploration. This results corroborates the idea that the an optimization/minimization approach can be utilized to determine optimal D_{min} and D_{max} results. These results are further corroborated by the topologies from the new library: all the two-variable results are able to return identical results for D_{min} and D_{max}. Furthermore, these results are always equal to or better than the results from the one-variable optimization. Therefore, this example appears to answer hypothesis 1 in the affirmative.

Hypothesis 2: By exploring and analyzing the optimal minimum and maximum diameter values for meso-scale truss structures designed using the Size, Matching, and Scaling method, a direct relationship between these two values can be determined and exploited. This relationship will allow for one of the two diameter values to be expressed as a function of the other. Consequently, the two-variable minimizations outlined in Hypothesis 1 can be simplified to a one-variable minimization problem, thereby reducing overall design time.

The diameter determination results from the first and second unit-cell libraries return different results. Firstly, when using the 28% assumption with the original unit-cell library, it can be seen that the SMS method can return diameter results very similar to the results from the two-variable optimizations. In addition, the overall design time is significantly reduced. These results, combined with the results from Example 1, suggest that, for the original library, a one-variable assumption is valid and beneficial for the method, as it reduces the overall design time significantly. However, when the new library is utilized, the one-variable optimization, though faster, does not return optimal diameter results. When the two-variable results are compared for the three topologies generated using the new method, it can be seen that the optimal D_{min}/D_{max} ratios are not equal. These results not only imply that optimal diameter ratios are highly dependently on the make-up of the unit-cell topology, but are unlikely to conform to a singular value. Therefore, it is unlikely that topologies generated using the new library will converge to any ratio. Based on these observations, it can be seen that hypothesis 2 is not valid for the new library, but may still be valid for the old one.

Hypothesis 3: The addition of unit-cell configurations, such as the cantley and octet configurations, will provide the SMS method with more options for the generation of the lattice topology. This, in turn, will allow for the placement of unit-cell structures that are better-suited for specific loading conditions, thereby improving structural stiffness. Although the design time will be slightly increased for a larger library, this increased time will be outweighed but the benefit conferred by improved structural performance.

The results from the three topologies generated using the new unit-cell library show that only two configuration are even considered in the construction in the topology of the structure: the crossed and diagonal structures. When the stiffness results of these three topologies are compared, the topology composed entirely of the crossed configuration returns the best stiffness results. The other topologies show that, as the unit-cells are replaced with diagonal configurations, that the stiffness results gradually worsen. This result implies that more configurations do not improve the results of the structure and, in fact, can reduce the performance of the structure. When comparing design time, it can be seen that results are mixed. The new library actually causes a reduction in design time for structures utilizing constrained minimization. However, if least-squares minimization is used, the results are opposite: design time increases. More information is necessary before a definitive conclusion can be made about the change in design time when a new library is utilized. The results in from this example, are counter to the statements made in Hypothesis 3.

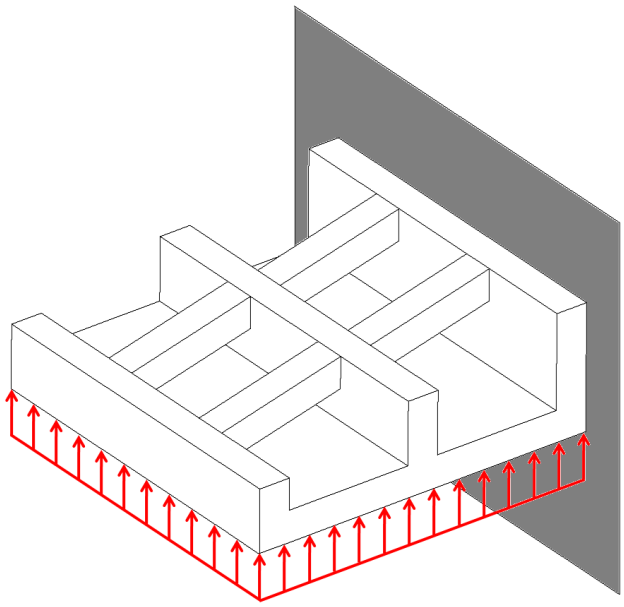

Figure 52: Problem definition of the 3-D L-bracket example.

Table 27: Initial properties for the 3-D specialized L-bracket.

Length (mm)	110	Loading (N/mm^2)	0.595
Width (mm)	110	Unit-Cell Size (mm)	10
Height (mm)	40	Total Unit-Cell Count	203
Elastic Modulus (N/mm)	1960	Target Volume (mm^3)	10000

5.4 Example 4: 3-D Specialized L-Bracket

5.4.1 Problem Description

The fourth and final design example is a specialized 3-D L-bracket. This bracket is a simplified version of a proprietary aircraft component. The bracket contains three vertical walls and one base. Between the three walls are four support beams. The bracket is fixed along its rear face and a distributed load of 0.595 N/mm^2 is supplied along the bottom face. The objective of this problem is to achieve a target volume of 10,000 mm^3 while minimizing the average deflection of the bottom face of the bracket. The design problem is shown in Fig. 52. Table 27 summarizes the initial conditions for the design problem. It is important to note that not all initial specifications are provided. For simplification purposes, only the bounding dimensions, total number

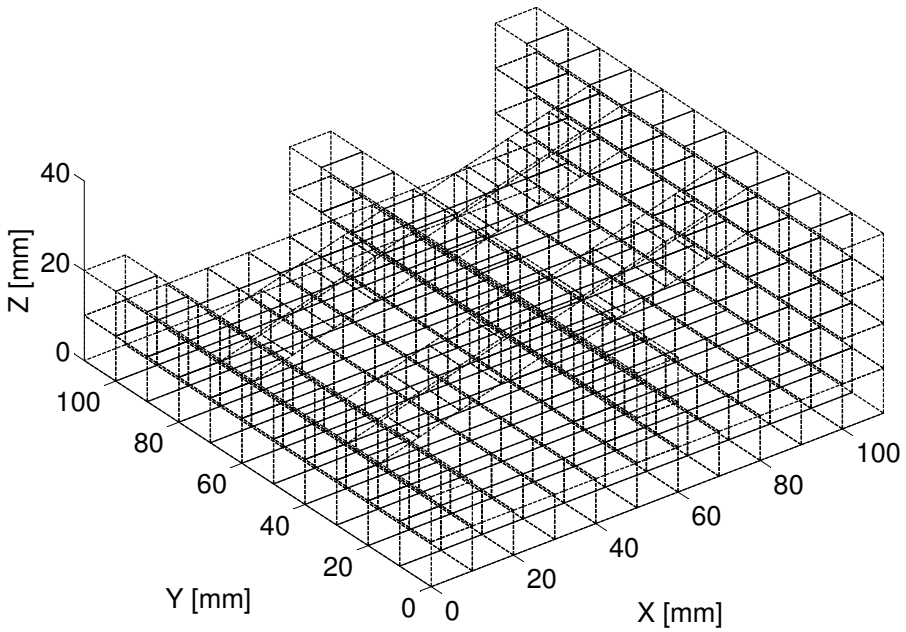

Figure 53: Base-lattice for the 3-D L-Bracket.

of unit-cells, and unit-cell size are provided.

5.4.2 Ground Geometry and Solid-Body Analysis

The ground geometry for the L-bracket is shown in Figure 53. This geometry was generated manually using a combination of several bezier-interpolated surfaces.

The solid-body stress analysis for the L-bracket is shown in Figure 54. As can be seen, the highest stresses in the structure are expected to occur on the four beams of the L-bracket and in particular on the two rear beams. Furthermore, the stress distribution appears to be fairly symmetric throughout the structure. Based on these values, the SMS method should allocate the largest strut diameters along the beams of the L-bracket. Conversely, the method should allocate the smallest diameters to the front corners of the bracket.

With the stress values are known, the unit-cell library can be used to determine the location and sizes of the struts to use in each unit-cell. As with Example 2, both the original and modified unit-cell library will utilized to generate the topology of the structure in order to compare the results from the two libraries.

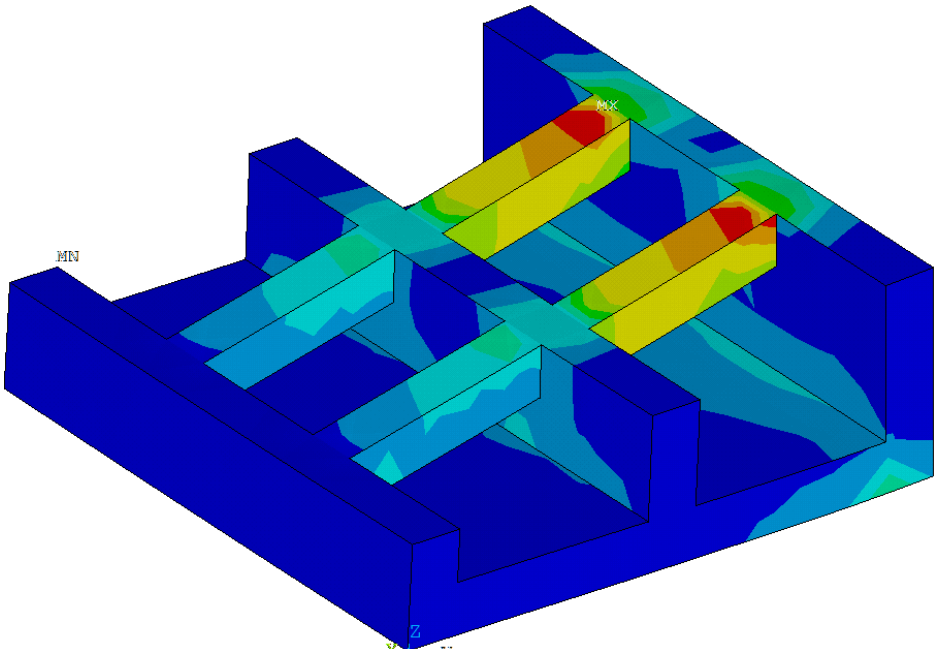

Figure 54: Solid-body model of the 3-D L-Bracket.

5.4.3 The Original Unit-Cell Library

The topology of the structure generated using the original unit-cell library is shown in Figure 55. A side view and overhead view are provided in Figure 56. As Figures 55 and 56 show, the thickest struts occur along the beams connecting the rear and middle faces. The thinnest struts occur on the bottom face near the far corners of the beam. This resultant topology appears to match intuitive expectations for the topology of the structure.

For the L-bracket, the cutoff diameter, D_{cutoff}, was also utilized. The topology after this cutoff diameter was utilized is shown in Figure 57. As can be seen, the utilization of this cutoff diameter has unanticipated affects on the topology of the structure. Because the cutoff diameter indiscriminately removes diameter values that fall below a certain value, it may remove some struts from the structure that are critical for the performance of the structure. For instance, in this example, the cutoff diameter has removed struts that are critical for the correct application of the loading and boundary conditions. Furthermore, some struts are removed that may

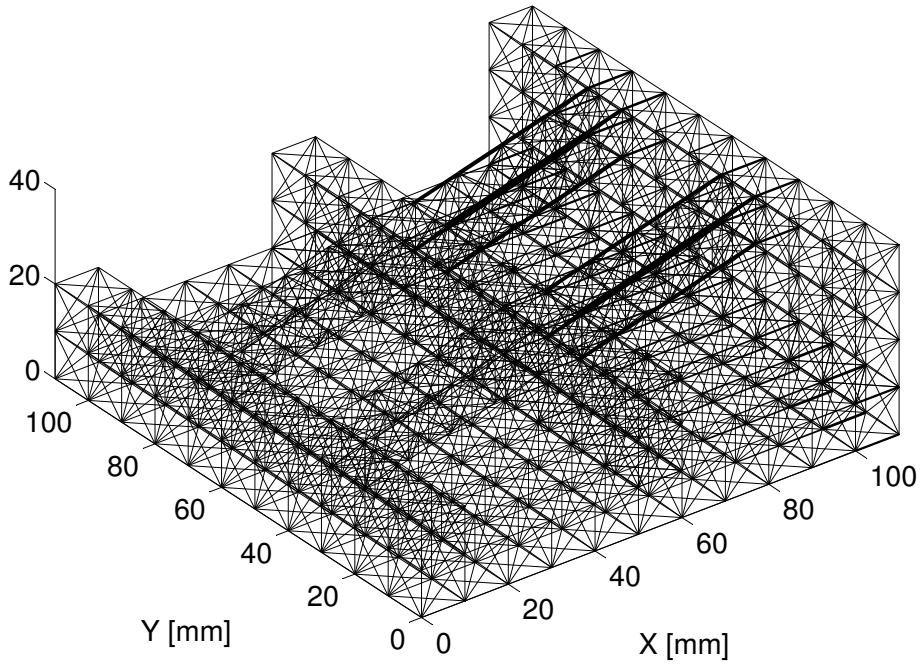

Figure 55: Completed topology for the 3-D L-Bracket.

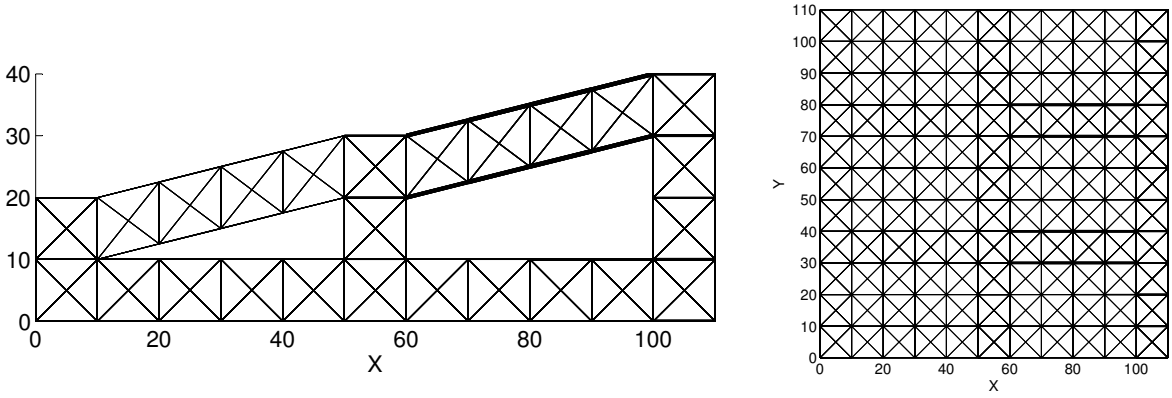

Figure 56: Side-view (left) and overhead view (right) of the completed topology for the 3-D L-Bracket.

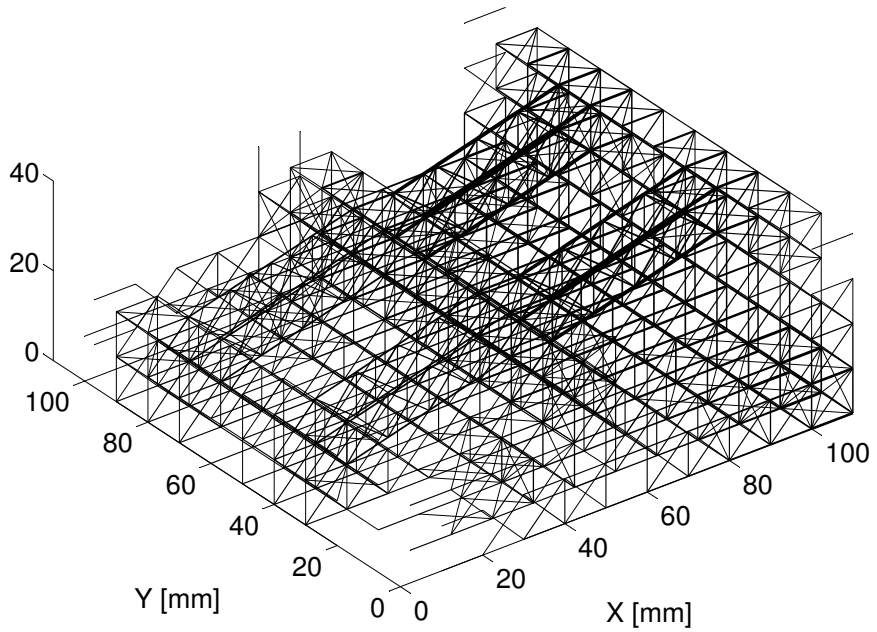

Figure 57: Topology of the 3-D L-Bracket after the cutoff diameter is implemented.

connect adjacent load-bearing struts to one another. Because these struts are critical for the satisfactory function of the completed truss structure, an accurate analysis of the truss structure cannot be made while using a cutoff diameter approach to topology alteration. Furthermore, when deflection results are compared before and after the cutoff diameter are implemented, deflection results are actually better before implementation. Therefore, for this example, the use of D_{cutoff} was excluded.

The diameter results from the 28% Assumption, the constrained minimization, and the least-squares minimization were determined. As with Examples 1 and 2, for each of the determination method, five separate trials were completed. The average values for D_{min}, D_{max}, D_{cutoff}, D_{min}/D_{max}, design time, volume, and deflection were taken. For this example, the average displacement of a select number of nodes on the bottom face was used as the primary metric for deflection. For all three methods, the upper and lower bounds for D_{min} and D_{max} were set to 0.01 mm and 5 mm, respectively. The values from each of the five trials is provided in Appendix E.1

In addition to the three optimization discussed in the previous section, a design

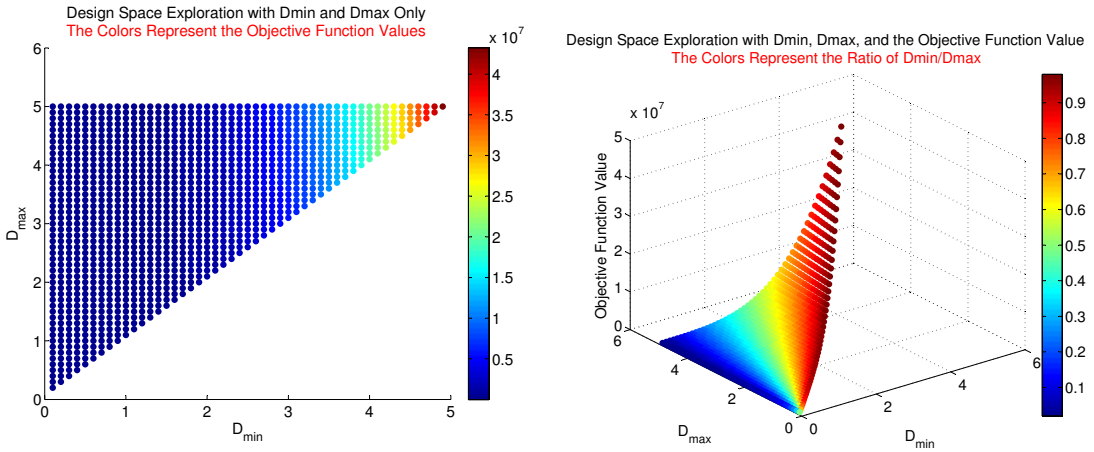

Figure 58: Plot of the design space for the L-bracket.

Table 28: Design space exploration results for the L-bracket.

Deflection (mm)	0.2379
Volume (mm^3)	10045
Design Time (s)	29418.0
D_{min} (mm)	0.4
D_{max} (mm)	2.4
D_{cutoff} (mm)	N/A
D_{min}/D_{max}	16.67

space exploration/grid search was conducted. In this example, D_{min} and D_{max} were iterated from 0.1 mm to 5 mm and and incremented in steps of 0.1 mm. The results of the exploration are plotted in Figure 58. The diameter values that returned the lowest objective function value are shown in Table 28. The analysis time, tip displacement, and volume are provided as well. Based on the information in Table 28, it can be expected that the minimum and maximum diameters determined by the three sizing methods should be near 0.4 mm and 2.4 mm, respectively. It can also be expected that the final tip displacement of the structure should be at or near 0.2379 m.

5.4.3.1 Results Comparison

The compiled results for all three diameter determination results and the design space exploration are shown in Table 29 for the L-bracket design problem. From

Table 29: Diameter determination results for the L-bracket using the original unit-cell library.

	28% Assumption	Constrained Optimization	Least-Squares Minimization	Design Space Exploration
Deflection (mm)	0.2685	0.2358	0.2179	0.2379
Volume (mm^3)	10000	10000	10000	10045
Design Time (s)	251.1894	816.4605	1105.3	29418.0
D_{min} (mm)	0.4872	0.1695	0.3000	0.4
D_{max} (mm)	1.7399	3.5878	2.9844	2.4
D_{cutoff} (mm)	N/A	N/A	N/A	N/A
D_{min}/D_{max}	28	4.72	10.05	16.67
Objective Function Value	0.0721	0.0556	0.0475	0.2573

Table 29, it can be seen that all four methods are able to converge to the target volume of 10,000 mm^3. However, beyond this value, the results for the methods vary widely. Firstly, it can be seen that the D_{min}/D_{max} ratios differ widely for each method. These results suggest that a 28% assumption for the diameter ratio would be incorrect. When deflection results are observed, it is seen that this is, indeed the case; the 28%, one-diameter optimization returns the worst deflection results of the four methods. Another interesting observation is that, unlike the other examples to this point, the two-variable optimizations do not return identical results. Here, the constrained optimization returns inferior results to the least-square minimization results, indicating that the least-squares minimization method is superior for this design problem. When design times are compared, the 28% method, unsurprisingly, returns results the quickest. The constrained optimization converges the second most quickly and the least-squares method returns results the slowest.

When the three methods are compared to the design space exploration, the results align with expectations. Both the two-variable optimizations are able to return better overall results than the design space exploration and are able to do so much more quickly than the exploration. These results imply that optimization is the better method to take in order to determine the ideal D_{min} and D_{max} values.

5.4.3.2 Summary

In this section of the design problem, the 3-D L-bracket was designed using the original unit-cell library. For this topology, the three diameter determination methods and a design space exploration were performed. From the deflection and design time results, several conclusions can be drawn:

- Unlike with the previous examples, all three diameter determination methods return different results for the diameter values, deflection, and design time. Based on these results, the least-squares minimization returns the best overall results but with the cost of the slowest design time. The 28% method, on the other hand, has the opposite effect.

- The design space exploration, even with a coarse increment, takes a long time to complete and does not return the most optimal results. This result further confirms the idea that a full, exhaustive exploration used by Graf is not an ideal systematic method for determining the D_{min} and D_{max} values. Instead, two-variable optimization appears to be much better.

- When the D_{min}/D_{max} ratios are compared, it can be seen that all four methods return different values. More importantly, it can be seen that none of them, save for the obvious one-variable optimization, have a D_{min}/D_{max} near 28%. This implies that a 28% assumption is invalid for this design problem. However, interestingly, if the deflection results are compared, there is not a huge deviation between the 28% method and the two-variable methods. This implies that several D_{min}/D_{max} ratios can result in deflections near the optimum.

In the following section, the modified library will be used to generate topologies for the l-bracket. These results will then be compared to the results from this section.

5.4.4 The Modified Unit-Cell Library

In this section, topologies created using the modified library will be generated for the L-bracket problem. In total, four unique topologies were created by varying the weighting values of the selection equation, Equation 12. The topology and diameter determination results are provided for each of the weighting values.

5.4.5 Selection Method 1

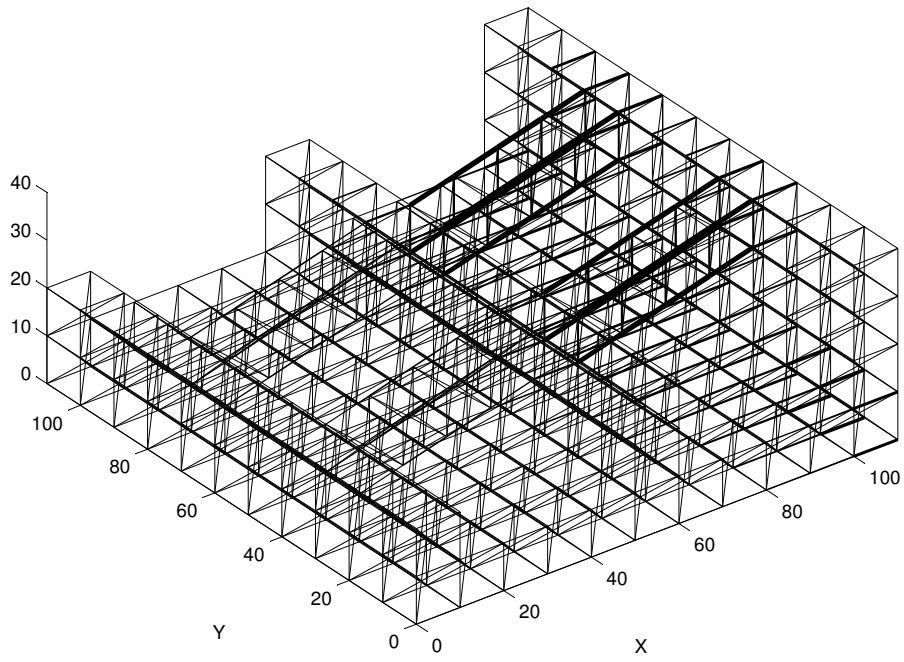

Figure 59: Topology for the first selection variant of the L-bracket.

Table 30: Diameter determination results for the first selection variant of the L-bracket.

	28% Assumption	Constrained Optimization	Least-Squares Minimization
Deflection (m)	0.3132	0.2485	0.2476
Volume (m^2)	9955	10000	10000
Design Time (s)	562.59	1306.7	1673.4
D_{min} (m)	0.6123	0.3708	0.3954
D_{max} (m)	2.1868	5.0094	4.7664
D_{cutoff} (m)	N/A	N/A	N/A
D_{min}/D_{max}	28	7.40	8.30
Objective Function Value	0.3024	0.0618	0.0613

In the first selection variant, the weighting values were set as: $W_v = 0$, $W_{nv} = 1$, $W_p = 1$. These weight values resulted in a topological make-up of all 203 unit-cell regions being composed with diagonal unit-cell configurations. The topology and diameter determination results are provided in Figure 59 and Table 30. The values in Table 30 are averaged from five separate runs. These runs are shown in Appendix E.2.

The compiled results in Table 30 show that all results are, once again, able to reach the optimal volume value. The 28% method is able to converge in less than half the time than either of the two-variable minimizations. However, the deflection results are considerably worse than either of the two-variable optimizations. Between the two-variable methods, the constrained optimization is able to return 366.7 seconds, or 21.9% faster. However, the deflection results are slightly worse.

5.4.6 Selection Method 2

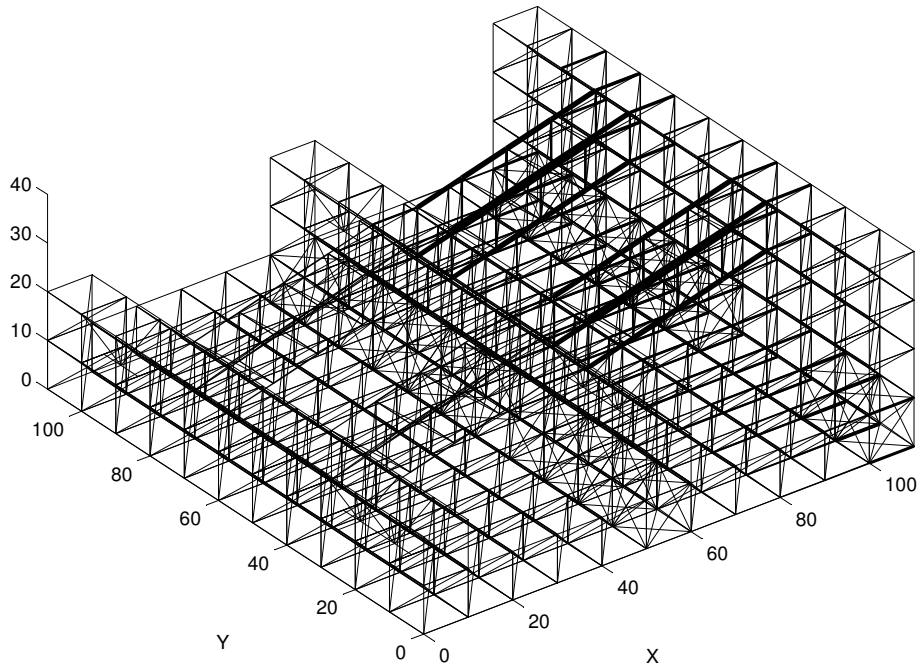

Figure 60: Topology for the second selection variant of the L-bracket.

Table 31: Diameter determination results for the second selection variant of the L-bracket.

	28% Assumption	Constrained Optimization	Least-Squares Minimization
Deflection (m)	0.3199	0.2531	0.2509
Volume (m^2)	9963	9991	10002
Design Time (s)	571.52	1190.0	1536.3
D_{min} (m)	0.5990	0.3497	0.3884
D_{max} (m)	2.1393	5.1551	4.7662
D_{cutoff} (m)	N/A	N/A	N/A
D_{min}/D_{max}	28	6.78	8.15
Objective Function Value	0.2403	0.0722	0.0711

For the second selection variant, the weighting values were set as: $W_v = 0$, $W_{nv} = 0$, $W_p = 1$. With these values, the topology generated by the SMS method was as follows. Here, 17 unit-cells were mapped with the crossed configuration, 6 were mapped with

the paramount 1 configuration, and the remaining 180 cells were mapped with the diagonal configuration. The topology and average diameter determination results are provided in Figure 60 and Table 31. The individual iteration results are shown in Appendix E.3.

The survey of diameter determination methods shows similar trends to the first variation. Firstly, the one-variable method is more than twice as fast as the next-best alternative, but is once again unable to return deflection results at or near the value of the other two methods. Between the two-variable methods, the constrained minimization approach converges faster, but the non-linear least squares minimization returns slightly better results. The D_{min}/D_{max} varies for each of the methods but are relatively close between the two-variable methods. However, neither of the ratios are near the predicted value of 28%, once again implying that the assumption is not a valid one.

5.4.7 Selection Method 3

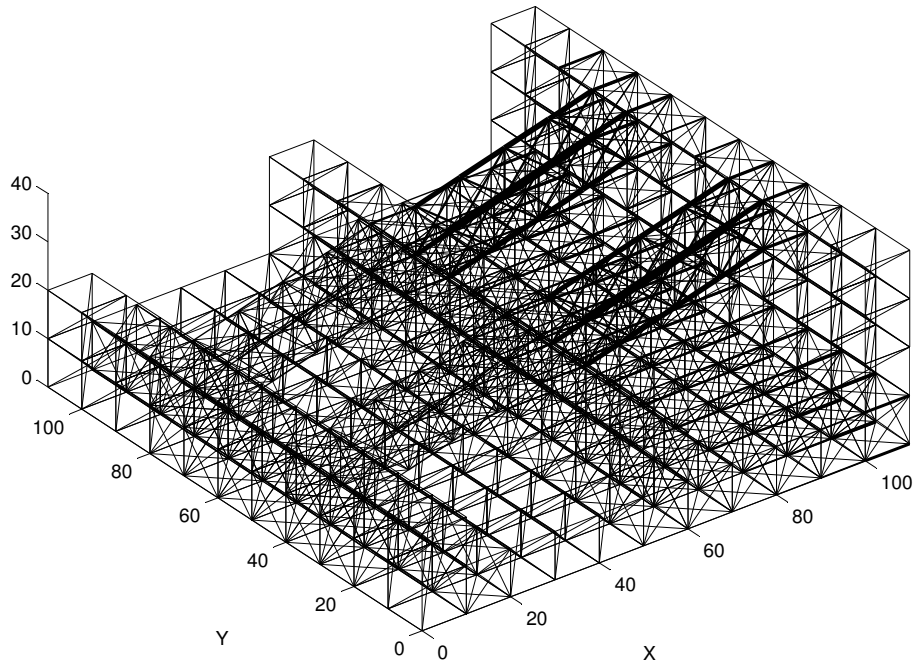

Figure 61: Topology for the third selection variant of the L-bracket.

Table 32: Diameter determination results for the third selection variant of the L-bracket.

	28% Assumption	Constrained Optimization	Least-Squares Minimization
Deflection (m)	0.3149	0.2369	0.2301
Volume (m^2)	10032	9996	10002
Design Time (s)	396.89	903.06	1286.1
D_{min} (m)	0.5488	0.2208	0.3131
D_{max} (m)	1.9599	5.8401	4.9706
D_{cutoff} (m)	N/A	N/A	N/A
D_{min}/D_{max}	28	3.78	6.30
Objective Function Value	0.2009	0.0577	0.0533

The third selection variant, shown in Figure 61, has weighting values set at: $W_v = 1$, $W_{nv} = 0$, $W_p = 1$. With these values, the topology generated contained two configurations: 125 crossed configurations and 78 diagonal configurations. The average diameter determination results are provided in Table 32. The individual iteration results are shown in Appendix E.4.

Relative to one another, the diameter determination results follow the same trends as the first two selection variants: the least-squares minimization returns the best deflection values but at the cost of a design time more than three times longer than the fastest method: the 28% assumption. However, the 28% assumption returns poor deflection results relative to the two diameter determination methods. The constrained minimization approach utilizing the line-search method returns deflection results very close to the the least-squares minimization and is able to converge 383.0 seconds, or 29.8% faster.

5.4.8 Selection Method 4

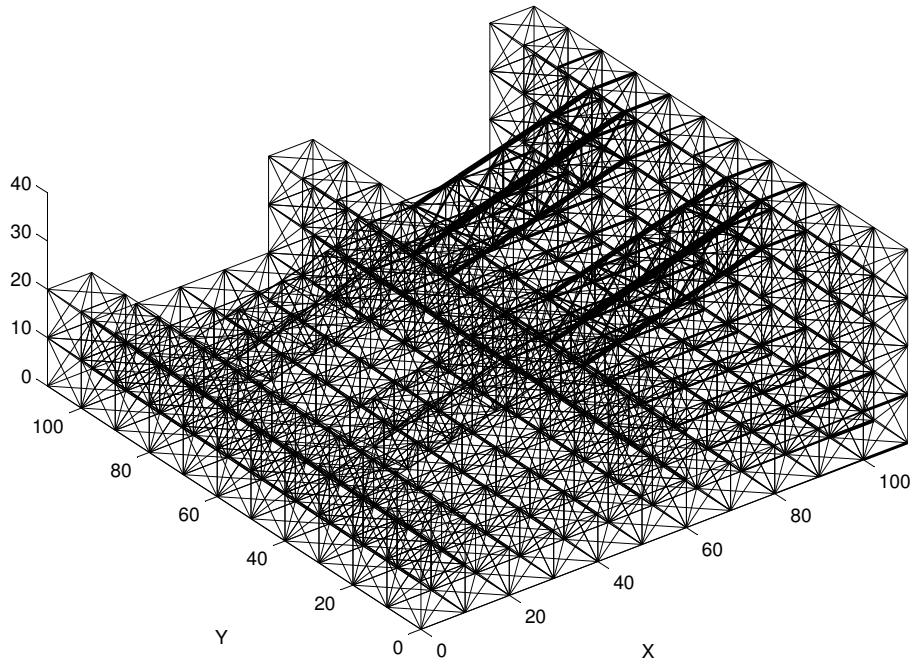

Figure 62: Topology for the fourth selection variant of the L-bracket.

Table 33: Diameter determination results for the fourth selection method of the L-bracket.

	28% Assumption	Constrained Optimization	Least-Squares Minimization
Deflection (m)	0.3234	0.2154	0.2125
Volume (m^2)	10046	10002	10002
Design Time (s)	337.13	667.36	819.63
D_{min} (m)	0.5303	0.2036	0.2612
D_{max} (m)	1.8940	5.8644	5.3264
D_{cutoff} (m)	N/A	N/A	N/A
D_{min}/D_{max}	28	3.47	4.90
Objective Function Value	0.3143	0.0468	0.0456

The final selection variant has weighting values set at: $W_v = 5$, $W_{nv} = 0$, $W_p = 1$. The final topology using these weighting values is dominated with the crossed configuration. Here, the topology contains 202 crossed configurations and 1 diagonal

Table 34: Compiled deflection results for the L-bracket.

	28% Assumption	Constrained Optimization	Least-Squares Minimization
Original Library	0.2685	0.2358	0.2179
Selection Variant1 [203 diagonal]	0.3132	0.2485	0.2476
Selection Variant 2 [17 crossed, 6 paramount 1, 180 diagonal]	0.3199	0.2531	0.2509
Selection Variant 3 [125 crossed, 78 diagonal]	0.3149	0.2369	0.2301
Selection Variant 4 [202 crossed, 1 diagonal]	0.3234	0.2154	0.2125

configuration. The topology and average diameter determination results are provided in Figure 62 and Table 33. The individual iteration results are shown in Appendix E.5.

As with the three previous selection variants, the diameter determination methods appear to have similar performances for the fourth selection variant.

5.4.9 Results Comparison

In this section, the results from the five variants of the L-bracket example will be compared. Table 34 shows the average deflection results returned by the five separate topologies.

From Table 34, some key observations can be made:

- On the whole, the 28% is worst, and the least-squares best. The constrained minimization is close to the least squares, but is slightly worse.
- As the number of crossed configurations increases, the deflection also appears to improve. This results suggests that the crossed configuration is generally the best configuration for all loading scenarios using the SMS method.
- When comparing the variants from the new library with the original library, the original library is superior in all cases except for against variant 4, where nearly all the topology is composed with the crossed configuration from the new

Table 35: Compiled design time results for the L-bracket.

	28% Assumption	Constrained Optimization	Least-Squares Minimization
Original Library	251.2	816.5	1105.3
Selection Variant1 [203 diagonal]	562.6	1306.7	1673.4
Selection Variant 2 [17 crossed, 6 paramount 1, 180 diagonal]	571.5	1190.0	1536.3
Selection Variant 3 [125 crossed, 78 diagonal]	396.9	903.1	1286.1
Selection Variant 4 [202 crossed, 1 diagonal]	337.1	667.4	819.6

library. This observation supports two separate ideas. First, it corroborates the idea that the crossed configuration is the superior configuration and that the introduction of other unit-cells will only reduce the overall stiffness of the structure. Second, it shows that the crossed configurations from the second library are generally superior than their equivalents from the original library.

The compiled design time results for all four topologies are shown in Table 35.

The compiled design time results all follow similar trends, regardless of the type of topology of the l-bracket. In particular, the following conclusions can be drawn from Table 35:

- For every variant, the 28%, one variable assumption converges fastest. This result is as expected, since only one variable need be optimized. However, the cost of a reduced time is a large drop is overall structural performance, as indicated in Table 34.

- Between the two variable methods, the optimization time for constrained minimization is always significantly shorter than least-squares minimization, indicating that it is consistently the faster of the two-variable methods.

- When comparing the selection variants with the original library, it can be seen that the optimization time for the original library is considerably shorter for

Table 36: Compiled diameter ratio results for the L-bracket.

	28% Assumption	Constrained Optimization	Least-Squares Minimization
Original Library	28	4.72	10.05
Selection Variant1 [203 diagonal]	28	7.40	8.30
Selection Variant 2 [17 crossed, 6 paramount 1, 180 diagonal]	28	6.78	8.15
Selection Variant 3 [125 crossed, 78 diagonal]	28	3.78	6.30
Selection Variant 4 [202 crossed, 1 diagonal]	28	3.47	4.90

the original library except for against variant 4. Because both the original configuration and variant 4 are dominated by the crossed configuration, this result implies that the newly-optimized crossed configuration has another advantage over the original configuration in that optimization converges more quickly.

- The design time for variants 1-3 are significantly higher, suggesting that the introduction of additional configurations into the topology lengthens the overall optimization time of the structure. This observation is especially apparent in variant 2, which converges the most slowly because it is composed of three separate configurations. Furthermore, if selection variant 1 is compared to variant 4, it can be seen that, if the topology is composed entirely of diagonal or crossed configurations, the crossed configuration will still converge faster.

The compiled D_{min}/D_{max} ratios for all four topologies are shown in Table 36. From Table 36, the following observations were made:

- None of the diameter determination ratios for the two variable optimizations are close to the approximated 28% taken by the one-variable approach. This result disproves the idea that there exists a set ratio between D_{min} and D_{max} for the old or new library. Furthermore, this wide variation in D_{min}/D_{max} ratios explains why the results from the one-variable optimization are so poor relative

to the two-variable optimizations: the ideal ratio is actually much lower for the L-bracket.

- Between the five different variations of the L-bracket, it can be seen that the ratios change for the two-variable optimizations. This result suggests that the D_{min}/D_{max} ratio is highly dependent on the topology of the structure. It is therefore unlikely, because the new library contains multiple entries, that a set ratio will ever exist between D_{min} and D_{max}.

- The ratios for the constrained minimization are always lower for constrained optimization than least-squares minimization. Because the stiffness results for constrained optimization and least-squares minimization are very similar, with least squares slightly more accurate, it can be inferred that a wide diameter ratio can result in near optimal results.

5.4.10 Research Questions Revisited

In this example, a three-dimensional l-bracket was designed using the SMS method. Both the original library and modified unit-cell library were utilized to generate five unique topologies for the method. Based on the diameter determination values from step 6 of the SMS method, some key results could be obtained. These results have a direct impact on the research questions and hypothesis driving this research.

Hypothesis 1: By utilizing the unit-cell approach and combining it with a constrained optimization of two diameter values: a minimum allowable diameter and a maximum allowable diameter, against volume and stiffness constraints, a systematic design method can be developed for the design of mesoscale truss structures. By exploring various optimization approaches and selecting the best method, analysis time can be minimized and structural performance can be maximized.

As with the cantilever beam, the optimizations appear to be largely successful in determining the optimal values of D_{min} and D_{max} for the L-bracket. When compared to the design space exploration, design time is not only reduced, but results are also more accurate. This result confirms hypothesis 1 for the L-bracket.

Hypothesis 2: By exploring and analyzing the optimal minimum and maximum diameter values for meso-scale truss structures designed using the Size, Matching, and Scaling method, a direct relationship between these two values can be determined and exploited. This relationship will allow for one of the two diameter values to be expressed as a function of the other. Consequently, the two-variable minimizations outlined in Hypothesis 1 can be simplified to a one-variable minimization problem, thereby reducing overall design time.

The diameter determination results and, in particular, the deflection and D_{min}/D_{max} ratio results, show that no real relationship exists between D_{min} and D_{max}, as the the ratio between the two varies for both the old and new libraries. Furthermore, results suggest that, for the new library, the D_{min}/D_{max} changes depending on which configurations and how many of that configuration are mapped to the topology. Also, results from the diameter determination indicate that a wide range of diameter ratios can result in optimal or near-optimal results. All these results show that a set ratio is unlikely to result in optimal diameter values for all topologies created using the SMS method.

Hypothesis 3: The addition of unit-cell configurations, such as the Cantley and octet configurations, will provide the SMS method with more options for the generation of the lattice topology. This, in turn, will allow for the placement of unit-cell structures that are better-suited for specific loading conditions, thereby improving structural stiffness. Although the design time will be slightly increased for a larger library, this increased time will be outweighed but the benefit conferred by improved structural performance.

The four topology variations for the SMS method show that only three of the seven topologies in the library are even considered in this design example. Furthermore, the optimized topologies show that, in general, the more crossed configurations that compose the structure, the better it performs. Consequently, selection variant four, the variant dominated with the crossed configurations performs the best of all the variants. Furthermore, none of the variants save the fourth one are able to perform better than the configuration built using the original library. Even if stiffness is not considered, it can be seen that topologies generated using configurations besides the crossed configuration converge more slowly than those configured using only the crossed topology. Thus, not only is performance reduced, design time is also significantly increased when new topologies are introduced. Therefore, in this research, it appears that no advantage occurs when a new library is utilized. Therefore, This example problem appears to invalidate Hypothesis 3.

CHAPTER VI

CLOSURE

6.1 Summary

Additive manufacturing as a technology has revolutionized manufacturing and design as a whole. This technology has allowed designers to achieve a level of complexity and customizability impossible to achieve using traditional manufacturing processes. Mechanical structures can now reach a level of complexity surpassing even designer imagination or capability. Once such classification of structures, mesoscale lattice structures, are particularly complex and difficult to design, but provide unequalled benefit for designers who desire structures with high strength-to-weight ratios. Although several design approaches and algorithms have been developed to address the design of mesoscale truss structures, all require some form of complex, multivariable optimization that is both time-consuming and stochastic. In previous research, a novel approach, termed the "unit-cell" approach, to lattice design, was presented that did not require massive topological optimization. The method that was developed utilizing this approach, the SMS method, proved to be highly successful in generating topologies without optimization. However, the implementation of the method resulted in some key research issues that must be addressed. These issues form the three research questions of this thesis. These research questions will be discussed in earnest in the following sections.

6.2 Research Questions and Hypotheses

In this thesis, three research question and hypothesis pairs were presented. Throughout the various chapters of this thesis, the modified SMS method was tested and

results were used to answer these research questions. In the following sections, the research questions will be discussed one-by-one.

6.2.1 Research Question and Hypothesis 1

The first research question and hypothesis are repeated below:

> **Research Question 1**: Can an optimization method for the design of mesoscale truss structures be developed to determine strut diameters for topologies designed using the unit-cell approach?

> **Hypothesis 1**: By utilizing the unit-cell approach and combining it with a constrained optimization of two diameter values: a minimum allowable diameter and a maximum allowable diameter, against volume and stiffness constraints, a systematic design method can be developed for the design of mesoscale truss structures. By exploring various optimization approaches and selecting the best method, design time can be minimized and structural performance can be maximized.

In order to address this research question, a new SMS method was presented. In particular, a sixth step was added to the method that deals solely in the determination of the two most critical diameter values in the truss structure: D_{min} and D_{max}. In this sixth step, two optimization routines were used to determine D_{min} and D_{max}, one utilizing a constrained minimization approach and one using a nonlinear, least-squares approach. For comparative purposes, a design space exploration was also completed. This step was then utilized in three of design examples of varying complexity. For the three design examples, the optimization results were highly

promising. Both optimizations were able to return the same optimal value, indicating that both are equally capable of solving the design problem. Furthermore, both of these optimizations were able to return results equal or better than the design exploration. In terms of design time, the methods were able to return results consistently faster. Therefore, based on these results, it appears that optimization is not only a good alternative to a manual exploration of diameter values, but is preferred because it is able to return more optimal results in less time. Therefore, the results of this research confirm Hypothesis 1.

> According to the results of this research, an optimization approach for diameter determination is valid and preferred over a manual search of diameter values. Between the two two-variable optimizations, results indicate that the least-squares minimization is generally more accurate than constrained minimization. However, the stiffness from the least-squares minimization are not significantly better than those of the constrained minimization approach. Furthermore, design time is significantly increased, usually by 20-30%, in order to attain this slightly improved performance. Therefore, no obvious choice can be made between which method is better for determining diameter values. Instead, the designer must make a choice: whether to sacrifice design time for slightly improved overall performance.

6.2.2 Research Question and Hypothesis 2

The second research question and hypothesis are listed below:

> **Research Question 2**: Can the two-variable optimization proposed in Hypothesis 1 be simplified in order to decrease analysis time?

Hypothesis 2: By exploring and analyzing the optimal minimum and maximum diameter values for meso-scale truss structures designed using the Size, Matching, and Scaling method, a direct relationship between these two values can be determined and exploited. This relationship will allow for one of the two diameter values to be expressed as a function of the other. Consequently, the two-variable minimizations outlined in Hypothesis 1 can be simplified to a one-variable minimization problem, thereby reducing overall design time.

In previous research, an assumption was discovered by Graf suggesting that a ratio between D_{min} and D_{max} may exist. In particular, it was assumed that a D_{min}/D_{max} ratio of 28% would result in the best possible stiffness values. However, this assumption was not sufficiently tested and validated against optimization. In this research, this 28% assumption was tested alongside the two-variable optimizations. Design times and stiffness results were compared to test this assumption.

Results from the design examples show that this assumption is able to return topology results much faster than either of the two-variable methods. Furthermore, when using a combination of the original unit-cell library and the simpler design examples (the 3-D cantilever and the 2-D simply-loaded beam), the results from the one-variable optimization are equivalent to the two-variable optimizations. These results explain why Graf made the 28% assumption originally. However, it is likely that this correlation is purely coincidental as the one-variable optimization did not return optimal results for the more complex example: the 3-D L-bracket.

When the new library is utilized, the diameter ratios are highly varied because they depend heavily on the topology of the structure and the configurations that are selected. Therefore, based on this observation, it would be unlikely that the D_{min} and D_{max} values for configurations generated using the new library could ever be expressed using a simple linear relationship, whether it be 28% or not.

The design results from Examples 4 also reveal that a larger range of diameter values may result in near-optimal results. For instance, for the five topology variations presented, the D_{min}/D_{max} ratios returned by the constrained minimization and least-squares minimization vary by roughly $\pm 2\%$. However, stiffness result are very close between the two results. This indicates that stiffness results do not change within $\pm 2\%$ of the optimal ratio. In summary, the results from this research invalidate Hypothesis 2.

Diameter determination utilizing the one-variable approach is significantly faster than the two-variable optimizations. However, stiffness results from both the original unit-cell library and the modified library do not match the assumed 28% relationship between D_{min} and D_{max}. Furthermore, results from the new library indicate that the D_{min}/D_{max} ratio varies widely with the topological makeup of the truss structure. Therefore it is unlikely that a set D_{min}/D_{max} ratio will ever exist between topologies generated using the SMS method.

6.2.3 Research Question and Hypothesis 3

Research Question 3: Will the expansion of the unit-cell library to include additional unit-cell configurations improve the performance of structures designed using the SMS method? If so, will the added benefit justify an increased overall design time?

Hypothesis 3: The addition of unit-cell configurations, such as the Cantley and octet configurations, will provide the SMS method with more options for the generation of the lattice topology. This, in turn, will allow for the placement of unit-cell structures that are better-suited for specific loading conditions, thereby improving structural stiffness. Although the design time will be slightly increased for a larger library, this increased time will be outweighed but the benefit conferred by improved structural performance.

The original SMS method contained only one entry in the library, the crossed configuration. As a result, only this entry was selected for all topologies generated using the SMS method. In this research, a new library was presented that included an additional six configurations as well as a newly optimized version of the original configuration. Along with this new library, a selection method was developed that selected configurations for use based on performance criteria and manual weighting values. By using the modified library along with the selection method, several different topologies were generated and stiffness results were compared.

Results from both examples 3 and 4 show that only three of the seven configurations in the unit-cell library are considered in selection due to their performance: the diagonal configuration, the crossed configuration, and the paramount 1 configuration. However, despite the selection of these configurations by the method, stiffness results indicate that topologies generated solely using the crossed topology perform better. This result is most evident when comparing the topology variations in the cantilever and L-bracket examples. In general, the topologies with a larger relative ratio of crossed configurations perform better. Furthermore, when design times are compared for this example, overall design time is significantly reduced when the crossed configuration is utilized. Therefore, not only is performance better, but design time is as well. Therefore, from the perspective of this research, Hypothesis 3 is invalidated:

According to stiffness and design time results, the addition of six more unit-cell entries to the unit-cell library is not justified. When other configurations besides the crossed unit-cell are selected, both stiffness results worsen and design times increase. Therefore, in the scope of this research, there appears to be no added benefit when increasing the size unit-cell library.

This statement can only be made with the caveat that it is only true with the given library and set of loading conditions. It is highly possible that the reason the expanded unit-cell library was so ineffective in the generation of topologies is because the library simply does not have enough configurations such that there is at least one configuration that can compete with the original "crossed" configuration. By adding more entries into this library, it is possible to improve the performance of the library. Furthermore, the library was only tested using a fairly narrow set of design problems: those that are statically loaded and those that only take into account axial and shear loading. It is very possible that one of the configurations in the library could excel at other design problem scenarios, such as fatigue, torsion, or compliant mechanisms.

Another possibility could be to reconsider entirely the way the unit-cell library is generated and utilized. As results from the design examples indicate, the SMS method appears to always prefer one type of optimal configuration. Given these results, it could be beneficial to approach the concept of the unit-cell library in a different manner. Rather than continually fill the library with more configurations, it may be possible to create a single configuration that has its topology optimized purely for each of the six stress conditions used in the unit-cell library. These six configurations would then be the only configurations used in the unit-cell library. Such a task would eliminate the need for the continual process of adding configurations to the unit-cell library as well as the need for a selection heuristic.

6.3 Future Work

Although several critical research issues have been addressed by this research, there are still other technical and conceptual improvements that can be incorporated into the SMS method. These improvements could potentially be research questions for future research conducted for the SMS method.

6.3.1 Diameter Determination

There are some potential areas for improvement in the diameter determination step of the SMS method. For instance, the benefit of one variable optimization has already been shown to reduce design time drastically. Although a linear, direct correlation between D_{min} and D_{max} has been disproved in this research, there may still be the possibility of determining a higher order, nonlinear relationship between these two values. It is believed that the ratio of D_{min} and D_{max} may be related to the type of topology generated by the SMS method. Therefore, if a correlation could be found based on this observation, then a one variable assumption could still be made.

A second area of improvement in diameter determination is to find a more robust algorithm for unessential struts. The cutoff diameter concept utilized by Graf and in this research is shown to work well in simpler examples, such as the cantilever beam and 2-D simply-loaded beam. However, the use of the same cutoff diameter concept does not work for the more complex L-bracket example. Instead, the opposite effect occurs. This issue occurs because the cutoff diameter haphazardly removes important struts that, although small, are still critical for the performance of the truss structure. Therefore, it is important to improve the process for removing struts these unessential struts. Such a process would likely require a more complex algorithm than the simple removal of small diameters. Instead, a comparison must be made between struts and their adjacent connections to determine their relative importance.

6.3.2 Unit-Cell Library

In addition to improvements in the method itself, the unit-cell library and selection method for unit-cells all have potential regions for improvement. Future work in the unit-cell library can take one of two directions.

6.3.2.1 The Current Unit-Cell Library Formulation

The first direction is the expansion and modification of the unit-cell library as it is currently formulated.

One particular region of improvement is in the selection method itself. The current selection method was created based on empirical understanding of the performance of the SMS method. Furthermore, this selection algorithm requires manual manipulation of weighting values in order to determine lattice topology. In order to improve the selection process for unit-cells, a more generalized and autonomous selection method will be necessary. This selection method must not only take into account several factors, such as the stress distribution of the solid-body analysis, empirical performance, and interactions between adjacent unit-cell regions. Another possibility is the idea of implementing the ability for the configuration to "learn" what types of configurations excel depending on the preferences of the designer.

A second region of improvement for the unit-cell library is the incorporation of more unit-cells. Currently, the library contains seven entries. However, the inclusion of more entries can potentially improve the topologies generated by the SMS method or allow them to be catered for certain design criterion. Furthermore, an even larger library could also change the answer to Research Question 3. It is possible that Hypothesis 3 was invalidated simply because the right entries were not utilized. In the future, if more entries are added to the library, then it is very possible that some configurations would result in better selection and performance, thus validating Hypothesis 3.

Finally, future work may exist in the optimization of the current configurations. As mentioned in Chapter 4, the optimization process in ANSYS did not return the best results when only beam elements were used. For the crossed configuration, when truss elements were used, the results were improved. This observation warrants further research into the best type of finite-element necessary to ensure good optimization of unit-cells. Also, current entries can potentially be further optimized to include higher order stress or other loading scenarios, such as fatigue loading, torsion, or bending. This could not only improve performance of configurations in the lattice, but could also improve the selection and mapping process for unit-cells.

6.3.3 A New Unit-Cell Library Formulation

The second direction for possible improvement is a complete reformulation of the unit-cell library, as discussed in the answer to Research Question 3. Rather than start with a set number of configurations and optimize these configurations for the six separate stress conditions, it may be possible to simply start with a generalized ground structure and optimize that for those same six configurations. Therefore, rather than having to select from many different configurations, each stress direction will only have one, highly-optimized configuration, resulting in a library with only six entries. All topologies would then be generated using these six configurations. Such an alternative could vastly simplify the selection and mapping of unit-cells, thus improving both performance and design time.

6.3.4 Base Lattice Generation

Ideally, the SMS method should be completely autonomous save for the initial specification of the design problem. However, the current implementation of the method requires manual interfacing between the user and the method, particularly in the generation of the base lattice. Currently, the base lattice is generated using a combination of manual, bezier-interpolated surfaces. Both the dimensions and positions of

the regions are manually specified. However, the base lattice should ideally be generated autonomously and the unit-cell regions should be sized and placed automatically in the structure. Unfortunately, the generation of this lattice is very similar to the creation of a mapped mesh in finite-element analysis, which is inherently a complex and time-consuming one. There is no simple or quick solution to this problem.

Another potential area of future work for the base lattice is the optimization of the size and distribution of unit-cell regions. As mentioned in example problem 3 of Chapter 5, a cursory exploration of the 3-D cantilever problem revealed that the performance of a structure designed using the SMS method is related to the size of its unit-cell regions. Therefore, in order to further improve the performance of structures designed using the SMS method, an area of future work could be the development of an optimization routine to determine the size of unit-cell regions.

6.3.5 Other Improvements

Other areas of potential work in the SMS method include the addition of other design concepts, such as stiffening skins that can surround the lattice structures. These stiffening skins have been documented to improve the stiffness of lattice structures and would be a critical feature in the development of the SMS method. Another area of future work for the SMS method is the integration of the method into a CAD or FEA system in order to provide ease of accessibility for designers.

6.4 Contributions

The research conducted in this thesis and the SMS method in general have significant contributions in the design of truss structures.

6.4.1 Design with Minimal Optimization

The primary contribution of this method is the development of a systematic design method for truss structures that does not require lengthy optimization of a large

number of design variables. As a result, this method removes the primary concern for designers in the use of mesoscale truss structures in design: design time. As a result, the SMS method removes significant barrier for entry into the design of mesoscale truss structures that designers would otherwise face using lengthy, multivariable optimization.

6.4.2 Starting Point for Topological Optimization

The SMS has largely been presented in the context of being a competing method against topological optimization. However, such a mindset may not be correct, as it may be possible to use the SMS method in conjunction with topological optimization rather than in competition with it. In particular, the results from the SMS method may be used as a good starting point for optimization in the ground structure approach to optimization. In most design cases, the SMS method will likely provide a starting point much closer to the global optimum than a randomly generated lattice or an identically sized lattice. Furthermore, if a better method for unessential strut removal is developed, the topology for the SMS may already have struts removed from the structure. This fewer number of struts can drastically reduce the overall optimization time in topological optimization.

6.4.3 Testing Bed for New Lattice Configurations

The introduction of a new systematic method for inputting, optimization, and selection of unit-cell configurations will give designers the ability to implement and test new configurations in an efficient manner. Rather simply generating an identically-sized structure, designers can now create specialized lattices using their customized lattice configurations. Utilizing the SMS method will allow these designers to delve deeper into understanding the performance and characteristics of new unit-cell configurations.

6.5 Closure

In the long term, the goal of this research and subsequent work in this area is to provide researchers and designers with a package of tools that can generate lattice structures for use in the design process. The benefits of mesoscale truss structures are numerous and, thanks to the advent of additive manufacturing, are within the grasp of modern-era designers. With the SMS method method, designers and manufacturers have taken another step to the utilizing of the full power of cellular structures. This method, and others like it, will only help designers to improve and expand their designs by opening up new and promising avenues of research. Although much future work is still necessary in the SMS and the design of cellular structures, the potential benefits are enormous. Continued research will not only test the limits of design research, but will also change the way manufacturing and design are approached for years to come.

APPENDIX A

UNIT-CELL OPTIMIZATION EXAMPLE

Figure 63: Example of unit-cell optimization process, part 1.

Example of the unit-cell optimization process

Unit-cell configurations are optimized using the process outlined in Section 4.1 (p. 63-71). An example of this process is shown here. In particular, we will deal with the optimization of the "Cantley" unit-cell configuration for the τ_{xy} shear direction (see Fig. 23, p. 73).

(1) The process begins with the definition of the "starting," or "default," configuration. The default configuration for the Cantley configuration is shown below. See function, "*getDefaultUnitCell.m*" for definitions of all seven unit-cell configurations.

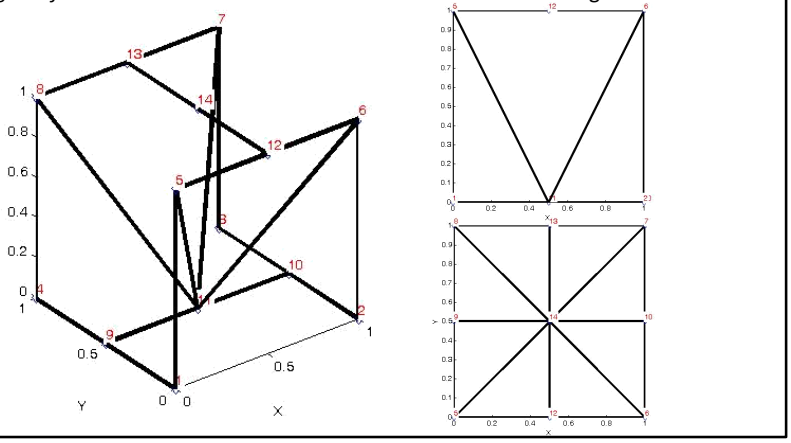

Figure 64: Example of unit-cell optimization process, part 2.

Example of the unit-cell optimization process

(2) Next, boundary conditions are applied to the configuration from (1). There are a total of six sets of boundary conditions that can be applied to the configuration; each set of boundary conditions represents one of the six stress directions used in the SMS method, σ_{xx}, σ_{yy}, σ_{zz}, τ_{xy}, τ_{xz}, τ_{yz}. Furthermore, each of the six sets of boundary conditions has multiple, individual loading conditions. For instance, there exist four separate cases that fall into the τ_{xy} boundary condition: τ_{xy}, $-\tau_{xy}$, τ_{yx}, $-\tau_{yx}$. All four of these conditions must be applied to the configuration and optimized. The results of these four optimizations will then be combined to form the final structure in Step (4). Below, the Cantley configuration is applied with the four loading conditions representing the τ_{xy} stress. See the script, "step3a_optimizeXY.m" in the "Unit Cell Optimization" folder and the function, "getUnitCellLoads.m" for more details.

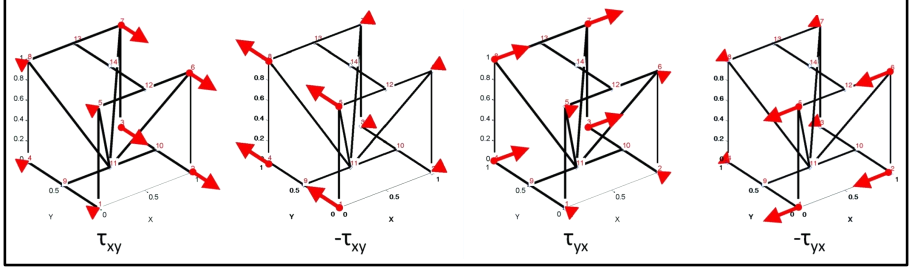

Figure 65: Example of unit-cell optimization process, part 3.

Example of the unit-cell optimization process

(3) After the boundary conditions are applied, the configuration can be optimized. Here, the strut diameters are optimized to minimize volume while maintaining a strain energy constraint of -.5 mJ. Optimizations are performed in the ANSYS software package. The ANSYS code for optimization is written in MATLAB in APDL format. Then, ANSYS is run in batch mode via MATLAB. After optimization is complete, results are automatically taken from ANSYS back into MATLAB. Therefore, the user should never have to manually interface with ANSYS. See "writeAPDLOPT_Seobj.m" function and "step3a_optimizeXY.m" script for more details. The figures below show the four completed optimizations for the Cantley configuration for τ_{xy}.

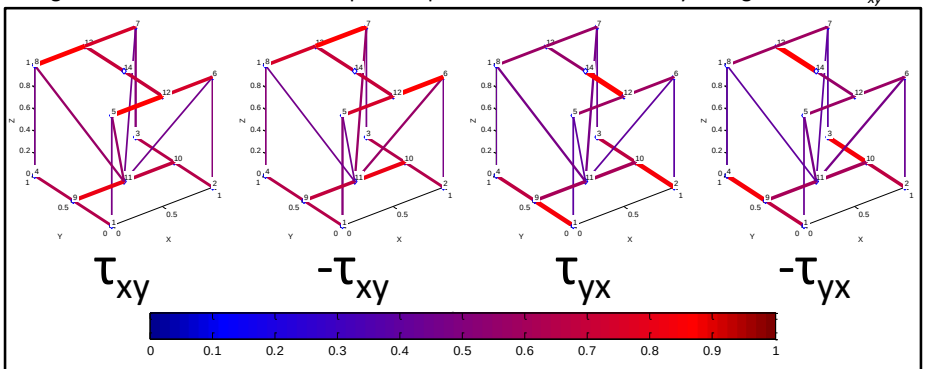

Thicker struts are signified by the color red. Thinner struts are indicated by the color blue.

Figure 66: Example of unit-cell optimization process, part 4.

Example of the unit-cell optimization process

(4) After optimization is complete for every loading condition in the set, the configurations are combined to form the final configuration. This process is completed by simply comparing all the configurations and retaining the largest diameter value existing between them. An example of this process for the Cantley is shown below.

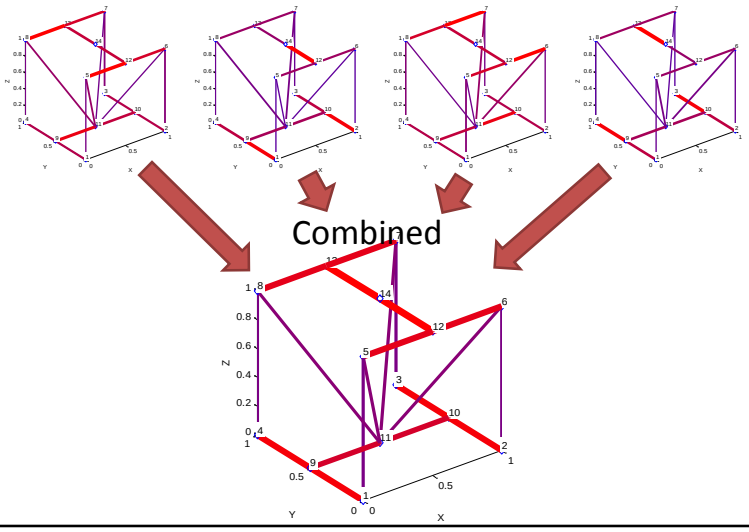

Figure 67: Example of unit-cell optimization process, part 5.

Example of the unit-cell optimization process

(5) In the final step, the diameter values of the configuration are normalized against the largest diameter value present in all seven optimized configurations for the τ_{xy} stress condition. In this case, the largest diameter value present in all the configurations just so happens to be within the Cantley configuration (1.38). The diameters are normalized to this value, as shown below. The completed configuration can then be stored in the unit-cell library. See the "UCLIBRARY_UNNORM_COMPILED.txt" and "UCLIBRARY_NORM.txt" files for the diameter values of all the configurations before and after normalization. See the "step6_NormalizeUCLibrary.m" script for the normalization process.

Diameters before normalization
1.33
1.33
1.33
1.33
1.15
1.15
1.24
1.24
1.24
1.24
1.38
1.38
0.74
0.74
0.74
0.74
0.66
0.66
0.66
0.66

$$D^{norm}_{j,k,l} = D_{j,k,l} / D^{max}_{l}$$

Diameters after normalization
0.96
0.96
0.96
0.96
0.83
0.83
0.90
0.90
0.90
0.90
1.00
1.00
0.54
0.54
0.54
0.54
0.48
0.48
0.48
0.48

Figure 68: Example of unit-cell optimization process, part 6.

Notes

If desired, a cutoff diameter can be implemented in the unit-cell library to remove struts from the unit-cell library below a certain value. This can be accomplished using the "step5_RemoveCutoffs.m" script. If no cutoff is required, then a cutoff of 0 should be used.

For more information on the optimization of unit-cell configurations, consult the "Procedure.txt" file in the "Unit-Cell Optimization" folder.

APPENDIX B

SELECTION EQUATION EXAMPLE

Figure 69: Example of use of the rating equation, part 1.

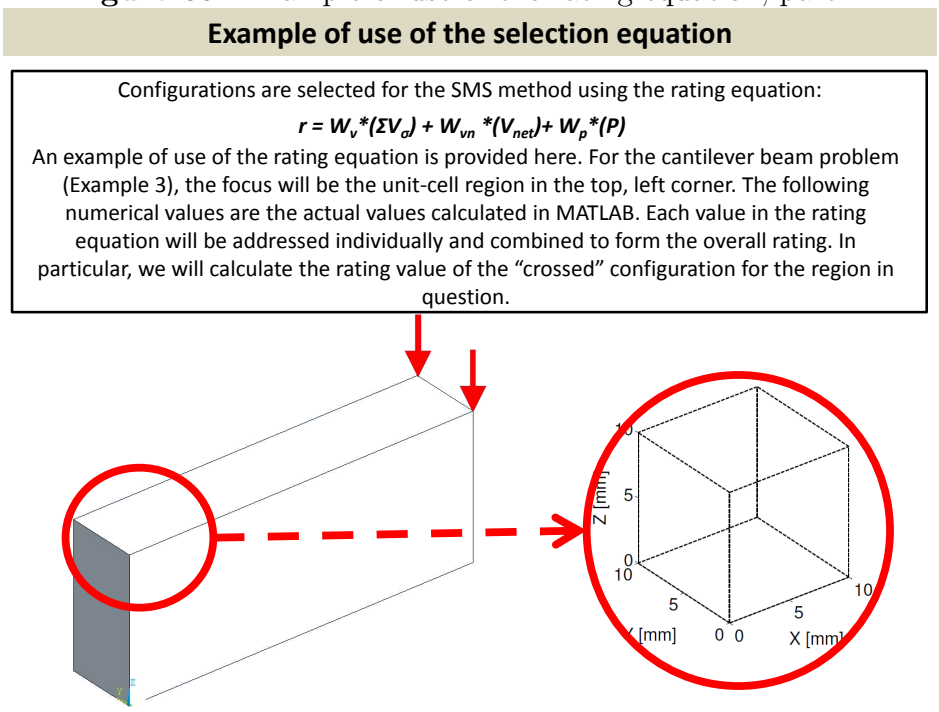

Figure 70: Example of use of the rating equation, part 2.

(1) Calculation of "ΣV_σ"

(a) Average stress values are taken for each of the six primary stress directions (σ_{xx}, σ_{yy}, σ_{zz}, τ_{xy}, τ_{xz} , τ_{yz}) and normalized.

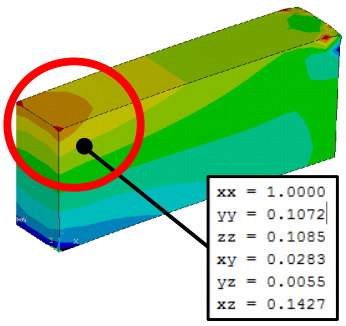

(b) Diameter values for each of the six variants (*xx*, *yy*, *zz*, *xy*, *xz*, *yz*) are taken from the unit-cell library. These values are already normalized.

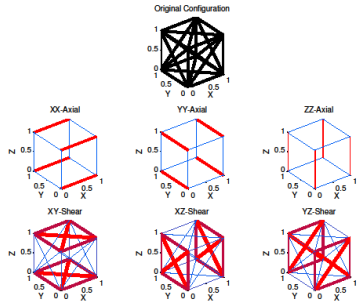

(c) Volumes are calculated for each of the variants by multiplying the normalized stress values from (a), labeled "***w***", with the diameter values from (b), labeled "***d***", and then calculating the volume of each strut as a cylinder. Then, all the volumes are summed to find the net volume:

$$V_{xx} = \Sigma(w_{xx} * \pi * d_{xx}^2/4) = 0.1267$$

Similarly, $V_{yy} = 0.1240$, $V_{zz} = 0.1134$, $V_{xy} = 0.6943$, $V_{yz} = 0.6961$, $V_{xz} = 0.6933$

$$\Sigma V_\sigma = V_{xx} + V_{yy} + V_{zz} + V_{xy} + V_{yz} + V_{xz} = 2.4478$$

Figure 71: Example of use of the rating equation, part 3.

(2) Calculation of "V_{net}" and "ΣP"

(d) The net volume is simply calculated by combining all the variants and removing overlapping struts. Then, the net volume is calculated by summing the volumes of each remaining strut as cylinder (see "mapUnitCells2Region2.m" function).

$$V_{net} = 0.1386$$

(e) P_{xx}, P_{yy}, P_{zz}, P_{xy}, P_{xz}, P_{yz} are directly found using the Performance Table. ΣP is the sum of all these values. For the crossed configuration:

	XX Axial	YY Axial	ZZ Axial	XY Axial	YZ Axial	XZ Axial
Crossed	0.0745	0.0693	0.0375	0.0810	0.0747	0.0752
Cantilev	0.5599	0.4883	0.0559	0.5418	0.5553	0.2628
Octet	0.2281	0.2023	0.1050	0.1004	0.0891	0.0863
Paramount 1	0.0917	0.0907	0.0500	0.9865	0.3904	0.3734
Diagonal	0.0743	0.0704	0.0390	0.1166	0.0881	0.0956
Paramount 2	1.0000	1.0000	1.0000	0.6043	0.5569	0.5462
Midpoint	0.1058	0.0955	0.0507	1.0000	1.0000	1.0000

$P_{xx} = 0.0745$, $P_{yy} = 0.0693$, $P_{zz} = 0.0375$, $P_{xy} = 0.0810$, $P_{yz} = 0.0747$, $P_{xz} = 0.0752$

$$\Sigma P = P_{xx} + P_{yy} + P_{zz} + P_{xy} + P_{yz} + P_{xz} = 0.4122$$

(f) Weighting values are manually set in order to vary the importance of the three attributes.

$$W_v = 1,\ W_{vn} = 1,\ W_p = 1$$

Figure 72: Example of use of the rating equation, part 4.

(3) Ratings Calculation

(g) With the individual volumes (ΣV_σ), the net volume (V_{net}), and the performance value (ΣP) known, the rating values of the configuration can be calculated for the region.

***r(crossed)* = (1*0.1386) + (1*0.4122) + (1*2.4478) = 2.9986**

(h) For the unit-cell region, a rating is calculated for each of the seven configurations:

***r(crossed)* = 2.9986**
***r(Cantley)* = 5.8787**
***r(octet)* = 7.3686**
***r(paramount 1)* = 4.4428**
***r(paramount 2)* = 9.1128**
***r(diagonal)* = 2.7069**
***r(midpoint)* = 6.8149**

(i) The configurations with the lowest rating is selected and mapped to the region. Mapping is completed by first adding extra nodes to the region using linear interpolation. Once this step is completed, struts can be mapped very easily to the structure (see "mapUnitCells2Region2.m" function). Varying the weighting values will change the type of configuration selected.

r(selected) = min(r) = diagonal configuration

APPENDIX C

INDIVIDUAL OPTIMIZATIONS TRIALS FOR THE 2-D SIMPLY-LOADED BEAM

Table 37: Individual trial results using the 28% assumption for the 2-D simply-loaded beam.

Run	D_{min} (m)	D_{max} (m)	D_{cutoff} (m)	D_{min}/D_{max}	Deflection (m)	Volume (m^2)	Design Time (s)
1	0.0103	0.0369	0.0110	28	0.0119	0.0201	18.9443
2	0.0103	0.0369	0.0110	28	0.0119	0.0201	19.0497
3	0.0103	0.0369	0.0110	28	0.0119	0.0201	18.9480
4	0.0103	0.0369	0.0110	28	0.0119	0.0201	18.8847
5	0.0103	0.0369	0.0110	28	0.0119	0.0201	19.0583
	0.0103	**0.0369**	**0.0110**	**28**	**0.0119**	**0.0201**	**18.9770**

Table 38: Individual trial results using constrained minimization for the 2-D simply-loaded beam.

Run	Dmin (m)	Dmax (m)	Dcutoff (m)	Dmin/Dmax	Deflection (m)	Volume (m^2)	Design Time (s)
1	0.0100	0.0378	0.0107	26.43	0.0119	0.0201	39.0263
2	0.0100	0.0378	0.0107	26.43	0.0119	0.0201	39.2485
3	0.0100	0.0378	0.0107	26.43	0.0119	0.0201	39.0892
4	0.0100	0.0378	0.0107	26.43	0.0119	0.0201	40.5302
5	0.0100	0.0378	0.0107	26.43	0.0119	0.0201	39.1614
	0.0100	**0.0378**	**0.0107**	**26.43**	**0.0119**	**0.0201**	**39.4111**

Table 39: Individual trial results using least-squares minimization for the 2-D simply-loaded beam.

Run	Dmin (mm)	Dmax (mm)	Dcutoff (mm)	Dmin/Dmax	Deflection (mm)	Volume (mm^3)	Design Time (s)
1	0.0100	0.0378	0.0107	26.45	0.0119	0.0201	110.7300
2	0.0100	0.0378	0.0107	26.45	0.0119	0.0201	105.7138
3	0.0100	0.0378	0.0107	26.45	0.0119	0.0201	107.4543
4	0.0100	0.0378	0.0107	26.45	0.0119	0.0201	106.6233
5	0.0100	0.0378	0.0107	26.45	0.0119	0.0201	105.1423
	0.0100	**0.0378**	**0.0107**	**26.45**	**0.0119**	**0.0201**	**107.1327**

APPENDIX D

INDIVIDUAL OPTIMIZATIONS TRIALS FOR THE 3-D CANTILEVER BEAM

D.1 Old Library

Table 40: Individual trial results using the 28% assumption and the original library for the cantilever beam.

Run	D_{min} (mm)	D_{max} (mm)	D_{cutoff} (mm)	D_{min}/D_{max}	Deflection (mm)	Volume (mm^2)	Design Time (s)
1	0.6967	2.4884	0.7415	28	0.5724	1600	2.7358
2	0.6967	2.4884	0.7415	28	0.5724	1600	2.7565
3	0.6967	2.4884	0.7415	28	0.5724	1600	2.7617
4	0.6967	2.4884	0.7415	28	0.5724	1600	2.6376
5	0.6967	2.4884	0.7415	28	0.5724	1600	2.7704
	0.6967	**2.4884**	**0.7415**	**28**	**0.5724**	**1600**	**2.7572**

Table 41: Individual trial results using constrained minimization and the original library for the cantilever beam.

Run	D_{min} (mm)	D_{max} (mm)	D_{cutoff} (mm)	D_{min}/D_{max}	Deflection (mm)	Volume (mm^2)	Design Time (s)
1	0.6864	2.5073	0.7319	0.2738	0.5723	1600	21.2625
2	0.6864	2.5073	0.7319	0.2738	0.5723	1600	20.9841
3	0.6864	2.5073	0.7319	0.2738	0.5723	1600	21.9210
4	0.6864	2.5073	0.7319	0.2738	0.5723	1600	22.4093
5	0.6864	2.5073	0.7319	0.2738	0.5723	1600	20.3646
	0.6864	**2.5073**	**0.7319**	**0.2738**	**0.5723**	**1600**	**21.3883**

Table 42: Individual trial results using least-squares minimization and the original library for the cantilever beam.

Run	D_{min} (mm)	D_{max} (mm)	D_{cutoff} (mm)	D_{min}/D_{max}	Deflection (mm)	Volume (mm^2)	Design Time (s)
1	0.6860	2.5080	0.7316	0.2735	0.5723	1600	17.6796
2	0.6860	2.5080	0.7316	0.2735	0.5723	1600	17.3704
3	0.6860	2.5080	0.7316	0.2735	0.5723	1600	17.6098
4	0.6860	2.5080	0.7316	0.2735	0.5723	1600	17.6256
5	0.6860	2.5080	0.7316	0.2735	0.5723	1600	17.9440
	0.6860	**2.5080**	**0.7316**	**0.2735**	**0.5723**	**1600**	**17.6459**

D.2 Selection Variant 1 - 10 Crossed Configurations

Table 43: Individual trial results using the 28% assumption and selection variant 1 for the cantilever beam.

Run	D_{min} (mm)	D_{max} (mm)	D_{cutoff} (mm)	D_{min}/D_{max}	Deflection (mm)	Volume (mm^2)	Design Time (s)
1	0.6967	2.4884	0.7415	28	0.5724	1600	2.7358
2	0.6967	2.4884	0.7415	28	0.5724	1600	2.7565
3	0.6967	2.4884	0.7415	28	0.5724	1600	2.7617
4	0.6967	2.4884	0.7415	28	0.5724	1600	2.6376
5	0.6967	2.4884	0.7415	28	0.5724	1600	2.7704
	0.6967	**2.4884**	**0.7415**	**28**	**0.5724**	**1600**	**2.7572**

Table 44: Individual trial results using constrained minimization and selection variant 1 for the cantilever beam.

Run	D_{min} (mm)	D_{max} (mm)	D_{cutoff} (mm)	D_{min}/D_{max}	Deflection (mm)	Volume (mm^2)	Design Time (s)
1	0.6864	2.5073	0.7319	0.2738	0.5723	1600	21.2625
2	0.6864	2.5073	0.7319	0.2738	0.5723	1600	20.9841
3	0.6864	2.5073	0.7319	0.2738	0.5723	1600	21.9210
4	0.6864	2.5073	0.7319	0.2738	0.5723	1600	22.4093
5	0.6864	2.5073	0.7319	0.2738	0.5723	1600	20.3646
	0.6864	**2.5073**	**0.7319**	**0.2738**	**0.5723**	**1600**	**21.3883**

Table 45: Individual trial results using least-squares minimization and selection variant 1 for the cantilever beam.

Run	D_{min} (mm)	D_{max} (mm)	D_{cutoff} (mm)	D_{min}/D_{max}	Deflection (mm)	Volume (mm^2)	Design Time (s)
1	0.6860	2.5080	0.7316	0.2735	0.5723	1600	17.6796
2	0.6860	2.5080	0.7316	0.2735	0.5723	1600	17.3704
3	0.6860	2.5080	0.7316	0.2735	0.5723	1600	17.6098
4	0.6860	2.5080	0.7316	0.2735	0.5723	1600	17.6256
5	0.6860	2.5080	0.7316	0.2735	0.5723	1600	17.9440
	0.6860	**2.5080**	**0.7316**	**0.2735**	**0.5723**	**1600**	**17.6459**

D.3 Selection Variant 2 - 8 Crossed, 2 Diagonal Configurations

Table 46: Individual trial results using the 28% assumption and selection variant 2 for the cantilever beam.

Run	D_{min} (mm)	D_{max} (mm)	D_{cutoff} (mm)	D_{min}/D_{max}	Deflection (mm)	Volume (mm^2)	Design Time (s)
1	0.6967	2.4884	0.7415	28	0.5724	1600	2.7358
2	0.6967	2.4884	0.7415	28	0.5724	1600	2.7565
3	0.6967	2.4884	0.7415	28	0.5724	1600	2.7617
4	0.6967	2.4884	0.7415	28	0.5724	1600	2.6376
5	0.6967	2.4884	0.7415	28	0.5724	1600	2.7704
	0.6967	**2.4884**	**0.7415**	**28**	**0.5724**	**1600**	**2.7572**

Table 47: Individual trial results using constrained minimization and selection variant 2 for the cantilever beam.

Run	D_{min} (mm)	D_{max} (mm)	D_{cutoff} (mm)	D_{min}/D_{max}	Deflection (mm)	Volume (mm^2)	Design Time (s)
1	0.6864	2.5073	0.7319	0.2738	0.5723	1600	21.2625
2	0.6864	2.5073	0.7319	0.2738	0.5723	1600	20.9841
3	0.6864	2.5073	0.7319	0.2738	0.5723	1600	21.9210
4	0.6864	2.5073	0.7319	0.2738	0.5723	1600	22.4093
5	0.6864	2.5073	0.7319	0.2738	0.5723	1600	20.3646
	0.6864	**2.5073**	**0.7319**	**0.2738**	**0.5723**	**1600**	**21.3883**

Table 48: Individual trial results using least-squares minimization and selection variant 2 for the cantilever beam.

Run	D_{min} (mm)	D_{max} (mm)	D_{cutoff} (mm)	D_{min}/D_{max}	Deflection (mm)	Volume (mm^2)	Design Time (s)
1	0.6860	2.5080	0.7316	0.2735	0.5723	1600	17.6796
2	0.6860	2.5080	0.7316	0.2735	0.5723	1600	17.3704
3	0.6860	2.5080	0.7316	0.2735	0.5723	1600	17.6098
4	0.6860	2.5080	0.7316	0.2735	0.5723	1600	17.6256
5	0.6860	2.5080	0.7316	0.2735	0.5723	1600	17.9440
	0.6860	**2.5080**	**0.7316**	**0.2735**	**0.5723**	**1600**	**17.6459**

D.4 Selection Variant 3 - 10 Diagonal Configurations

Table 49: Individual trial results using the 28% assumption and selection variant 3 for the cantilever beam.

Run	D_{min} (mm)	D_{max} (mm)	D_{cutoff} (mm)	D_{min}/D_{max}	Deflection (mm)	Volume (mm^2)	Design Time (s)
1	0.6967	2.4884	0.7415	28	0.5724	1600	2.7358
2	0.6967	2.4884	0.7415	28	0.5724	1600	2.7565
3	0.6967	2.4884	0.7415	28	0.5724	1600	2.7617
4	0.6967	2.4884	0.7415	28	0.5724	1600	2.6376
5	0.6967	2.4884	0.7415	28	0.5724	1600	2.7704
	0.6967	**2.4884**	**0.7415**	**28**	**0.5724**	**1600**	**2.7572**

Table 50: Individual trial results using constrained minimization and selection variant 3 for the cantilever beam.

Run	D_{min} (mm)	D_{max} (mm)	D_{cutoff} (mm)	D_{min}/D_{max}	Deflection (mm)	Volume (mm^2)	Design Time (s)
1	0.6864	2.5073	0.7319	0.2738	0.5723	1600	21.2625
2	0.6864	2.5073	0.7319	0.2738	0.5723	1600	20.9841
3	0.6864	2.5073	0.7319	0.2738	0.5723	1600	21.9210
4	0.6864	2.5073	0.7319	0.2738	0.5723	1600	22.4093
5	0.6864	2.5073	0.7319	0.2738	0.5723	1600	20.3646
	0.6864	**2.5073**	**0.7319**	**0.2738**	**0.5723**	**1600**	**21.3883**

Table 51: Individual trial results using least-squares minimization and selection variant 3 for the cantilever beam.

Run	D_{min} (mm)	D_{max} (mm)	D_{cutoff} (mm)	D_{min}/D_{max}	Deflection (mm)	Volume (mm^2)	Design Time (s)
1	0.6860	2.5080	0.7316	0.2735	0.5723	1600	17.6796
2	0.6860	2.5080	0.7316	0.2735	0.5723	1600	17.3704
3	0.6860	2.5080	0.7316	0.2735	0.5723	1600	17.6098
4	0.6860	2.5080	0.7316	0.2735	0.5723	1600	17.6256
5	0.6860	2.5080	0.7316	0.2735	0.5723	1600	17.9440
	0.6860	**2.5080**	**0.7316**	**0.2735**	**0.5723**	**1600**	**17.6459**

APPENDIX E

INDIVIDUAL OPTIMIZATIONS TRIALS FOR THE 3-D L-BRACKET

E.1 Old Library

Table 52: Individual trial results using the 28% assumption and the original library for the L-bracket.

Run	D_{min} (mm)	D_{max} (mm)	D_{cutoff} (mm)	D_{min}/D_{max}	Deflection (mm)	Volume (mm^3)	Design Time (s)
1	0.4872	1.7399	N/A	28	0.2685	10000	256.4006
2	0.4872	1.7399	N/A	28	0.2685	10000	249.0863
3	0.4872	1.7399	N/A	28	0.2685	10000	247.0695
4	0.4872	1.7399	N/A	28	0.2685	10000	256.8973
5	0.4872	1.7399	N/A	28	0.2685	10000	246.4932
	0.4872	**1.7399**	**N/A**	**28**	**0.2685**	**10000**	**251.1894**

Table 53: Individual trial results using constrained minimization and the original library for the L-bracket.

Run	D_{min} (mm)	D_{max} (mm)	D_{cutoff} (mm)	D_{min}/D_{max}	Deflection (mm)	Volume (mm^3)	Design Time (s)
1	0.1695	3.5878	N/A	4.72	0.2358	10000	812.0288
2	0.1695	3.5878	N/A	4.72	0.2358	10000	806.6286
3	0.1695	3.5878	N/A	4.72	0.2358	10000	816.8155
4	0.1695	3.5878	N/A	4.72	0.2358	10000	826.5960
5	0.1695	3.5878	N/A	4.72	0.2358	10000	820.2335
	0.1695	**3.5878**	**N/A**	**4.72**	**0.2358**	**10000**	**816.4605**

Table 54: Individual trial results using least-squares minimization and the original library for the L-bracket.

Run	D_{min} (mm)	D_{max} (mm)	D_{cutoff} (mm)	D_{min}/D_{max}	Deflection (mm)	Volume (mm^3)	Design Time (s)
1	0.3000	2.9844	N/A	10.05	0.2179	10000	1102.5
2	0.3000	2.9844	N/A	10.05	0.2179	10000	1106.4
3	0.3000	2.9844	N/A	10.05	0.2179	10000	1113.3
4	0.3000	2.9844	N/A	10.05	0.2179	10000	1102.9
5	0.3000	2.9844	N/A	10.05	0.2179	10000	1101.6
	0.3000	**2.9844**	**N/A**	**10.05**	**0.2179**	**10000**	**1105.3**

E.2 Selection Variant 1 - 203 Diagonal Configurations

Table 55: Individual trial results using the 28% assumption and selection variant 1 for the L-bracket.

Run	D_{min} (mm)	D_{max} (mm)	D_{cutoff} (mm)	D_{min}/D_{max}	Deflection (mm)	Volume (mm^3)	Design Time (s)
1	0.6123	2.1868	N/A	28	0.3132	9955	567.71
2	0.6123	2.1868	N/A	28	0.3132	9955	555.38
3	0.6123	2.1868	N/A	28	0.3132	9955	563.17
4	0.6123	2.1868	N/A	28	0.3132	9955	566.93
5	0.6123	2.1868	N/A	28	0.3132	9955	559.74
	0.6123	**2.1868**	**N/A**	**28**	**0.3132**	**9955**	562.59

Table 56: Individual trial results using constrained minimization and selection variant 1 for the L-bracket.

Run	D_{min} (mm)	D_{max} (mm)	D_{cutoff} (mm)	D_{min}/D_{max}	Deflection (mm)	Volume (mm^3)	Design Time (s)
1	0.3708	5.0094	N/A	7.40	0.2485	10000	1288.1
2	0.3708	5.0094	N/A	7.40	0.2485	10000	1287.8
3	0.3708	5.0094	N/A	7.40	0.2485	10000	1294.9
4	0.3708	5.0094	N/A	7.40	0.2485	10000	1295.4
5	0.3708	5.0094	N/A	7.40	0.2485	10000	1367.2
	0.3708	**5.0094**	**N/A**	**7.40**	**0.2485**	**10000**	1306.7

Table 57: Individual trial results using least-squares minimization and selection variant 1 for the L-bracket.

Run	D_{min} (mm)	D_{max} (mm)	D_{cutoff} (mm)	D_{min}/D_{max}	Deflection (mm)	Volume (mm^3)	Design Time (s)
1	0.3954	4.7664	N/A	8.30	0.2476	10000	1642.8
2	0.3954	4.7664	N/A	8.30	0.2476	10000	1691.4
3	0.3954	4.7664	N/A	8.30	0.2476	10000	1703.7
4	0.3954	4.7664	N/A	8.30	0.2476	10000	1685.5
5	0.3954	4.7664	N/A	8.30	0.2476	10000	1643.5
	0.3954	**4.7664**	**N/A**	**8.30**	**0.2476**	**10000**	1673.4

E.3 Selection Variant 2 - 17 Crossed, 6 Paramount 1, 180 Diagonal Configurations

Table 58: Individual trial results using the 28% assumption and selection variant 2 for the L-bracket.

Run	D_{min} (mm)	D_{max} (mm)	D_{cutoff} (mm)	D_{min}/D_{max}	Deflection (mm)	Volume (mm^3)	Design Time (s)
1	0.5990	2.1393	N/A	28	0.3199	9963	548.65
2	0.5990	2.1393	N/A	28	0.3199	9963	571.02
3	0.5990	2.1393	N/A	28	0.3199	9963	574.76
4	0.5990	2.1393	N/A	28	0.3199	9963	572.89
5	0.5990	2.1393	N/A	28	0.3199	9963	590.26
	0.5990	**2.1393**	**N/A**	**28**	**0.3199**	**9963**	**571.52**

Table 59: Individual trial results using constrained minimization and selection variant 2 for the L-bracket.

Run	D_{min} (mm)	D_{max} (mm)	D_{cutoff} (mm)	D_{min}/D_{max}	Deflection (mm)	Volume (mm^3)	Design Time (s)
1	0.3497	5.1551	N/A	6.78	0.2531	9991	1151.1
2	0.3497	5.1551	N/A	6.78	0.2531	9991	1195.7
3	0.3497	5.1551	N/A	6.78	0.2531	9991	1423.2
4	0.3497	5.1551	N/A	6.78	0.2531	9991	1088.4
5	0.3497	5.1551	N/A	6.78	0.2531	9991	1091.8
	0.3497	**5.1551**	**N/A**	**6.78**	**0.2531**	**9991**	**1190.0**

Table 60: Individual trial results using least-squares minimization and selection variant 2 for the L-bracket.

Run	D_{min} (mm)	D_{max} (mm)	D_{cutoff} (mm)	D_{min}/D_{max}	Deflection (mm)	Volume (mm^3)	Design Time (s)
1	0.3884	4.7662	N/A	8.15	0.2509	10002	1512.2
2	0.3884	4.7662	N/A	8.15	0.2509	10002	1555.3
3	0.3884	4.7662	N/A	8.15	0.2509	10002	1540.0
4	0.3884	4.7662	N/A	8.15	0.2509	10002	1553.9
5	0.3884	4.7662	N/A	8.15	0.2509	10002	1520.3
	0.3884	**4.7662**	**N/A**	**8.15**	**0.2509**	**10002**	**1536.3**

E.4 Selection Variant 3 - 125 Crossed, 78 Diagonal Configurations

Table 61: Individual trial results using the 28% assumption and selection variant 3 for the L-bracket.

Run	D_{min} (mm)	D_{max} (mm)	D_{cutoff} (mm)	D_{min}/D_{max}	Deflection (mm)	Volume (mm^3)	Design Time (s)
1	0.5488	1.9599	N/A	28	0.3149	10032	407.48
2	0.5488	1.9599	N/A	28	0.3149	10032	413.93
3	0.5488	1.9599	N/A	28	0.3149	10032	382.27
4	0.5488	1.9599	N/A	28	0.3149	10032	395.72
5	0.5488	1.9599	N/A	28	0.3149	10032	385.06
	0.5488	**1.9599**	**N/A**	**28**	**0.3149**	**10032**	**396.89**

Table 62: Individual trial results using constrained minimization and selection variant 3 for the L-bracket.

Run	D_{min} (mm)	D_{max} (mm)	D_{cutoff} (mm)	D_{min}/D_{max}	Deflection (mm)	Volume (mm^3)	Design Time (s)
1	0.2208	5.8401	N/A	3.78	0.2369	9996	880.90
2	0.2208	5.8401	N/A	3.78	0.2369	9996	879.46
3	0.2208	5.8401	N/A	3.78	0.2369	9996	899.07
4	0.2208	5.8401	N/A	3.78	0.2369	9996	927.57
5	0.2208	5.8401	N/A	3.78	0.2369	9996	928.28
	0.2208	**5.8401**	**N/A**	**3.78**	**0.2369**	**9996**	**903.06**

Table 63: Individual trial results using least-squares minimization and selection variant 3 for the L-bracket.

Run	D_{min} (mm)	D_{max} (mm)	D_{cutoff} (mm)	D_{min}/D_{max}	Deflection (mm)	Volume (mm^3)	Design Time (s)
1	0.3131	4.9706	N/A	6.30	0.2301	10002	1167.7
2	0.3131	4.9706	N/A	6.30	0.2301	10002	1182.4
3	0.3131	4.9706	N/A	6.30	0.2301	10002	1413.6
4	0.3131	4.9706	N/A	6.30	0.2301	10002	1426.6
5	0.3131	4.9706	N/A	6.30	0.2301	10002	1240.3
	0.3131	**4.9706**	**N/A**	**6.30**	**0.2301**	**10002**	**1286.1**

E.5 Selection Variant 4 - 202 Crossed, 1 Diagonal Configurations

Table 64: Individual trial results using the 28% assumption and selection variant 4 for the L-bracket.

Run	D_{min} (mm)	D_{max} (mm)	D_{cutoff} (mm)	D_{min}/D_{max}	Deflection (mm)	Volume (mm^3)	Design Time (s)
1	0.5303	1.8940	N/A	28	0.3234	10046	327.63
2	0.5303	1.8940	N/A	28	0.3234	10046	325.22
3	0.5303	1.8940	N/A	28	0.3234	10046	356.46
4	0.5303	1.8940	N/A	28	0.3234	10046	355.10
5	0.5303	1.8940	N/A	28	0.3234	10046	321.25
	0.5303	**1.8940**	**N/A**	**28**	**0.3234**	**10046**	**337.13**

Table 65: Individual trial results using constrained minimization and selection variant 4 for the L-bracket.

Run	D_{min} (mm)	D_{max} (mm)	D_{cutoff} (mm)	D_{min}/D_{max}	Deflection (mm)	Volume (mm^3)	Design Time (s)
1	0.2036	5.8644	N/A	3.47	0.2154	10002	673.60
2	0.2036	5.8644	N/A	3.47	0.2154	10002	662.24
3	0.2036	5.8644	N/A	3.47	0.2154	10002	662.94
4	0.2036	5.8644	N/A	3.47	0.2154	10002	668.74
5	0.2036	5.8644	N/A	3.47	0.2154	10002	669.30
	0.2036	**5.8644**	**N/A**	**3.47**	**0.2154**	**10002**	**667.36**

Table 66: Individual trial results using least-squares minimization and selection variant 4 for the L-bracket.

Run	D_{min} (mm)	D_{max} (mm)	D_{cutoff} (mm)	D_{min}/D_{max}	Deflection (mm)	Volume (mm^3)	Design Time (s)
1	0.2612	5.3264	N/A	4.90	0.2125	10002	829.71
2	0.2612	5.3264	N/A	4.90	0.2125	10002	837.26
3	0.2612	5.3264	N/A	4.90	0.2125	10002	813.67
4	0.2612	5.3264	N/A	4.90	0.2125	10002	806.29
5	0.2612	5.3264	N/A	4.90	0.2125	10002	811.21
	0.2612	**5.3264**	**N/A**	**4.90**	**0.2125**	**10002**	**819.63**

REFERENCES

[1] "Image: Honeycomb lattice." [online] http://www.cammmetals.com/portfolio.html.

[2] "Image: Invisalign braces." [online] http://www.invisalign.com/Pages/default.aspx.

[3] "Image: Metal foam." [online] http://www.neatorama.com/2010/01/30/metal-foam-is-lighter-than-aluminum-stronger-than-steel/.

[4] "Image: Phonak hearing aid." [online] http://www.phonak.com/.

[5] "Image: Sls manifold." [online] http://www.designnews.com/article/511949-Additive_Manufacturing_Technology_Expands.php.

[6] "Matlab r2011a documentation, optimization toolbox: fmincon active set algorithm." [online] http://www.mathworks.com/help/toolbox/optim/.

[7] Achtziger, W., "On simultaneous optimization of truss geometry and topolgy," *Structural Multidisciplinary Optimization*, vol. 33, pp. 285–304, 2007.

[8] Allaire, G., Jouve, F., and Maillot, H., "Topology optimization for minimum stress design with homogenization method," *Structurural Multidisciplinary Optimization*, vol. 28, pp. 87–98, 2004.

[9] Allaire, G. and Kohn, R. V., "Optimal design for minimum weight and compliance in plane stress using external microstructures," *Europ. J. Mech. A/Solids*, vol. 12, no. 6, pp. 839–878, 1993.

[10] Ashby, M. F., Evans, A., Fleck, N. A., Gibson, L. J., Hutchinson, J. W., and Wadley, H. N. G., *Metal Foams: A Design Guide*. Woburn, MA: Butterworth-Heinemann, 2000.

[11] Bendsøe, M. P., *Optimization of Structural Topology, Shape, and Material*. Berlin Heidelberg: Springer-Verlag, 1995.

[12] Bendsøe, M. P. and Kikuchi, N., "Generating optimal topologies in structural design using a homogenization method," *Computer Methods in Applied Mechanics and Engineering*, vol. 71, pp. 197–224, 1988.

[13] Bendsøe, M. P. and Sigmund, O., *Topology Optimization: Theory, Methods and Applications*. Springer, 2003.

[14] Burns, S. A., *Recent advances in optimal structural design*. American Society of Civil Engineers, 2002.

[15] Cantley, R. W., "Molded plastic truss work," 2002.

[16] Chapra, S. C. and Canale, R. P., *Numerical Methods for Engineers*. McGraw-Hill, 6 ed., 2010.

[17] Chiras, S., Mumm, D. R., Evans, A. G., Wicks, N., Hutchinson, J. W., Dharmasena, K., Wadley, H. N. G., and Fichter, S., "The structural performance of near-optimized truss core panels," *International Journal of Solids and Structures*, vol. 39, no. 15, pp. 4093–4115, 2002.

[18] Chu, C., Engelbrecht, S. S., Graf, G. C., and Rosen, D. W., "A comparison of synthesis methods for cellular structures with application to additive manufacturing," in *Solid Freeform Fabrication Symposium*, (Austin, TX), Aug. 4-6 2008.

[19] Chu, C., Graf, G. C., and Rosen, D. W., "Design for additive manufacturing of cellular structures," in *Computer-Aided Design & Applications Conference*, (Orlando, FL), June 23-27 2008.

[20] Deshpande, V. S., Ashby, M., and Fleck, N., "Foam topology bending versus stretching dominated architectures," *Acta Materialia*, vol. 49, pp. 1035–1040, 2001.

[21] Deshpande, V. S., Fleck, N. A., and Ashby, M. F., "Effective properties of the octet-truss lattice material," *Journal of Mechanics and Physics of Solids*, vol. 49, no. 8, pp. 1747–1769, 2001.

[22] Dewhurst, P. and Srithongchai, S., "An investigation of minimum-weight dual-material symmetrically-loaded wheels and torsion arms," *Journal of Applied Mechanics*, vol. 72, pp. 196–202, 2005.

[23] Dorn, W., Gomory, R., and Greenberg, H., "Automatic design of optimal structures," *Journal Mechanica*, vol. 3, pp. 25–52, 1964.

[24] Engelbrecht, S. S., "Design of meso-scale cellular structure for rapid manufacturing," Master's thesis, Georgia Institute of Technology, 2009.

[25] Gibson, L. J. and Ashby, M. F., *Cellular Solids: Structure and Properties*. Cambridge, U.K.: Cambridge University Press, 1997.

[26] Gould, N., Orban, D., and Toint, P., "Numerical methods for large-scale nonlinear optimization," *Acta Numerica*, vol. 14, pp. 299–361, 2005.

[27] Graf, G. C., "Development of specialized base primitives for meso-scale conforming truss structures," Master's thesis, Georgia Institute of Technology, 2009.

[28] Haber, R., Bendsøe, M. P., and Jog, C., "A new approach to variable topology shape design using a constraint on the perimeter," *Structural Optimization*, vol. 11, pp. 1–12, 1996.

[29] Hibbeler, R. C., *Mechanics of Materials*. Pearson Prentice Hall, 7 ed., 2008.

[30] Jacobs, P. F., *Rapid Prototyping & Manufacturing: Fundamentals of Stereolithography*. TX: Mcgraw-Hill, September 1993.

[31] Johnston, S. R., Reed, M., Wang, H., and Rosen, D. W., "Analysis of mesostructure unit cells comprised of octet-truss structures," in *Solid Freeform Fabrication Symposium*, (Austin, TX), pp. 421–432, 2006.

[32] Kennedy, J. and Eberhart, R. C., "Particle swarm optimization," in *IEEE International Conference on Neural Networks*, (Piscataway, NJ), pp. 1942–1948, 1995.

[33] Legault, M. R. and Msselman, M., "The rise of rapid manufacturing," *High Performance Composites*, vol. 17, pp. 32–37, July 2009.

[34] Liu, G., *Meshfree Methods: Moving Beyond the Finite Element Method*. CRC Press, 2 ed., 2009.

[35] Michell, A. G. M., "Limits of economy of material in frame structures," *Philosophy Magazine*, vol. 6, pp. 589–597, 1904.

[36] Özisik, M. N. and Orlande, H. R. B., *Inverse Heat Transfer*. New York, NY: Taylor & Francis, 2000.

[37] Patel, J. and Choi, S., "Topology optimization for meso-structured materials under uncertainty," in *2008 ASME iDETC/CIE*, (New York, NY), 2008.

[38] Pederson, P., "On optimal shapes in materials and structures," *Structural Multidisciplinary Optimization*, vol. 19, pp. 169–182, 2000.

[39] Press, W. H., Teukolsky, S. A., Vettering, W. T., and Flannery, B. P., "Chapter 15," in *Numerical Recipes in C*, ch. 15, Cambridge, U.K.: Cambridge University Press, 2nd ed., 1992.

[40] Rao, S. S., *Engineering Optimization: Theory and Practice*. John Wiley & Sons, Inc., 4 ed., 2009.

[41] Reddy, J. N., *An Introduction to the Finite Element Method*. Tata McGraw-Hill, 3 ed., 2006.

[42] Rosen, D. W., Gibson, I., and Stucker, B., *Additive Manufacturing Technologies*. Springer, 2010.

[43] Rozvany, G. I. N., *Topology Optimization in Structural Mechanics*. Springer, 2003.

[44] Rozvany, G. I. N., Guerin, O., Logo, J., and Pomenzanski, V., "Exact analytical theory of topology optimization with some pre-existing members or elements," *Structural Multidisciplinary Optimization*, vol. 4, pp. 585–594, 2007.

[45] Rozvany, G. I. N. and Zhou, M., "The coc algorithm, part i: Cross-section optimization or sizing," *Computer Methods in Applied Mechanics and Engineering*, vol. 89, pp. 281–308, 1991.

[46] Seepersad, C. C., Allen, J. K., McDowell, D. L., and Mistree, F., "Robust design of cellular materials with topological and dimensional imperfections," *ASME Journal of Mechanical Design*, vol. 128, p. 1285, 2006.

[47] Selyugin, S., "On optimal geometrically non-linear trusses.," *Structural Multidisciplinary Optimization*, vol. 29, pp. 113–124, 2005.

[48] Sigmund, O., "A 99 line topology optimization code written in matlab," *Structural Multidisciplinary Optimization*, vol. 21, pp. 120–127, 2001.

[49] Tai, K., Cui, G., and Tapabrata, R., "Design synthesis of path generating compliant mechanisms by evolutionary optimization of topology and shape," *ASME Journal of Mechanical Design*, vol. 124, pp. 492–500, 2002.

[50] Wallach, J. and Gibson, L., "Mechanical behaviour of a three-dimensional truss material.," *International Journal of Solids and Structures*, vol. 38, pp. 7181–7196, 2001.

[51] Wang, A. J. and McDowell, D. L., "Optimization of a metal honeycomb sandwich beam-bar subjected to torsion and bending," *International Journal of Solids and Structures*, vol. 40, no. 9, pp. 2085–2099, 2003.

[52] Wang, H., Chen, Y., and Rosen, D., "A hybrid geometric modeling method for large scale conformal cellular structures," in *ASME Computers and Information in Engineering Conference*, Sept. 24-28 2005.

[53] Wang, H. and Rosen, D. W., "An automated design synthesis method for compliant mechanisms with application to morphing wings," in *ASME Mechanisms Conference*, Sept. 10-13 2006.

[54] Wang, H. V., *A Unit-Cell Approach for Lightweight Structure and Compliant Mechanism*. PhD thesis, Georgia Institute of Technology, December 2005.

[55] Wang, H., *A unit-cell approach for lightweight structure and compliant mechanism*. PhD thesis, Georgia Institute of Technology, 2005.

[56] Watts, D. M. and Hague, R. J., "Exploiting the design freedom of rm," in *Proc Solid Freeform Fabrication Symposium*, (Austin, TX), pp. 656–667, 2006.

[57] Wholers, T. T., "Wohlers report 2008," 2008.

[58] Wooten, J., "Aeronautical case studies using rapid manufacture," in *Rapid Manufacturing* (Hopkinson, N., Hague, R., and Dickens, P., eds.), ch. 15, John Wiley & Sons, 2006.

[59] Xia, Q. and Wang, M. Y., "An optimization-based approach for the design of lightweight truss-like structures," *Computer-Aided Design (Submitted)*, 2008.

[60] Yang, R. and Chuang, C., "Optimal topology design using linear programming," *Computers & Structures*, vol. 52, pp. 265–275, 1994.

[61] Zhou, K. and Li, J., "The exact weight of discretized michell trusses for a central point load," *Structural Multidisciplinary Optimization*, vol. 28, pp. 69–72, 2004.

[62] Zhou, M., Shyy, Y., and Thomas, H., "Checkerboard and minimum member size control in topology optimization," *Structural Multidisciplinary Optimization*, vol. 21, pp. 152–158, 2001.